Investigating The Production of Transforming Growth Factor Alpha (TGF -α) In 3D Hepatocyte And Natural Killer (NK) Cell Models.

Maynooth University
National University of Ireland Maynooth

This thesis is submitted to Maynooth University for the Degree of
Master of Science (Research)

By

Joana Amoanab (BSc Hons.)

October 2023

Department of Biology

Head of Department: Prof. Paul Moynagh

Supervisor: Dr. Mark Robinson

Table of Contents

List of Figures

List of Tables

DECLARATION

I have read and understood the Departmental policy on plagiarism.

I declare that this thesis is my own work and has not been submitted in any form for another degree or diploma at any university or other institution of tertiary education. Information derived from the published or unpublished work of others has been acknowledged in the text and a list of references is given.

Signature:

Date: 29th September, 2023

List of Abbreviations

2D	2-dimensional	LPS	Lipopolysaccharide
3D	3-dimensional	IFN	Interferon
AIH	Autoimmune hepatitis	Ig	Immunoglobulin
ALD	Alcohol-associated liver disease	IL	Interleukin
ALD	Alcoholic liver disease	KC	Kupffer cell
ANOVA	Analysis of variance	mAb	Monoclonal antibody
ASM	Advanced suspension medium	NAFLD	Non-alcoholic fatty liver disease
BSA	Bovine serum albumin	*G6PD*	Glucose-6-Phosphate Dehydrogenase
CLD	Chronic liver disease	*MYC*	MYC Proto-Oncogene
CXCR6	C-X-C chemokine receptor type 6	*VEGFA*	Vascular endothelial growth factor A
CYP	Cytochrome	*SREBF1*	Sterol regulatory element binding transcription factor 1
DMSO	Dimethyl sulfoxide	CSF2	Colony Stimulating Factor 2
ECM	Extra-cellular matrix	*ALB*	Albumin
FACS	Fluorescence-activated cell sorting	*AFP*	Alpha- feto Protein
FBS	Fetal bovine serum	*ADAM17*	A disintegrin and metalloprotease 17
FMO	Flourescence minus one	*HIF1A*	Hypoxia Inducible Factor 1 Subunit Alpha
FSC	Forward scatter	*TNFA*	Tumor Necrosis Factor Alpha
HBV	Hepatitis B virus	EDTA	Ethylenediaminetetraacetic acid
HC	HappyCell ASM		
HCC	Hepatocellular carcinoma		
HCV	Hepatitis C virus		
HSC	Hepatic stellate cell		

Acknowledgement

I would like to begin by expressing my heartfelt gratitude to God for guiding me throughout my research journey and Masters studies. Without Him, none of this would have been possible.

I am profoundly thankful to my supervisor, Dr. Mark Robinson, for his invaluable guidance, encouragement, and expertise that shaped my research. I extend my appreciation to the members of the Robinson lab, particularly Shauna O'Neill, for her exceptional assistance, dedication, and support, which significantly contributed to the success of my work.

I am indebted to the Irish Research Council for their generous funding, without which my research project would have remained a distant dream. Their support made it possible for me to explore and expand the boundaries of knowledge in my field.

I am also grateful to my academic advisor and assessor , Martina Schroeder, and Eoin McNamee, for their insightful feedback, advice, and unwavering support at every stage of my thesis.

To my friends at Maynooth University, your camaraderie and encouragement made my time here not only academically fulfilling but also personally enriching.

A special thank you goes out to my family and loved ones for their constant prayers, unwavering support, and belief in my abilities. Your love has been my greatest motivation.

In closing, I would like to express my appreciation to all those who have played a part, big or small, in my academic journey. Your contributions have been instrumental, and I am truly grateful.

Abstract

The human liver is a complex organ with pivotal roles in metabolism, detoxification, and immune responses. Transforming growth factor-alpha (TGF-α), a ligand of the epidermal growth factor receptor (EGFR), is known for its involvement in cell proliferation, differentiation, and tissue repair, particularly in liver regeneration. This study investigates the intricate interplay between NK cells and hepatocytes, focusing on TGF-α production within a three-dimensional (3D) co-culture model.

In this research, 3D culture systems demonstrate a significant enhancement in hepatocyte proliferation when exposed to recombinant TGF-α. This highlights the substantial influence of the cellular environment on TGF-α effects and suggests that the 3D culture system is a better model to assess the impact of TGF-α signalling on hepatocytes. Gene expression analyses reveal distinct patterns between 2D and 3D models, further emphasizing the importance of the latter.

Additionally, this study explores the production of TGF-α by liver-resident NK cells and their potential role in liver regeneration. Transcriptional analysis confirms the presence of *TGFA* expression within CD56^{Bright} liver-resident NK cells, suggesting their involvement in modulating the local TGF-α environment. However, co-culture experiments involving NK cells and hepatocyte cell lines reveal an unexpected absence of TGF-α production, highlighting the complex and context-specific nature of immune responses within the liver microenvironment.

While this research advances our understanding of the context-dependent effects of TGF-α, further investigations are essential to elucidate the regulatory pathways governing TGF-α production by NK cells and its impact on liver regeneration. Ultimately, these findings hold promise for innovative therapeutic strategies in the treatment of liver-related pathologies, offering hope to patients in need of liver repair and regeneration therapies.

Chapter 1   Introduction

1.1 The Human Liver

The liver is a crucial organ that plays a central role in the metabolism of nutrients and the elimination of waste metabolites. It is the largest solid organ in the body, and its proper functioning is essential for overall health and well-being (Trefts et al., 2017). The principal role of this organ is to regulate the transport of substances while also ensuring their absorption from the digestive system before they are introduced into the systemic circulation (Trefts et al., 2017). In addition to its role in digestion, the liver performs other various functions to support immunity, detoxification, protein synthesis and vitamin storage (Russell, 2003). The majority of hepatic functions are executed by the hepatocytes, the primary parenchymal cells, which constitute approximately 60-70% of liver cells and approximately 80% of the total liver volume (Michalopoulos, 2007). The remaining 20% is comprised of non-parenchymal cells such as Kupffer cells, stellate cells, endothelial cells, and lymphocytes (Gao, 2016).

Various liver diseases, including fatty liver, liver fibrosis, and cirrhosis, have been identified as potential disruptors of the liver's physiological processes (Friedman, 2010). One of the most fascinating aspects of the liver is that, following hepatic injury, the liver possesses a unique capacity for self-repair, rendering it the sole internal organ in the human body with the ability to regenerate itself (Michalopoulos, 2007). In response to hepatic injury, all the liver cell types are activated and each of these cell types contributes to the process of liver regeneration (Tsuchida & Friedman, 2017). The mechanisms underlying liver regeneration remain incompletely elucidated. A deeper understanding of the cellular regulation of liver regeneration may provide novel strategies to enhance this process therapeutically in the context of chronic liver disease and liver transplantation.

1.2 Structure of the human liver

The human liver, comprising approximately 2.5% of total body weight, boasts a remarkable anatomical intricacy crucial to its diverse physiological functions (Lorente et al., 2020). It is situated in the upper right quadrant of the abdominal cavity, comprising four discernible lobes—namely the right, left, caudate, and quadrate lobes—the liver's dominant right lobe encompasses approximately 60-70% of its total mass (Standring, 2020). These lobes are demarcated by three pivotal fissures: the left sagittal fissure, the right sagittal fissure, and the transverse fissure, which houses the porta hepatis—a gateway for the hepatic artery, portal vein, and bile duct to interface with the liver's internal milieu (Standring, 2020).

At the microscopic level, the liver's functional architecture is characterized by hepatic lobules, hexagonal structures wherein hepatocytes radiate outward from a central vein (Leiskau & Baumann, 2017). These hepatocytes, the *sine qua non* of hepatic parenchyma, organize into plates and the spaces between these hepatocyte plates are occupied by sinusoids, capillary-like vessels lined with specialized endothelial cells. Sinusoids serve as the conduits through which blood flows, carrying oxygenated blood from branches of the hepatic artery and nutrient-rich, deoxygenated blood from the portal vein (Gao, 2016; Trefts et al., 2017).

Within this microcosm of hepatocytes and sinusoids, Kupffer cells stand sentinel as specialized macrophages lining the sinusoidal walls (Bilzer et al., 2006a). Fulfilling a dual mandate of immune defense and erythrocyte degradation, these phagocytes contribute indispensably to the liver's homeostatic equilibrium (Bilzer et al., 2006a). Concurrently, the bile canaliculi, interconnecting passageways forged between adjacent hepatocytes, coalesce to form bile ductules—a tributary network that culminates in the bile ducts, conduits for transporting bile synthesized by hepatocytes (Hohenester et al., 2012).

Portal triads, strategically positioned at the lobular corners, encompass branches of the hepatic artery, portal vein, and bile duct, orchestrating the quintessential trinity of vascular and ductal conduits to each lobule (Leiskau & Baumann, 2017; Lorente et al., 2020).

The liver receives its blood supply through two main sources: the hepatic artery, originating from the celiac trunk, and the portal vein, which transports nutrient-rich blood from the gastrointestinal tract, pancreas, and spleen (Lorente et al., 2020). The convergence of these vessels at the porta hepatis ensures an efficient supply of oxygen and nutrients to the hepatocytes.

The biliary system, integral to hepatic function comprises bile canaliculi, small channels that weave between adjacent hepatocytes and merge to form bile ductules. These ductules converge to create bile ducts, which are essential for the transportation of bile produced by hepatocytes to the gallbladder and duodenum (Standring, 2020). The gallbladder acts as a storage and concentration reservoir for bile, releasing it in response to hormonal signals during the digestive process (Standring, 2020).

The liver is not only a metabolic powerhouse but also a responsive organ with rich lymphatic drainage and innervation (Yang, 2020). Lymphatics within the liver drain into hepatic lymph nodes, contributing to immune surveillance. The hepatic plexus provides sympathetic and parasympathetic nerve fibres to the liver, regulating various physiological processes (Gao, 2016; Trefts et al., 2017).
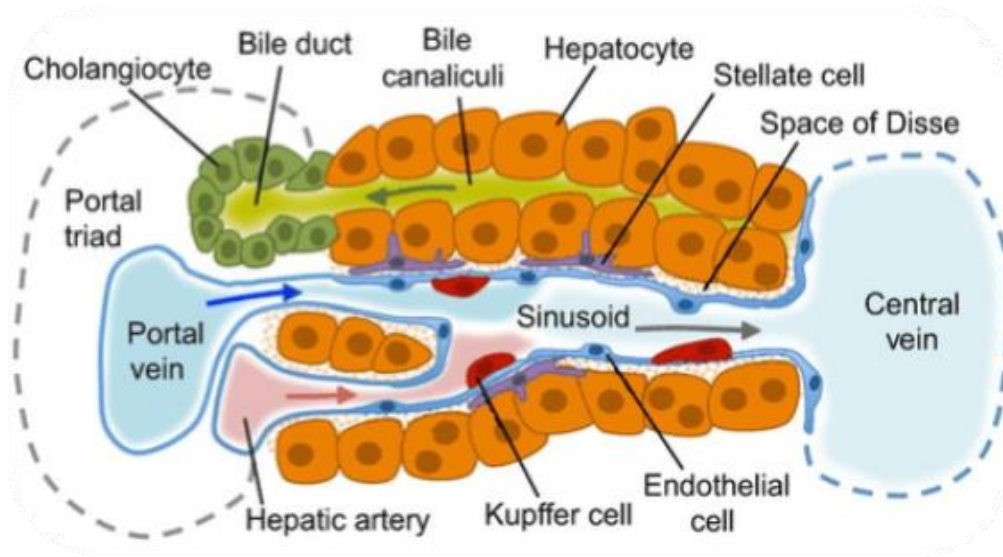
Figure 1. 1: Liver Anatomy and Functional Components

Figure 1.1 illustrates from Gordillo et al., 2015, the structural components of the liver, highlighting the lobule as the functional unit. The lobule is depicted as a hexagon, with a portal triad (comprising the bile duct, portal vein, and hepatic artery) at each corner and a central vein at the midpoint. Hepatocytes, the primary parenchymal cells, play a crucial role in liver function. Biliary epithelial cells (BECs), also known as cholangiocytes, make up 3% of the liver mass and line the biliary tree, modifying bile produced by hepatocytes. Bipotential BECs, residing in the canals of Hering, have the capacity to differentiate into either BECs or hepatocytes in response to liver injury. Additionally, the liver's non-parenchymal cell fraction includes hepatic stellate cells (HSCs), resident macrophages (Kupffer cells), liver sinusoidal endothelial cells (LSECs), portal fibroblasts, and non-resident immune cells. LSECs, characterized by fenestrae and the absence of a basement membrane, facilitate the filtration of metabolites, proteins, drugs, and other substances into the space of Disse.

1.3 Functions of the human liver

The human liver plays a multifaceted role in maintaining homeostasis and supporting various physiological processes (Figure 1.2) within the body, making it indispensable for overall health and well-being.

One of the liver's foremost functions is regulating metabolism. In the realm of carbohydrate metabolism, the liver acts as a guardian of blood glucose levels (Leiskau & Baumann, 2017). During periods of fasting or heightened energy demand, it undertakes gluconeogenesis, synthesizing glucose from non-carbohydrate precursors such as amino acids and glycerol (Leiskau & Baumann, 2017). Conversely, in times of glucose abundance, the liver converts excess glucose into glycogen, stored for future use.

The metabolism of cholesterol and lipoproteins, which are necessary for the creation of bile acids and steroid hormones (Chiang & Ferrell, 2018), is another critical function of the liver. The control of cholesterol levels in the body is largely dependent on the enzyme HMG CoA. According to Moore and Dalley (2006) and Guyton (2006), the HMG CoA molecule is essential for both the manufacture of cholesterol and the uptake of cholesterol from lipoproteins and chylomicrons.

In protein metabolism, the liver takes center stage, synthesizing approximately 15% of the entire protein content in the human body, with the majority of this protein being taken up by the circulatory system (Gao, 2016). The proteins including albumin, crucial for maintaining blood volume and pressure, and a myriad of clotting factors such as fibrinogen and prothrombin. This ensures effective blood clotting and the maintenance of vascular integrity (Leiskau & Baumann, 2017).

The liver's detoxification prowess is equally remarkable. It is the body's chief detoxifying organ, metabolizing drugs, neutralizing toxins, and converting toxic ammonia, a byproduct of

protein metabolism, into urea (Chiang & Ferrell, 2018). Enzymes residing in the liver, notably the cytochrome P450 family, facilitate the breakdown of drugs, toxins, and xenobiotics, detoxifying the bloodstream and preventing the accumulation of harmful substances (Zanger & Schwab, 2013).

The liver produces bile, an essential digestive fluid. This fluid, comprising bile salts, cholesterol, and bilirubin, emulsifies fats, fostering their absorption within the small intestine (Gebhardt, 1992; Hofmann, 1999). Without bile, the process of fat digestion and subsequent absorption of fat-soluble vitamins would be severely compromised (Hofmann, 1999).

As a storage reservoir, the liver houses glycogen, a polysaccharide that can be rapidly converted into glucose to maintain blood sugar levels during periods of fasting or heightened energy demands (Exton, 1987). Additionally, the liver stores fat-soluble vitamins (A, D, E, and K), releasing them into the bloodstream as required to support various bodily functions (Heubi et al., 2007; Russell, 2000).

The liver also plays a role in regulating blood composition as it monitors and controls levels of glucose, amino acids, and lipids in the bloodstream, ensuring that these essential components are maintained at optimal levels (Postic & Girard, 2008). Additionally, the liver contributes to electrolyte balance and actively removes harmful substances from the blood, promoting overall health (Cederbaum, 2012).

Kupffer cells, within in the liver, act as vigilant sentinels guarding the bloodstream (Bilzer et al., 2006). They intercept pathogens and toxins, phagocytosing foreign particles, and participating in immune responses, exemplifying the liver's crucial role in immunological defense (Bilzer et al., 2006).
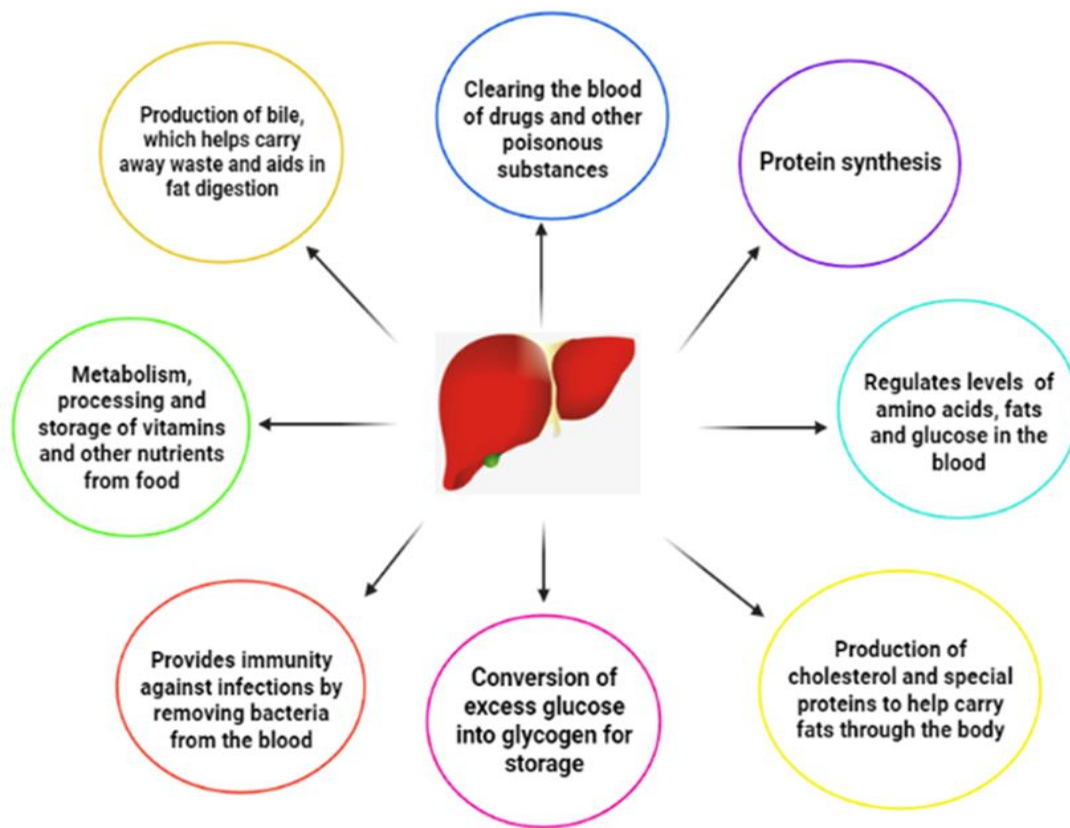
Figure 1. 2: Functions of The Liver

1.4 Aetiology of liver disease

Acute liver disease, characterized by a sudden and severe onset of liver dysfunction, can arise from various aetiologies, such as viral infections, drug toxicity, or metabolic disorders (Tapper & Parikh, 2018). This condition manifests rapidly over a short period, giving rise to clinical manifestations like jaundice, abdominal pain, and nausea (Stravitz & Lee, 2019). Timely identification and intervention are imperative to avert progression to acute liver failure (Stravitz & Lee, 2019).

In contrast, chronic liver disease entails a prolonged and persistent hepatic disorder marked by gradual, sustained injury to liver tissue, resulting in a progressive decline or loss of liver

function (Bataller & Brenner, 2005). This functional impairment encompasses the liver's diminished capacity to synthesize clotting factors and other crucial proteins, as well as its reduced ability to excrete bile and detoxify metabolic by-products (Bataller & Brenner, 2005). The pathology of chronic liver disease revolves around a persistent cycle of inflammation, tissue destruction, and subsequent regeneration, culminating in the deposition of extracellular matrix—a process commonly referred to as fibrosis and cirrhosis (Tapper & Parikh, 2018).

Chronic liver disease poses a substantial global health challenge, impacting millions of individuals and imposing a significant burden on healthcare systems (Asrani et al., 2019). The array of underlying causes for chronic liver disease is wide-ranging and encompasses factors such as prolonged alcohol abuse, infections, autoimmune diseases, and genetic and metabolic disorders (Singal & Shah, 2019).

Non-alcoholic fatty liver disease (NAFLD) has emerged as a predominant chronic hepatic condition with a global prevalence estimated to affect approximately 25% of the population (Younossi et al., 2016). However, regional disparities exist, with notably higher incidence rates observed in Western nations, where it afflicts up to 30-40% of adults (Younossi et al., 2016). The intimate association between NAFLD and obesity, which has attained epidemic proportions, is evident, with an estimated 80-90% of obese individuals experiencing NAFLD (Younossi et al., 2016). This underscores NAFLD as a direct consequence of the escalating worldwide prevalence of weight-related health issues. Insulin resistance, metabolic syndrome, and type 2 diabetes further compound the risk, while sedentary lifestyles and consumption of high-calorie, processed foods perpetuate the crisis (Eslam et al., 2020).

Alcoholic liver disease (ALD) remains a formidable adversary within the domain of chronic liver disorders, contributing to a staggering 50% of liver-related mortalities on a global scale (Gao & Bataller, 2011). Nevertheless, the prevalence of ALD exhibits substantial regional

variation, with nations in Eastern Europe, such as Russia, grappling with its onslaught in up to 70% of liver disease (Rehm et al., 2013). Chronic and excessive alcohol consumption stands as the root cause of ALD, a behavior pattern transcending geographical boundaries. Genetic variations in alcohol metabolism introduce an additional layer of complexity to risk assessment, influencing the progression of ALD (Stickel & Hampe, 2012).

Viral hepatitis, specifically chronic hepatitis B and C, exerts a significant impact on global health. Approximately 257 million individuals contend with chronic hepatitis B, while 71 million endure chronic hepatitis C (WHO, 2017). Prevalence rates are notably elevated in regions with limited healthcare access and inadequate vaccination programs. Transmission primarily occurs through contact with infected blood or bodily fluids, with risky behaviors such as unprotected sexual intercourse and needle sharing among intravenous drug users serving as prominent transmission pathways (WHO, 2017).

Autoimmune liver diseases, while less prevalent compared to other aetiologies of chronic liver diseases, nonetheless impact a substantial segment of the population, with estimated prevalence rates ranging from 50 to 200 cases per 100,000 individuals (Manns et al., 2010). These conditions are characterized by an aberrant immune response targeting hepatocytes. Genetic factors play a significant role, as evidenced by autoimmune hepatitis, which exhibits a predilection for females and displays familial aggregation, implying a genetic predisposition (Liberal et al., 2013).

Although individual genetic and metabolic disorders affecting the liver are infrequent, they collectively contribute a notable proportion, approximately 5-10%, to the overall burden of chronic liver diseases (Bacon et al., 2011). Conditions such as hemochromatosis, affecting 1 in 200 individuals of Northern European descent, and Wilson's disease, occurring in 1 in 30,000

individuals globally, underscore the profound influence of genetics on hepatic health (Pietrangelo, 2010; Roberts & Schilsky, 2008).

Drug-Induced Liver Injury (DILI), while relatively uncommon, has the potential to precipitate acute liver failure, with an incidence of approximately 10-15 cases per 10,000 individuals exposed to medications (Chalasani et al., 2008). The aetiology of DILI frequently links back to specific drugs, including certain antibiotics (e.g., isoniazid), anti-seizure medications (e.g., valproate), over-the-counter drugs like acetaminophen (in excessive doses), and select supplements, particularly when consumed inappropriately or by individuals with pre-existing liver conditions (Reuben et al., 2010).

Cystic fibrosis-related liver disease is a prevalent complication of cystic fibrosis, affecting approximately 30-40% of individuals with this genetic disorder (Debray et al., 2011). The condition arises from genetic mutations inherent to cystic fibrosis, leading to hepatic complications through the aberrant transport of substances within cells (Colombo et al., 2002).

1.5 Liver Fibrosis and cirrhosis

1.5.1 Liver Fibrosis

Liver fibrosis is a pathological condition characterized by the aberrant deposition of extracellular matrix (ECM) proteins, notably collagen, within the hepatic tissue (Friedman, 2008a). This condition is a prominent feature in diverse manifestations of chronic liver diseases, representing a substantial burden on global healthcare (Bataller & Brenner, 2005).

The aetiology of liver fibrosis is rooted in prolonged or recurrent hepatocellular injury, which triggers an excessive accumulation of fibrous connective tissue and consequent structural tissue remodeling (Schuppan & Kim, 2013). The accumulation of ECM proteins ultimately leads to the

disruption of the liver's structural integrity, resulting in the formation of a fibrous scar (Hernandez-Gea & Friedman, 2011).

Untreated liver fibrosis invariably progresses to cirrhosis, signifying a critical juncture in the continuum of liver pathology. This transition is marked by a gradual deterioration of hepatic function (Tsochatzis et al., 2014). In its advanced stages, liver fibrosis ends in liver failure, a condition that may necessitate a liver transplant, and in severe cases, can be fatal (Schuppan & Kim, 2013).

1.5.2 Liver Cirrhosis

As previously discussed, liver fibrosis is a progressive condition that can ultimately result in cirrhosis, which represents the terminal stage of hepatic tissue scarring. This condition presents a significant risk to an individual's holistic well-being warranting in-depth investigation and consideration.

Cirrhosis is characterized by profound impairments in the liver's fundamental functions, including detoxification processes, nutrient metabolism, protein synthesis, and regulation of blood clotting mechanisms (Friedman, 2008). A key consequence of cirrhosis is the development of portal hypertension, arising from the cumulative fibrotic changes that obstruct hepatic blood flow (Garcia-Tsao et al., 1985). Consequently, elevated pressure within the portal vein, a major conduit for blood from the digestive organs, leads to a range of complications, notably variceal bleeding, and ascites (Garcia-Tsao et al., 1985).

Variceal bleeding, a potentially life-threatening event, ensues when dilated blood vessels in the oesophagus or stomach rupture due to elevated portal pressure (Garcia-Tsao & Lim, 2009).

Concurrently, ascites manifests as the accumulation of fluid within the abdominal cavity, further exacerbating the burden of cirrhosis (Ginès et al., 2004).

In addition to these complications, individuals suffering from cirrhosis face an escalated risk of developing HCC, particularly in cases associated with chronic viral hepatitis or prolonged alcohol consumption (Singal et al., 2009; Tsochatzis et al., 2014). Therefore, early detection and timely intervention through routine surveillance using imaging modalities are essential in managing this heightened risk (Singal et al., 2009).

Furthermore, the cognitive repercussions of cirrhosis are substantial. Hepatic encephalopathy, arising from the liver's compromised ability to metabolize toxins, presents as cognitive dysfunction, confusion, and, in severe instances, coma (Felipo, 2013). This emphasizes the profound and wide-ranging impact of cirrhosis on neurological function.

As cirrhosis progresses, the liver's diminishing functional capacity approaches a critical threshold, marking the onset of liver failure (Bernal et al., 2015). Acute liver failure manifests suddenly and severely, necessitating immediate medical intervention, while chronic liver failure mandates long-term management and often requires advanced therapeutic strategies (Bernal et al., 2015).

Cirrhosis remains a significant concern, as it contributes substantially to both morbidity and mortality among individuals suffering from chronic liver diseases. In 2019, cirrhosis was responsible for 2.4% of global fatalities (Abbafati et al., 2020). The Global Burden of Disease (GBD) study in 2019 provided estimates at global and regional levels for the number of deaths and age-standardized death rates (ASDRs) associated with cirrhosis in the same year. The global estimate for cirrhosis-related deaths in 2019 was 1,472,000, representing a 10% increase from 2010. Eastern Mediterranean region exhibited the lowest number of cirrhosis-related

deaths, totalling 146,000. Southeast Asia had the highest number of cirrhosis-related deaths, with a total of 443,000 (Global Burden of Disease 2019 Cirrhosis Collaborators, 2021).

Liver cirrhosis is expected to become more common in the coming years, primarily due to the lack of effective treatments for hepatic fibrosis and slowing down the progression of cirrhosis (Abbafati et al., 2020; WHO, 2017). In cases of advanced liver damage with significant impairment of liver function, the possible option available is liver transplantation.

Liver regeneration has gained recognition as a treatment for individuals with end-stage liver disease (Starzl et al., 1967). Since Thomas Starzl's groundbreaking first liver regeneration in 1967, outcomes for transplant recipients have steadily improved both in the short and long term. These improvements are attributed to advancements in immunosuppressive therapies, better assessments of donor-recipient compatibility, and improved management of post-transplant complications (Tsochatzis et al., 2014).

Recent times have seen a growing global population of people in need of transplantation, while the pool of available organ donors has not grown proportionally. This disparity between demand and supply of organs is a significant issue in the field of liver regeneration, contributing to approximately 15% mortality risk among patients on transplant waiting lists (Tsochatzis et al., 2014).

The shortage of deceased donor organs has led to the development of living donor liver transplantation, a relatively recent innovation that has gained prominence (Ghobrial et al., 2008). In living donor liver transplantation, a living donor provides a portion of their healthy liver to the recipient. Interestingly, both the donor's liver and the remaining liver in the recipient can regenerate, eventually fully restoring functionality. However, stringent medical evaluations are crucial to ensure the donor's well-being (Ghobrial et al., 2008).

13

After transplantation, the donor's remaining liver undergoes regeneration to regain its original size. At the same time, the transplanted liver adapts and grows to meet the recipient's metabolic needs, highlighting the remarkable regenerative potential of this vital organ (Michalopoulos & Bhushan, 2020).

These innovative approaches are rooted in the liver's exceptional regenerative capacity. Consequently, deepening our understanding of the mechanisms governing liver regeneration holds great promise for improving the management of liver failure and providing valuable insights into the care of patients who require extensive liver resections or transplantation (Michalopoulos & Bhushan, 2020).

1.6 Liver regeneration

Liver regeneration is a phenomenon that encompasses the reinstatement of hepatic volume to counter any liver damage or malfunction. The liver exhibits a unique ability to regenerate its lost volume, a phenomenon that is not observed in other internal organs. The remaining or transplanted liver typically goes through a rapid expansion process after surgical procedures such as partial hepatectomy or live donor liver transplantation in order to restore liver volume. Normally, hepatocytes exhibit quiescence but retain the ability to undergo proliferation upon induction by certain stimuli. The potential impact of mitogens such as HGF, TGF-α, and TGF-β1 on hepatocyte proliferation in animal models has been extensively studied.

The most commonly used model to study liver regeneration is the 70% partial hepatectomy (PHx) model in rodents, which was originally described by Higgins in 1931 (Higgins & Anderson 1931) and remains essentially unchanged today. However, the precise contribution of these factors to liver regeneration in humans remains unclear.

The process of liver regeneration after partial hepatectomy involves three primary stages namely initiation, proliferation, and termination of cellular proliferation. The beginning of each phase is initiated by a certain molecule set released in response to organ damage (Bhat et al., 2019). The earliest regeneration drivers are portal pressure changes and an increasing level of urokinase plasminogen activator (uPA) (Rmilah et al., 2019; Drixler et al., 2003).

1.6.1 Priming/ Initiation phase

The initiation stage of liver regeneration involves preparing hepatocytes for proliferation, which occurs within the first 5 hours after surgery. This phase is marked by the increased expression of several genes. During this initial phase, hepatocytes are induced to enter the G1 phase of the cell cycle by various cytokines (López-Luque & Fabregat, 2018) . This entry is driven by increased blood pressure in the hepatic sinusoids due to a mismatch in liver volume and incoming venous blood volume, causing turbulent flow (Michalopoulos, 2010) . This mechanical stimulation prompts sinusoidal endothelial cells (SECs) to release uPA, which in turn converts plasminogen to plasmin. This leads to the activation of matrix metalloproteinases (MMPs), resulting in the degradation of fibrinogen and remodeling of the ECM. This ECM remodeling releases growth factors, including hepatocyte growth factor (Rmilah et al., 2019).

The first phase of regeneration is primarily mediated by two proinflammatory cytokines: Tumor necrosis factor-alpha (TNF-α) and interleukin-6 (IL-6). These cytokines are mainly secreted by liver macrophages in response to bacterial lipopolysaccharide and components of the complement system (Min et al., 2016). IL-6 plays a central role by initiating cytoprotection and hepatocyte proliferation through its interaction with IL-6R and subsequent activation of gp130 (Tao et al., 2017). This activation triggers various signaling pathways, including JAK/STAT, MAPK, and PI3K/AKT pathways (Michalopoulos, 2013; Schmidt-Arras & Rose-

John, 2016). While gp130 is present on most cell surfaces, IL-6R is primarily located on hepatocytes. However, soluble forms of IL-6R can initiate trans-signaling in cells lacking the receptor, enhancing hepatocyte regenerative responses (Tao et al., 2017). Research by Modares et al. emphasized the crucial role of the trans-signaling pathway in liver regeneration after partial hepatectomy (PHx), as the activation of hepatocyte IL-6R alone was insufficient to initiate cell proliferation (Modares et al., 2019).

TNF-α has dual functions during this phase as it activates the NF-κB signaling pathway and induces inhibitory KB kinase through direct interaction with TNF-R1 on Kupffer cell surfaces. Additionally, TNF-α stimulates hepatocyte c-Jun N-terminal kinase (JNK), which phosphorylates the c-Jun transcription factor within the nucleus. This leads to the transcription of cyclin-dependent kinase 1 and promotes hepatocyte proliferation (Rmilah et al., 2019).

1.6.2 Proliferative phase

During the proliferative phase of liver regeneration, which is the second phase in the process, a series of complex molecular events take place to facilitate the restoration of liver tissue. This phase involves a transition from the G1 phase of the cell cycle to the M phase, and it is tightly regulated by specific mitogens. Some of these mitogens include HGF, TGF-α, EGF, and HB-EGF. They activate various pathways such as Ras-MAPK and PI3K/AKT, along with other stimulants like bile acids, VEGF, noradrenaline, IGFs, estrogen, and serotonin (Tao et al., 2017).

HGF, synthesized by mesenchymal liver cells, binds to the MET receptor, initiating a cascade of events. This binding triggers the phosphorylation of proteins involved in the PI3K and MAPK signaling pathways, including PI3K/AKT and extracellular-signal-regulated kinase 1/2 (ERK1/2). Activation of these pathways promotes liver cell proliferation, migration, and

differentiation, while also exerting antiapoptotic effects (Araújo et al., 2013; Puerta et al., 2016).

Epidermal growth factor receptor (EGFR), a transmembrane receptor with tyrosine kinase activity, interacts with EGF, TGF-α, AREG, epigen, and HB-EGF. This interaction activates signaling pathways such as MAPK, PI3K/AKT-mammalian target of rapamycin (mTOR), and STAT signaling, all of which contribute to the stimulation of hepatocyte proliferation. Studies have shown that mice lacking EGFR exhibit impaired liver regenerative capacity and delayed expression of cyclin D1, a critical cell cycle regulator (Berasain & Avila, 2014; Natarajan et al., 2007).

The Nuclear Factor Erythroid 2-Related Factor 2 (NRF2) transcription factors become activated in response to increased levels of reactive oxygen species (ROS) generated during the early stages of liver regeneration due to cellular damage. NRF2 plays a crucial role in regulating cell cycle progression by suppressing the transcription of Cyclin A2 and modulating the Wee1/Cdc2/Cyclin B1 pathway, which controls the initiation of the M phase. Additionally, NRF2 influences hepatocyte proliferation by modulating insulin/IGF-1 and Notch1 signaling and supporting hepatocyte differentiation through hepatocyte nuclear factor 4 alpha (HNF4α) activity (Morales-González et al., 2017; Zou et al., 2014).

Bile acids, the end products of cholesterol metabolism synthesized exclusively in the liver, serve as signaling molecules during liver regeneration. They activate membrane G-protein-coupled Bile Acid Receptor 1 (TGR5) and nuclear Farnesoid X Receptor (FXR) (Liu et al., 2015). FXR activation, in response to an increase in bile acid concentration following liver mass loss, inhibits bile acid synthesis and induces the FOXM1B gene (van de Laarschot et al., 2016). FOXM1B is a transcription factor that regulates DNA synthesis and mitosis through the activation of cyclin-dependent kinase 2 (CDK2), essential for the G1/S transition, and CDK1,

which oversees the S/M transition (Frankenberg et al., 2006). Activation of Fgfr4/β-Klotho by bile acids controls the termination of liver regeneration and the final organ size. This activation also regulates the Hippo signaling pathway, cellular senescence, and transcriptional activation (Alvarez-Sola et al., 2018).

TGR5, found on the surfaces of various liver cell types, including Kupffer cells (KCs), Sinusoidal Endothelial Cells (SECs), and Biliary Epithelial Cells (BECs), activates cAMP induction and inhibits nuclear factor kappa B (NF-κB) signaling (Péan et al., 2013). This results in reduced production of proinflammatory cytokines in immune cells and contributes to liver regeneration. TGR5 also facilitates the excretion of bile acids, maintains liver pH balance, and regulates bile acid polarity, safeguarding the regenerating liver from potential damage caused by excessively hydrophobic molecules (Merlen et al., 2017).

Wnt ligands, glycoproteins secreted primarily by nonparenchymal liver cells like KCs and SECs, play a crucial role in liver regeneration (Valizadeh et al., 2019). They activate signaling pathways by binding to the Frizzled receptor and coreceptors LRP5/6, leading to the accumulation of β-catenin in the cytoplasm. This accumulated β-catenin translocate to the nucleus, where it interacts with transcriptional factors of the T cell factor family, ultimately promoting the transcription of target genes such as cyclin D1, which drives hepatocyte proliferation (Preziosi et al., 2018; Russell & Monga, 2018).

Furthermore, Hedgehog (Hh) signaling, which plays a significant role in embryonic development and homeostasis, is also implicated in liver regeneration. This pathway regulates the morphogenesis of liver tissue during regeneration, ensuring the proper restoration of liver structure and function (Briscoe & Thérond, 2013; Chapouly et al., 2019).

1.6.3 Termination Phase

Upon reaching an appropriate size relative to the body, the liver undergoes a termination phase of regeneration, orchestrated by various molecules and pathways. Interleukin-1 (IL-1), produced by non-parenchymal liver cells, plays a crucial role by inhibiting the replication of liver cells triggered by growth factors such as HGF, EGF, and TGF-α (Liu & Chen, 2017). Another molecule, IL-6, exhibits a dual role in liver regeneration, acting both as a promoter and an inhibitor. Its impact is contingent on its timing and concentration, with the ability to decelerate cell growth by upregulating p21 expression.

Within this regulatory framework, proteins of the SOCS family assume a significant role in modulating the JAK/STAT signaling pathway. SOCS1 directly interacts with and inhibits JAK, while SOCS3 hinders the STAT3 pathway by binding to cytokine receptors. Notably, SOCS3 is pivotal in suppressing the IL-6-activated pathway (Khan et al., 2019).

Certain members of the TGF-β family serve as inhibitors of cell growth, with TGF-β1 specifically inducing cell death to correct excess liver mass (Addante et al., 2018). TGF-β1 is synthesized in platelets and the spleen, and the spleen appears to be involved in terminating liver regeneration by inhibiting HGF and its c-MET receptor (Marí & Morales, 2017).

HNF4-α emerges as a crucial regulator of hepatocyte differentiation and plays a pivotal role in terminating liver regeneration. Its expression initially decreases but later increases in the process, a critical aspect for the regeneration process. HNF4-α counters YAP and TGF-β/SMAD3, thereby aiding in averting excessive connective tissue production and fibrosis (Zhou et al., 2020).

Integrin-linked kinase serves as a suppressor of hepatocyte growth, residing beneath the cell membrane and associating with specific integrins of the ECM. Disruption of this interaction

can lead to an imbalance in liver size. Conversely, focal adhesion kinase, also linked to specific integrins, promotes hepatocyte growth (Michalopoulos, 2017).

The Hippo signaling pathway emerges as a pivotal determinant of final organ size. This pathway entails a cascade of kinases that activate tumor suppressors and coactivators, ultimately influencing the genes controlling cell growth and specialization. The Hippo pathway integrates various growth factor signals and maintains liver size by balancing positive and negative signals. Significantly, it is attuned to factors related to cellular structure and adhesion, enabling it to discern tissue integrity (Konishi et al., 2018).

1.7 Epidermal Growth Factor Receptor structure and expression

The Epidermal Growth Factor Receptor is a plasma membrane glycoprotein that belongs to the ErbB family of receptor tyrosine kinases (RTKs), which also includes ErbB-2, ErbB-3, and ErbB-4 (Yarden & Sliwkowski, 2001). It exhibits a domain outside of the cell that is rich in cysteine and is composed of two distinct regions (Lemmon & Schlessinger, 2010). Additionally, it contains a region that spans the cell membrane and a cytoplasmic tyrosine kinase domain that is highly conserved (Lemmon & Schlessinger, 2010). Upon ligand binding, ErbB proteins exhibit the capability to establish homo- or heterodimers with other ErbB family constituents (Citri & Yarden, 2006). This mechanism results in the initiation of subsequent signaling cascades that govern the modulation of cellular proliferation, expansion, and differentiation (Hynes & MacDonald, 2009).

EGFR has been linked to the differentiation and growth of epithelial cells, and also plays a role in the development of malignancies derived from epithelial cells (Hirsch et al., 2003; Jorissen et al., 2003). Upon the binding of a ligand, the EGFR undergoes dimerization, leading to the autophosphorylation of tyrosine residues on the receptor (Schlessinger, 2000). The existence

of phosphotyrosine residues promotes the recruitment of unique partners thus initiating varied downstream pathways (Pawson & Nash, 2003). The EGFR protein is responsible for regulating multiple cellular signals, including but not limited to cell proliferation, cell motility, and potential involvement in stem cell maintenance (Citri & Yarden, 2006; Hynes & MacDonald, 2009). Furthermore, it has been demonstrated that EGFR has the capability to modulate downstream effectors by directly translocating its internal domain to the nucleus (Komposch & Sibilia, 2015; Seshacharyulu et al., 2012). This activation results in the upregulation of genes related to the cell cycle, including Cyclin D1, and genes linked to inflammation, such as COX-2 (Komposch & Sibilia, 2015; Seshacharyulu et al., 2012).
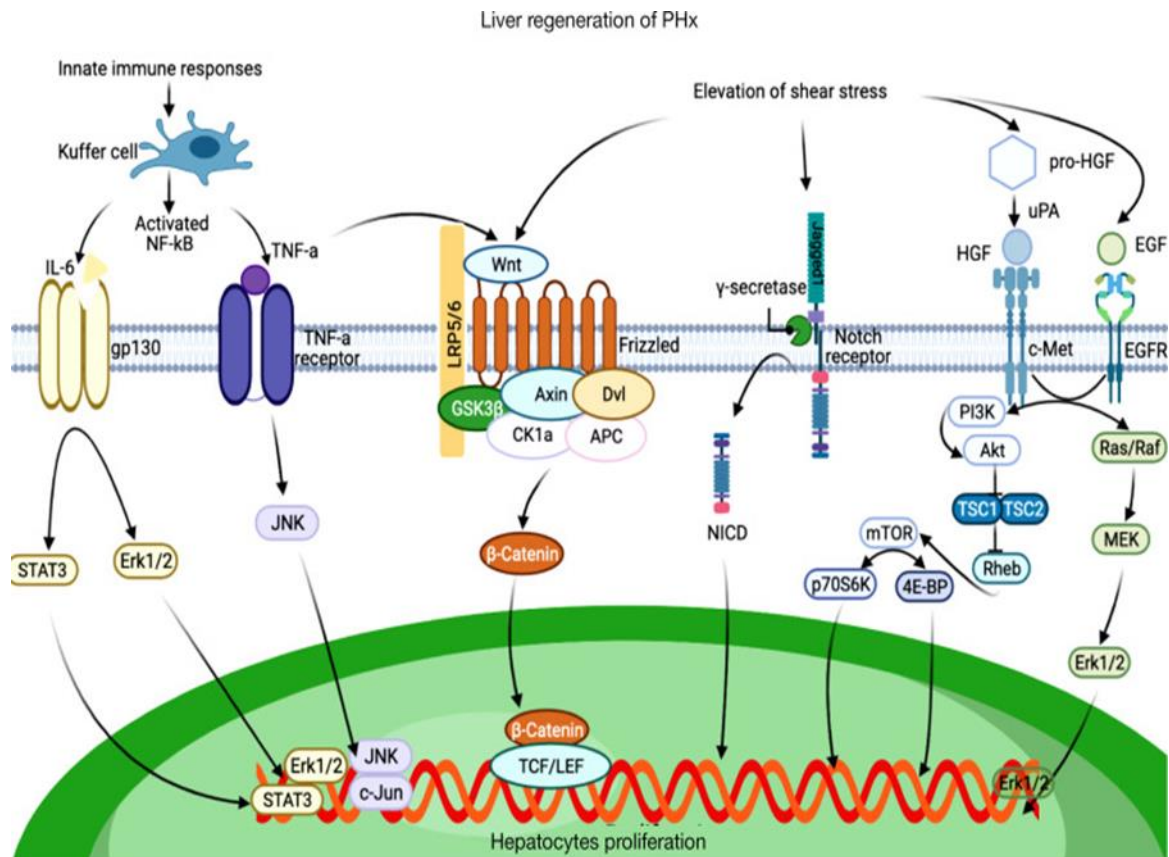
Figure 1. 3: Molecular Mechanisms in Liver Regeneration Following Partial Hepatectomy (PHx)

Figure 1.3 from Huang et al., 2021, illustrates the network of cytokines, growth factors, and signaling pathways involved in the process of liver regeneration after Partial Hepatectomy (PHx).

1.8 Molecular signals initiating liver regeneration.

HGFR and EGFR provide crucial signals for liver regeneration, as evidenced in a study by Zhang et al.,2018. HGFR and EGFR play complementary roles in initiating and promoting liver regeneration (Borowiak et al., 2004; Michalopoulos & Bhushan, 2020). These receptors are activated in response to specific growth factors (e.g., HGF for HGFR and EGF for EGFR), and their activation leads to the stimulation of signaling pathways that promote hepatocyte proliferation, tissue repair, and ultimately, liver regeneration (Michalopoulos, 2007). The coordination of these molecular signals is essential for successful liver regeneration and the maintenance of liver homeostasis (Michalopoulos, 2007). Understanding these signaling pathways and their regulation is important for developing strategies to enhance liver regeneration in cases of liver injury or disease.

1.8.1 HGF

Hepatocyte Growth Factor is a factor that induces morphogenic and angiogenic effects in a paracrine manner (Borowiak et al., 2004). The HGFR, also known as C-met, is a receptor that specifically binds to HGF. It is highly expressed on both parenchymal and nonparenchymal cells in the liver (Borowiak et al., 2004). The extracellular matrix of various organs contains an inactive form of HGF (Borowiak et al., 2004). A study conducted by Appasamy et al. (1993) has demonstrated a notable prevalence of HGF in the liver in comparison to other organs (Appasamy et al., 1993). The injection of HGF in the portal vein leads to liver expansion in normal rodents (Takahashi et al., 1995). Previous studies have indicated that the activation of C-met in cultures of hepatocytes leads to a significant mitogenic response and clonal expansion (Borowiak et al., 2004).

The activation and subsequent release of hepatocyte growth factors occurs within a timeframe of 30 minutes to 1 hour after partial hepatectomy (PHx), stimulated by uPA (Ding et al., 2010). Upon release, the active hepatocyte growth factors (HGFs) bind to their corresponding receptors located on the surface of hepatocytes. This binding event triggers the upregulation of cyclins and CDKs, ultimately resulting in a robust hepatocyte response (Huh et al., 2004). In response to hepatocyte activation and proliferation, proliferating endothelial and HSCs synthesize newly formed HGFs, resulting in a significant increase in HGF levels and subsequent rapid cellular expansion (Huh et al., 2004).

1.8.2 EGFR signaling

Endocytic sorting partially governs the regulation of EGFR signaling (Sorkin & Von Zastrow, 2009). After binding with a ligand, the EGFR is internalized and transported to the endosome. The stability of the ligand/EGFR complex and the ubiquitination process mediated by cbl family proteins are crucial factors in the degradation or recycling of EGFR (Sorkin & Von Zastrow, 2009). This has been previously reported in literature (Sorkin & Von Zastrow, 2009).

The EGFR pathway in the liver is an area of focus for researchers. According to the findings, EGFR is significantly present in the adult liver, as well as during developmental and regenerative stages, suggesting its essential functional importance (Komposch & Sibilia, 2015). The EGFR signaling pathway can be activated by various EGF receptor ligands, such as amphiregulin, EGF, HB EGF, betacellulin, epiregulin, and TGF-α (Singh & Harris, 2005). In both paracrine and autocrine signaling models, distinct functional variances are displayed by EGFR ligands (Singh & Harris, 2005). Some ligands such as EPGN, EGF, and HB-EGF in this group can generate strong mitogenic signals in the liver (Harris et al., 2003; Mehta & Besner, 2007). The specificity of these ligands for EGFR over other ErbB proteins, which can

form dimers with EGFR, has not been clearly established (Singh & Harris, 2005). Certain ligands like EGF and TGF-α are believed to have a significant impact on liver regeneration (Luetteke et al., 1999).

The activation of EGFR is commonly associated with four main downstream pathways: Ras/MAPK, PI3K/Akt, Stats, and phospholipase C-gamma 1 (PLCY1) pathways (Schlessinger, 2000). It is important to note that several studies have shown that the activation of EGFR through ligands in vitro can result in different downstream signaling pathways depending on the binding affinity of the ligands in various types of epithelial cells (Miaczynska et al., 2004). High affinity ligands, which constitute only 10% of the epidermal growth factor receptor (EGFR) pool, are responsible for activating the Ras/MAPK and PI3K/Akt pathways (Roepstorff et al., 2009). On the other hand, low affinity ligands, which make up 90% of the EGFR pool, have been found to induce the Stats and PLCY1 pathways (Roepstorff et al., 2009). When activated, the intracellular domain of the epidermal growth factor receptor (EGFR) can serve as a binding site for Src homology 2 (SH2) domains, specifically those of growth factor receptor-bound protein 2 (Grb2) and SHC adaptor protein (Shc) (Schlessinger, 2000). Grb2 or Shc proteins interact with Ras, subsequently leading to an interaction with Raf. This interaction ultimately triggers the activation of the entire MAP kinases pathway.

Furthermore, in the liver, the activation of EGFR-dependent Stats occurs independently of JAK kinase activation, which is contrary to the usual pattern. Stats may be consistently linked to EGFR and activated through direct phosphorylation by EGFR (Gu et al., 2020). In recent studies, it has been suggested that the Src-kinase may activate Stats by means of EGFR activation. The exact process by which PLCY1 is activated is not yet fully understood. However, current evidence suggests that PLCY1 is linked to EGFR and does not require tyrosine phosphorylation for activation. Upon activation, PLCY1 will generate two secondary

messengers, namely 1,2-diacylglycerol (DAG) and inositol 1,4,5-triphosphate (IP3) (Rhee, 2001). Activation of protein kinase C (PKC) can be facilitated by DAG, while Ca^{2+}-dependent pathways can be activated by IP3, as reported in a previous study.

1.9 EGFR Ligands

Epidermal growth factor receptor ligands are peptide growth factors that bind to and activate EGFR, a receptor tyrosine kinase involved in various cellular processes (Yarden & Sliwkowski, 2001). There are seven main EGFR ligands, namely, Epidermal growth factor (EGF), TGF-α, Heparin-binding EGF (HB-EGF), betacellulin, amphiregulin (AREG), Epiregulin (EREG), and Epigen (EPGN). These ligands differ in their expression, affinity, kinetics, and function. In this study, our focus will be directed towards the ligand TGF-α due to its unique attributes and interactions with EGFR.

1.9.1 TGF-α

The *TGFA* gene encodes for the protein known as transforming growth factor alpha (TGF-α) in humans (Machida et al., 1999). According to sources, TGF-αlpha is a significant growth factor in liver regeneration as it directly induces DNA synthesis in hepatocytes (Harada et al., 1999; Hoffmann et al., 2020). TGF-α is a polypeptide consisting of 50 amino acids that attach to the EGFR (Derynck, 1990). TGF-α is said to be produced in various types of cells. While a number of cell types, including hepatocytes and immune cells, can produce TGF alpha, the overall contribution of each cell type is unclear (Mead & Fausto, 1989). TGF-α is thought to have a significant role in cell proliferation and differentiation through an autocrine mechanism. It has been found that it has a sequence homology of 35% and a similar range of biological

activities as EGF. Cell proliferation of liver parenchymal cells also involves TGF-α (Harada et al., 1999; Mead & Fausto, 1989).

Membrane-bound TGF-α can be released from the cell membrane via cleavage by a protease called ADAM17 (also known as TACE) (Li et al., 2007). The activation of EGFR can be achieved by soluble forms and membrane bound forms of TGF-α that are produced through cleavage. Dimerization of EGFR is initiated by the binding of TGF-α, which leads to the phosphorylation of a protein-tyrosine kinase (Harris et al., 2003). EGFR undergoes autophosphorylation due to the activity of protein-tyrosine kinase, which affects the activation and signaling of other proteins involved in various signal transduction pathways (Brown, 1995; Citri & Yarden, 2006). The presence of TGF-α and its mRNA has been observed in both parenchymal and nonparenchymal cells of the liver in experimental animals (Hadjittofi et al., 2021). However, their occurrence in the human liver has not been extensively studied. Previous studies have examined TGF-α and its mRNA in various organs of experimental animals during their development, as referenced in (Hoffmann et al., 2020; Mead & Fausto, 1989). TGF-α expression has been observed during rat liver development in prior research. The investigation of TGF-α and its receptor expression in human liver development has been limited. The relevance of TGF alpha produced by liver-resident immune cells is currently unknown.

1.9.2 Amphiregulin

Amphiregulin (AREG), characterized by approximately 84-amino acid structure, serves as a pivotal regulator of cellular behavior through its interactions with the EGFR and human epidermal growth factor receptor 2 (HER2) on the cell membrane (Shoyab et al., 1989). AREG's structural configuration encompasses amino acid sequences that adopt a three-dimensional conformation, allowing for precise binding to the EGFR (Higashiyama et al.,

2008a). This interaction is facilitated by glycan residues attached to the protein, enhancing its affinity for the receptor and thereby initiating intracellular signaling cascades (Zaiss et al., 2015).

AREG exhibits a dynamic expression profile, with its synthesis and secretion being attributed to various cell types, including epithelial cells, fibroblasts, and immune cells (Schneider & Wolf, 2009). The expression of AREG can be modulated in response to a range of extracellular stimuli, such as growth factors, hormones, and tissue injury (Plowman et al., 1990). This adaptability underscores AREG's versatility in orchestrating a myriad of biological processes.

Upon interaction with EGFR, AREG activates downstream signaling pathways that hold central importance in regulating cell proliferation, growth, and survival. AREG's capacity to stimulate cell division is fundamental for tissue development, maintenance, and repair.

In the context of tissue injury, AREG plays a critical role in promoting cell migration and proliferation at the injury site, thus expediting tissue regeneration and the restoration of tissue integrity (Cook et al., 1997). Specifically, AREG's involvement in liver regeneration is noteworthy. In the liver, AREG is released in response to injury, and it stimulates the proliferation of hepatocytes, the main functional cells of the liver. This acceleration of hepatocyte division is crucial for the rapid restoration of liver tissue following damage, ensuring the organ's functional recovery.

In addition to its role in cell proliferation and tissue repair, AREG is a key player in guiding epithelial cell differentiation (Zaiss et al., 2013). Epithelial cells are essential for maintaining the structural and functional integrity of various tissues, including the skin, gastrointestinal tract, and respiratory system. Through EGFR activation, AREG influences the differentiation of epithelial cells, ensuring proper tissue architecture and function.

Beyond its involvement in cell growth and tissue repair, AREG exerts a regulatory influence on immune responses. It can modulate the behavior of immune cells and their interactions with other cell types, thereby shaping the immune landscape within tissues (Zaiss et al., 2013). This multifaceted role highlights AREG's significance in orchestrating diverse biological processes, ultimately contributing to tissue homeostasis and immune regulation.

1.9.3 Heparin-Binding Epidermal Growth Factor

Heparin-Binding Epidermal Growth Factor or HB-EGF, is a biologically significant protein consisting of approximately 87 amino acids (Mehta & Besner, 2007). Structurally, it possesses distinct domains that facilitate its binding to heparin, a glycosaminoglycan molecule (Mehta & Besner, 2007). This interaction with heparin serves as a crucial modulator of HB-EGF's activity and has profound implications for its binding to the Epidermal Growth Factor Receptor (EGFR) (Dao et al., 2018; Umata, 2004).

Upon binding to EGFR, HB-EGF initiates a complex cascade of intracellular signaling events. This cascade encompasses the activation of various kinases and transcription factors, ultimately leading to a plethora of cellular responses (Dao et al., 2018; Umata, 2004). These responses play a pivotal role in regulating cell behavior and function.

One of the central functions attributed to HB-EGF is its remarkable capacity to stimulate cell growth and proliferation (Umata, 2004). This influence extends to a diverse array of cell types, encompassing epithelial cells and specific immune cells. Through the activation of intricate signaling cascades within these cells, HB-EGF effectively promotes their expansion and multiplication, thereby contributing significantly to tissue growth and maintenance (Mehta & Besner, 2007).

Notably, HB-EGF emerges as a key protagonist in various tissue repair processes, with particular prominence in skin and gastrointestinal tract regeneration (Yamamoto et al., 2020). During wound healing, HB-EGF plays an instrumental role by facilitating the migration and proliferation of skin cells, thereby aiding in the restoration of damaged tissue (Dao et al., 2018; Umata, 2004). Furthermore, within the gastrointestinal system, HB-EGF actively supports mucosal repair and regeneration, ensuring the integrity and functionality of the digestive tract (Yamamoto et al., 2020).

In addition to its roles in tissue repair, HB-EGF exhibits a vital function in angiogenesis, the intricate process of new blood vessel formation (Chalothorn et al., 2005). This process holds paramount importance in various physiological and pathological conditions, encompassing wound healing, tumor growth, and cardiovascular diseases.

1.9.4 Epidermal Growth Factor

Epidermal Growth Factor (EGF) is a 53-amino acid protein characterized by the presence of three disulfide bonds crucial for maintaining its structural stability (Harris et al., 2003). EGF exerts its biological effects through binding to EGFR located on the cell surface, which initiates a cascade of intracellular signaling pathways.

In terms of cell biology, EGF plays pivotal roles in various cellular processes. Firstly, it promotes cell proliferation, a fundamental process in growth and tissue repair (Luetteke et al., 1999). Additionally, EGF influences cell differentiation, which is the process by which cells acquire specialized functions (Schlessinger et al., 2000). Moreover, EGF facilitates cell migration, particularly essential in processes like wound healing (Avraham & Yarden, 2011). Furthermore, EGF exhibits anti-apoptotic effects, effectively inhibiting programmed cell death (Luetteke et al., 1999).

Physiologically, EGF serves as a linchpin in embryonic development, significantly contributing to the formation of vital organs during this critical phase (Luetteke et al., 1999). Furthermore, in postnatal life, EGF plays a crucial role in wound healing, expediting the regeneration of skin and other tissues (Harris et al., 2003). Additionally, EGF is instrumental in tissue repair and regeneration following injury, demonstrating its importance in maintaining tissue integrity and function (Luetteke et al., 1999).

1.9.5 Betacellulin

Betacellulin (BTC) is a compact polypeptide composed of 80 amino acid residues. Its structural uniqueness underpins its capacity to bind to and activate EGFR, alternatively known as ErbB1 or HER1 (Yarden & Sliwkowski, 2001). Upon binding, BTC induces receptor dimerization, a pivotal event wherein two EGFR molecules associate, thereby facilitating the autophosphorylation of tyrosine residues within the receptor's intracellular domain (Carpenter & Cohen, 1979; Yarden & Sliwkowski, 2001).

BTC can stimulate diverse cellular processes, including cell proliferation, motility, and tissue regeneration (Roskoski, 2014). However, in certain contexts characterized by dysregulated EGFR signaling, such as cancer, BTC's involvement can foster disease progression (Singh & Harris, 2005). Dysregulation often occurs through mechanisms such as EGFR mutations or BTC overexpression, which can precipitate uncontrolled cellular growth and tumor formation (Singh & Harris, 2005).

BTC also plays a pivotal role in various physiological processes, notably in embryonic development, tissue regeneration, and homeostasis maintenance (Dunbar & Goddard, 2000). During embryogenesis, BTC assumes a particularly critical role in the intricate orchestration of tissue and organ development (Dunbar & Goddard, 2000).

1.9.6 Epiregulin

Epiregulin or EREG, constitutes a small, secreted protein displaying structural homology with other members of the EGFR family. This protein encompasses a conserved EGF-like domain, chiefly responsible for its binding affinity to EGFR (Odell et al., 2022). EREG plays a pivotal role as a growth factor, pivotal in triggering cellular growth and proliferation mechanisms (Cheng et al., 2021).

Upon binding to the EGFR, EREG activates a cascade of intracellular signaling pathways with profound implications on cellular behavior. These pathways are highly context-dependent and can culminate in cell division, cell survival, or differentiation (Zhang et al., 2007). EREG's multifaceted role extends to various physiological processes, encompassing embryonic development and tissue repair (Higashiyama et al., 2008).

EREG plays a critical role in the development and maintenance of epithelial tissues, including the epidermis and the mucosal lining of the gastrointestinal tract (Odell et al., 2022). Moreover, EREG is involved in mediating inflammatory responses, as it can be synthesized by immune cells and epithelial cells in response to inflammatory cues or tissue injury (Knight et al., 2012). In these contexts, EREG exerts its function by promoting tissue regeneration and repair processes (Komposch & Sibilia, 2015).

However, it is noteworthy that, akin to other growth factors, the production and activity of EREG are under stringent regulatory control within the body. This regulatory mechanism ensures the maintenance of proper cellular functions (Cheng et al., 2021; Odell et al., 2022).

1.9.7 Epigen

When epigen (EPGN) binds to EGFR, it induces receptor dimerization (pairing of two EGFR molecules) and activation of the receptor's intrinsic tyrosine kinase activity (Roepstorff et al., 2009). This leads to the autophosphorylation of tyrosine residues in the receptor's cytoplasmic domain, initiating downstream signaling cascades (Harris et al., 2003).

The downstream signaling pathways activated by EGPN play crucial roles in regulating cellular processes (Singh & Harris, 2005).

The activation of EGFR by EPGN and other ligands is tightly regulated, as dysregulation can lead to uncontrolled cell growth and contribute to the development and progression of various cancers (Harris et al., 2003).

1.10 Cells involved in liver regeneration

1.10.1 Hepatocytes

Hepatocytes, constituting approximately 60-70% of the total cellular population and occupying around 80% of the liver's overall volume, represent the predominant parenchymal cell type within the hepatic tissue (Jungermann & Kietzmann, 1996; Michalopoulos, 2007). These highly specialized cells play a pivotal role in a multitude of crucial physiological processes.

Positioned radially within the liver lobule, hepatocytes are in close proximity to sinusoids and capillaries, a strategic arrangement facilitating efficient interaction with the bloodstream. This spatial configuration optimizes the liver's ability to effectively perform its diverse functions by enabling the processing and filtration of blood as it courses through the lobule (Jungermann & Kietzmann, 1996).

Morphologically, hepatocytes are characterized by the presence of one or occasionally two centrally located round nuclei enveloped by a cytoplasmic matrix. This cytoplasm is replete with various organelles including mitochondria, endoplasmic reticulum, and Golgi apparatus, indicative of the cell's proficiency in executing a wide array of metabolic and synthetic functions (Jungermann & Kietzmann, 1996; Michalopoulos, 2007).

Remarkably, hepatocytes possess a robust regenerative capacity. Following injury or surgical resection, the remaining hepatocytes can rapidly proliferate and regenerate the lost tissue. This regenerative ability is crucial for the liver's capacity to recover from injuries and uphold its functionality (Michalopoulos, 2007).

1.10.2 Non-parenchymal cells

1.10.2.1 *Kupffer Cells (KCs)*

The hepatic Kupffer cells (KCs), being the resident macrophage in the liver, constitute the most extensive populace of resident tissue macrophages within the organism (Davies et al., 2013). Initially coined as "sternzellen" by Karl Wilhelm von Kupffer in 1876, Kupffer cells were initially believed to be a constituent of the liver blood vessel's endothelium.

Kupffer cells are known to be a crucial component of the innate immune response (Bilzer et al., 2006a). Their strategic positioning in the hepatic sinusoid enables them to effectively carry out the process of phagocytosis of various pathogens such as bacteria, bacterial endotoxins, viruses, and endogenous or foreign proteins that enter the liver through the portal or arterial circulation (Hritz et al., 2008). The production of various inflammatory, growth-mediated, vasoactive and chemotactic molecules, including TNFa and IL-6, is a significant function of KCs (Wan et al., 2014). These cells are considered the primary phagocytic agents of the reticular-endothelial system, which is now more accurately referred to as the mononuclear

phagocytic system (Sternberger, 1979). As a result, they are crucial for the liver's innate immunological functions as well as in liver regeneration (Knolle & Thimme, 2014).

1.10.2.2 *Hepatic Stellate Cells (HSCs)*

Hepatic stellate cells (HSCs), residing within the perisinusoidal space, also known as the space of Disse, are a specialized subtype of pericytes in the liver (Friedman, 2008). Their location places them in close proximity to hepatocytes and liver sinusoidal endothelial cells (LSECs), making them integral components of the liver microenvironment. HSCs are known for their distinctive morphology, characterized by a tapered body shape with oval-shaped nuclei. Importantly, these cells contribute significantly to the formation and maintenance of the hepatic basement membrane through the secretion of various extracellular matrix components such as laminin, proteoglycans, and type IV collagen (Friedman, 2008).

In the context of liver regeneration, HSCs play a pivotal role due to their strategic location near hepatic blood vessels. This positioning enables them to promptly respond to signals emanating from damaged liver tissue (Tsuchida & Friedman, 2017). The synthesized collagen provides structural support and aids in the formation of scar tissue, which is essential for wound closure and the restoration of tissue integrity. Additionally, glycoproteins contribute to the adhesive properties of the extracellular matrix, facilitating cell migration and tissue reorganization, further enhancing the regenerative process (Kisseleva & Brenner, 2021).

1.10.3 Liver resident immune cells

The human liver includes a variety of resident immune cells, which exhibit a wide range of diversity and consist of multiple subsets that display unique immunological roles (Crispe, 2014;

Thomson & Knolle, 2010) These distinct subpopulations comprise conventional T lymphocytes, B lymphocytes, innate NK cells, and mononuclear phagocytes (Crispe & Bigorgne, 2010). Recent scientific reports have identified the existence of Liver resident T cells, Liver resident NK cells, and macrophages that exhibit significant distinctions in comparison to those present in circulation (Peng et al., 2015).

Resident immune cells are present in the hepatic sinusoids and the space of Disse (Jenne & Kubes, 2013; Ohtani, 1988). Although various immune cell populations, such as Kupffer cells, have been identified in the liver, a comprehensive understanding of the complete spectrum of immune cells within the liver is still lacking, necessitating further research (Krenkel & Tacke, 2017; Kubes & Jenne, 2018).

The liver's immune cell population is composed of four distinct groups, including liver myeloid immune cell populations like dendritic cells, macrophages, and myeloid-derived suppressor cells (MDSC) (Krenkel & Tacke, 2017). Additionally, there are liver lymphoid immune cell populations such as NK cells, NK T cells, mucosal associated invariant T cells, and populations of CD1d-restricted invariant NKT cells (Peng et al., 2015). Hematopoietic progenitor cell populations and immune-regulating liver non-hematopoietic cell populations like HSCs and LSECs are also present (Gentek et al., 2014). Liver-resident cells play a vital role in regulating inflammation and maintaining organ homeostasis in a healthy adult liver (Lalor et al., 2002).

1.10.3.1 *Natural Killer (NK) Cells*

Natural Killer (NK) cells are a type of lymphocyte that belongs to the same family as T and B cells, originating from a shared progenitor (Cooper et al., 2001; Vivier et al., 2008). As a constituent of the innate immune system, NK cells exhibit rapid responses to diverse pathological stimuli (Vivier et al., 2008). Natural killer cells are primarily recognized for their

ability to eliminate cells that have been infected with viruses, as well as for their capacity to identify and regulate the initial stages of malignant tumor development (Cooper et al., 2001; Vivier et al., 2008). In addition to conferring immunity against pathogens, distinct natural killer cells are present in the placenta and potentially exert significant influence on gestation (Vivier et al., 2008).

NK cells were initially observed for their spontaneous cytotoxicity towards tumor cells, which does not require any prior activation or priming, unlike cytotoxic T cells that necessitate priming by antigen-presenting cells (Shimasaki et al., 2020; Vivier et al., 2011). They are designated based on their ability to perform this natural form of predation (Vivier et al., 2008). Furthermore, natural killer cells release cytokines, including IFNγ and TNFα, that stimulate the immune response of other cells such as macrophages and dendritic cells (Vivier et al., 2008).

Natural Killer cells can be categorized based on their expression of CD56 into two distinct subsets, namely CD56^{Bright} and CD56^{Dim} (Cooper et al., 2001). CD56^{Bright} NK cells are analogous to T helper cells in their ability to exert their effects through the secretion of cytokines (Cooper et al., 2001). The CD56^{Bright} subset of NK cells is the predominant population of NK cells, distributed across various anatomical sites such as bone marrow, secondary lymphoid tissue, liver, and skin (Cooper et al., 2001). The presence of hepatic NK cells was initially identified through electron microscopy of rat liver and subsequently referred to as "pit cells" (Cooper et al., 2001).

CD56^{Dim} NK cells are predominantly present in the peripheral blood. The CD56^{Dim} NK cells constitute a significant proportion of up to 90% of all NK cells present in the peripheral blood and spleen (Cooper et al., 2001). The CD56^{Dim} subset of natural killer cells consistently

expresses the CD16 receptor, which plays a crucial role in facilitating antibody-dependent cellular cytotoxicity (Cooper et al., 2001).

Liver NK cells have been extensively compared to peripheral blood NK cells, highlighting variations in activation status, cytotoxicity, and maturation (Cooper et al., 2001; Vivier et al., 2008). The activation of liver NK cells surpasses that of other tissues, as demonstrated by their elevated expression of the activation marker CD69, along with heightened levels of perforin and granzyme B (Vivier et al., 2008). As a result, there is an observed increase in cytotoxicity in comparison to NK cells found in peripheral blood (Vivier et al., 2008). The subset of CD56^{Dim} NK cells in the liver displays similarities to the circulating NK cell population in the peripheral blood (Vivier et al., 2008). Scientific discoveries suggest that there are significant distinctions between liver CD56^{Bright} NK cells and circulating NK, which implies the existence of a distinct liver-resident NK cell population referred to as liver-resident NK (Vivier et al., 2008). This population exhibits dependence on the chemokine receptor CXCR6 (Vivier et al., 2008). The current understanding of the development and differentiation of liver-resident NK cells is limited (Cooper et al., 2001; Vivier et al., 2008). The identification of cells representing various developmental stages of NK cells in the adult human liver suggests that the liver may serve as a site for differentiation of liver-resident NK cells and recruitment of NK cell precursors from peripheral blood (Vivier et al., 2008). The observation of distinct cell populations corresponding to different developmental phases of NK cells within the hepatic tissue of adult humans implies that the liver could potentially function as a location for the maturation of liver-resident NK cells and the attraction of NK cell progenitors from the peripheral blood (Cooper et al., 2001; Vivier et al., 2008).

1.11 Hypothesis

We hypothesise that liver resident natural killer (NK) cells possess the capacity to express TGF-α, and that co-culture of peripheral blood NK cells with hepatocytes is sufficient to induce TGF-α expression. We hypothesise that crosstalk between liver-resident NK cells and hepatocytes provide proliferative signals to hepatocytes, thereby contributing to liver regeneration.

1.12 Aim and Specific objectives.

1.12.1 Aims

I. To determine whether co-culture in the presence of hepatocytes induces TGF alpha expression in NK cell populations.

II. To determine whether NK cell-derived TGF alpha regulates hepatocyte proliferation.

1.12.2 Specific objectives

I. To define what EGFR ligands are expressed by liver-resident NK cells.

II. To determine whether 3D hepatocyte and immune cell co-culture results in an up-regulation of transforming growth factor alpha by immune cells.

III. To assess the ability of transforming growth factor alpha to modulate hepatocyte growth and proliferation in 3D models.

Chapter 2   Materials And Methods

2.1 Materials

Table 2. 1 Flow Cytometry Conjugated Antibodies

Antibody	Fluorochrome	Clone	Catalogue	Company
CD69	PE-Vio770	REA824	130-112-615	Miltenyi Biotec
CD45	Red Fluor710	H130	80-0459-T100	Tonbo Bioscience
CD56	BV711	NCAM16.2	563169	BD Bioscience
CD56	Vio Bright FITC	AF12-7H3	130-113-309	Miltenyi Biotec
CD3	VioBlue™	REA613	130-114-519	Miltenyi Biotec
CD3	APC	REA613	130-113-135	Miltenyi Biotec
CD16	VioGreen™	REA423	130-113-397	Miltenyi Biotec
CD16	PE	REA423	130-113-393	Miltenyi Biotec
CXCR6	APC	KO41E5	356006	Biolegend
CD14	APC	61D3	20-0149-T100	Tonbo Bioscience
Rat Anti-Mouse	FITC	-	MA5-16796	Invitrogen

Table 2. 2 Kits

Item	Catalogue	Company	Supplier
Comp Bead Kit	130-104-693	Miltenyi Biotec	Miltenyi Biotec
MojoSort™ Human NK Cell Isolation Kit	480054	Biolegend	Biolegend
LunaScript® RT Supermix Kit	10155444	New Legend Biolab	New Legend Biolab
Human TGF-α ELISA Kit	EHTFA	Invitrogen	Thermo Fisher Scientific
Zombie NR™ Fixable Viability Kit	423106	Biolegend	Biolegend
PureLink™ RNA Micro Kit	12183-016	Invitrogen	Thermo Fisher Scientific

Table 2. 3 Human Cell Lines

Cell Line	Cell Type	Tissue	Disease	Company
HepG2	Epithelial-like	Liver	HCC	ATCC
Huh7	Epithelial-like	Liver	HCC	ATCC

Table 2. 4 Cytokines and Functional Antibodies

Item	Clone	Catalogue	Company
TGF-α Monoclonal Antibody	IE8-G6	MA5-33316	Invitrogen
Human Recombinant Antibody	10016A	-	Peprotech
Human IL-15	-	130-095-764	Miltenyi Biotec

Table 2. 5 TaqMan Gene Expression Assays

Item	Catalogue	Company	Supplier
B2M	Hs99999907	Applied Biosystem	Thermo Fisher Scientific
HPRT1	Hs99999909	Applied Biosystem	Thermo Fisher Scientific
CSF2	Hs00929873	Applied Biosystem	Thermo Fisher Scientific
VEGFA	Hs00900055	Applied Biosystem	Thermo Fisher Scientific
MYC	Hs00153408	Applied Biosystem	Thermo Fisher Scientific
G6PD	Hs00166169	Applied Biosystem	Thermo Fisher Scientific
HIF1A	Hs00153153	Applied Biosystem	Thermo Fisher Scientific
ALB	Hs00609411	Applied Biosystem	Thermo Fisher Scientific
SREBF1	Hs01088691	Applied Biosystem	Thermo Fisher Scientific
AFP	Hs00173490	Applied Biosystem	Thermo Fisher Scientific
EGFR	Hs01076090	Applied Biosystem	Thermo Fisher Scientific
TGFA	Hs00608187	Applied Biosystem	Thermo Fisher Scientific
ADAM17	Hs01041915	Applied Biosystem	Thermo Fisher Scientific
TNFA	Hs00174128	Applied Biosystem	Thermo Fisher Scientific

Table 2. 6 Equipment/ Software

Equipment/ Software	Model	Company
Inverted Microscope	Inverted CKXS3	Olympus
Automated Cell Counter	Countess II	Thermo Fisher Scientific
Haemocytometer	Improved Neubauer	Baxter Scientific
CO_2 Incubator	Forma Steri-cycle	Thermo Fisher Scientific
Water Bath	SWB Series	Stuart
Biological Safety Cabinet Class II	Nuaire	Bender Med Systems
Biological Safety Cabinet Class II	Airstream	ESCO
Centrifuge	Sorrall ST40	Thermo Fisher Scientific
Centrifuge	AccuSpin Micro 17R	Fisher Scientific
Flow Cytometer	BD Accuri™ C6	BD Biosciences
Flow Cytometer	Attune NxT	Life Technologies
Microplate Reader	Clariostar	BMG Lab Tech
NanoDrop Spectrometer	NanoDrop 2000	Thermo Fisher Scientific
-80 Freezer	Ultra Low Temperature Freezer	New Brunswick Scientific
Thermal Cycler	MiniAmp Plus	Thermo Fisher Scientific
Real Time qPCR	StepOne Plus	Applied Biosystem
FlowJo	v10.7.1	Treestar Incorporated
GraphPad Prism	Prism 9	GraphPad Software Inc.

Table 2. 7 Plasticware and General Lab Consumables

Item	Catalogue	Company
5 Ml Serological Pipettes	19220002	Fisher Scientific
10 Ml Serological Pipettes	193001	Fisher Scientific
25 Ml Serological Pipettes	27219011	Fisher Scientific
15 Ml Facon Tubes	62.554.502	Sarstedt
50 Ml Facon Tubes	62.559.001	Sarstedt
12 Well Tissue Culture Plate	36620002	Fisher Scientific
96 Well Tissue Culture (Treated) Plate	36220006	Fisher Scientific
96 Well Flat Bottom Tissue Culture (Treated) Plate	02721057	Fisher Scientific
$25cm^3$ Cell Culture Flask	690175	Greiner
$75cm^3$ Cell Culture Flask	658175	Greiner
Transfer Pasteur Pipette (3ml)	13469108	Fisher Scientific
Sterile Cell Strainer (70μm)	22363548	Sarstedt
Filtropur S	83.1826.001	Sarstedt
5 Ml Polystyrene Round Bottom Tube (Flow Tubes)	3520544	Fisher Scientific
50 Ml Luer Syringe	300866	BD Plastipak
Microamp Fast 96 Well Reaction Plates	4346907	Applied Biosystem
Microamp Optical Adhesive Film	4311971	Applied Biosystem
Multiply- Pro Cup (0.2ml) PCR Tubes	72.737.002	Sarstedt
1.5 ML Microcentrifuge Tubes	3457	Thermo Fisher Scientific
Countess Cell Counting Chamber Slide	100078809	Thermo Fisher Scientific

Table 2. 8 General Reagents

	Item	Catalogue	Company	Supplier
Media/ Buffers	Molecular Grade Water	SH30538.03	HyClone™	Cytiva
	DMEM (1X) GlutaMAX	61965-026	Gibco™	Thermo Fisher Scientific
	RPMI 1640 (1X) GlutaMAX	61870-010	Gibco™	Thermo Fisher Scientific
	Fetal Bovine Serum	F9665	Sigma-Aldrich	Merck
	Happy Cell Media	VHCDM	Vale Life Sciences	Vale Life Sciences
	Bovine Serum Albumin (BSA)	SH30574.02	HyClone™	GE Life Sciences
	Penicillin-Streptomycin	15140-122	Gibco™	Thermo Fisher Scientific
	Hank's Balanced Salt Solution (HBSS)	SH30588.02	HyClone™	Cytiva
	Permeabilization Buffer (10x)	00-8333-56	Invitrogen	Thermo Fisher Scientific
	Fixation/Permeabilization Concentrate	00-5123-43	Invitrogen	Thermo Fisher Scientific
	Fixation/Perm Diluent	00-5223-56	Invitrogen	Thermo Fisher Scientific
Chemicals	Chloroform	J67241	Alfa Aesar	Thermo Fisher Scientific
	Ethanol Solution (Molecular grade)	BP8202-500	Fisher Bioreagents	Thermo Fisher Scientific
	Isopropanol	327272500	ACROS ORGANICS™	Thermo Fisher Scientific
	TRIzol™ Reagent	15596018	Ambion	Thermo Fisher Scientific
	Trypsin EDTA	MFCD00130286	Sigma-Aldrich	Merck

	DNase I	DN25	Sigma-Alrich	Merck
	EDTA (Ultra Pure™ 0.5M EDTA)	15575-038	Invitrogen	Thermo Fisher Scientific
	2-Mercaptoethanol	102511391	Sigma-Aldrich	Merck
	Ficoll-Paque™ PLUS	17144003	Cytiva	Cytiva
	Ammonium Chloride	199970010	ACROS ORGANICS™	Thermo Fisher Scientific
	Potassium Hydrogen Carbonate	450640010	ACROS ORGANICS™	Thermo Fisher Scientific
Others	Glycogen	G1767-1VL	Sigma-Aldrich	Merck
	Happy Cell ® Inactivation Solution	VHCIS	Vale Life Sciences	Vale Life Sciences
	TLR Grade® LPS	ALX-581-013-L002	Enzo Life Sciences	Enzo Life Sciences
	Carrier RNA	4382878	Applied Biosystems	Thermo Fisher Scientific
	Luna® Universal Probe qPCR Master Mix	10170225	New England Biolabs	New England Biolabs
	7AAD	13-6993-T500	Tonbo Biosciences	Tonbo Biosciences
	FcR Blocking Reagent	130-059-901	Miltenyi Biotec	Miltenyi Biotec
	Precision Count Beads	424902	Biolegend	Biolegend

2.2 Methods

2.2.1 General Cell Culture

In order to model the human liver environment as part of the research objectives, two hepatocyte cell lines were selected for use, namely HepG2 cells and Huh-7 cells. The Huh-7 cell line is a well-established immortalized cell line that was originally derived from a hepatocellular carcinoma (HCC) tumour (Kawamoto et al., 2020). This cell line was obtained from a 57-year-old Japanese male patient in the year 1982 (Kawamoto et al., 2020). The HepG2 cell line is also an immortalized cell line that was derived from a human liver carcinoma (Kawamoto et al., 2020). The liver tissue used for deriving this cell line came from a 15-year-old Caucasian male patient who was diagnosed with hepatocellular carcinoma (Kawamoto et al., 2020). Both these cell lines were cultured in Dulbecco's Modified Eagle Medium (DMEM) supplemented with 10% fetal bovine serum (FBS), a vital source of essential nutrients. Cultures were incubated in a humidified incubator at 37°C with 5% CO_2. Regular subculturing was performed in order to maintain the viability of the cells and prevent excessive confluency. Upon reaching a confluency level of 70-80%, the cells underwent subculturing (approximately every 2-3 days). The process employed in this study involved the utilization of trypsinization, a well-established enzymatic dissociation technique commonly employed to separate cells from the culture medium. The assessment of cell viability and concentration was conducted employing either a haemocytometer or an automated cell counter. To avoid contamination, thorough aseptic precautions were taken throughout the cell culture processes. Sterilization was performed on all equipment, culture vessels, and reagents prior to use. Biosafety cabinets were used throughout the procedure to provide a sterile environment and protect the cells from potential contaminants.

2.2.2 3D Cell Culture Setup (Happy Cell® ASM 3D Culture Medium)

Happy Cell® ASM (Advanced Serum-free Medium) 3D Culture Medium is a specialized cell culture medium that has been developed to provide for optimal cell development and nourishment in three-dimensional (3D) culture systems (Koledova, 2017). The major goal of this system is to aid in the growth and functioning of complex multicellular forms such as organoids, spheroids, and tissue models in a laboratory setting.

The 4X Happy Cell (HC) medium was used at a 1X final concentration in DMEM. In order to establish the 3D cell culture, HepG2 cells were grown at the required density in 1X HC in a 15 mL falcon. The contents of the tube were mixed before being placed in a humidified incubator set to 37°C and a CO2 concentration of 5% to allow spheroid formation. This incubation period was maintained for the duration of the trial under consideration. During the co-culture experiments media was replenished to ensure sufficient nutrient. Every 2-3 days 20% of the cell culture media was removed and replaced with fresh DMEM supplemented with IL-15 at 2ng/mL. The medium exchange was carefully done to minimize interruption to the 3D culturing system.

2.2.3 Cell Viability and Image Analysis

2.2.3.1 *Trypan Blue Exclusion Test*

The Trypan blue cell viability assay represents a widely utilized technique within the field of biology to assess the vitality of cells present in various settings, encompassing both controlled laboratory cultures and natural biological specimens. This method capitalizes on the unique property of Trypan blue dye to differentiate between living and dead cells, a process achieved by preferentially coloring non-living cells. Specifically, Trypan blue penetrates cells

characterized by compromised membranes, typically those that are dead or in the process of dying, resulting in their distinct blue staining.

To conduct the trypan blue assay, we mixed a small volume of cell suspension, typically around 10ul, with an equivalent volume of Trypan blue in an Eppendorf tube to achieve a 1:2 dilution. The mixture of cells and Trypan blue is thoroughly homogenized by pipetting up and down. After, 10ul of this mixture is loaded into the counting chamber of a haemocytometer, allowing it to be drawn beneath the coverslip via capillary action. We then count viable cells using a microscope and a hand-held counter. The determination of viable cell percentage entails a calculation method based on quantifying unstained cells (considered viable) in relation to the total cell count, encompassing both stained and unstained populations. This calculation offers an estimate of the sample's cell viability.

2.2.3.2 *WST-1 proliferation assay*

In this study, the WST-1 proliferation assay was utilized to evaluate the rates of cellular proliferation. This colorimetric assay measures the reduction of WST-1 (a tetrazolium salt) by mitochondrial dehydrogenases present within metabolically active cells.

The assay was carried out in according to the instructions of the manufacturer. Briefly, cells were carefully distributed into 96-well plates at specific densities, as per the experimental requirements. Subsequently, the cells were subjected to the designated experimental treatments for further investigation. At the end of the treatment period a volume of 10 uL of WST-1 reagent was added into each well and incubated for an additional period of 20 to 30 minutes. Using a microplate reader, the absorbance was measured at a wavelength of 440 nm using a reference wavelength of 650 nm. To account for non-specific signals, the background absorbance from a blank well (containing medium with WST-1 reagent but no cells) was also analysed and

subtracted from all sample readings. The absorbance values obtained from the WST-1 assay were used to calculate cell viability and proliferation rates.

2.2.3.3 *Image J software analysis*

Image J software was employed to evaluate cell confluency. The image analysis encompassed a series of sequential steps. First, we conducted cell segmentation using a threshold-based segmentation methodology. This step effectively distinguished cell areas from the background in the acquired images. Furthermore, we employed particle analysis to precisely quantify the number of cells present in each image. The cell density was subsequently computed as the total cell count divided by the image area.

All numerical data generated through the ImageJ analysis were automatically exported to a spreadsheet via Microsoft Excel. These data were then subjected to statistical evaluation and used for graphical representation.

2.2.4 TRIzol RNA Extraction

RNA extraction from 2D cell culture experiments was performed utilising the TRIzol method. The procedure involved the cells being treated with 1 ml of TRIzol reagent, and then vigorously shaken to ensure complete cell lysis and homogenization. The homogenized samples were subsequently subjected to an incubation period of 5 minutes at ambient temperature in order to facilitate the complete dissociation of the nucleoprotein complexes. A total of 0.2 mL of chloroform was added to the homogenate and vigorously shaken for 15 seconds to facilitate phase separation. The samples were then incubated for 3 minutes at room temperature before being centrifuged at 12,000 g for 15 minutes at 4°C. This process facilitated the separation of

the mixture into three distinct phases: an upper aqueous phase, which appeared colourless and contained RNA; an interphase, which exhibited a red coloration and contained DNA; and a lower organic phase, which contained proteins and lipids. The aqueous phase (containing RNA) was transferred carefully to a new RNase-free tube, avoiding any interphase or organic phase carryover. To precipitate the RNA, 0.5 mL of isopropanol was added, and the tubes were gently inverted to mix the contents. It is crucial to acknowledge that in cases where RNA quantities were low, a volume of 1ul of glycogen (G1767, Sigma, with a concentration of 20 mg/mL) was introduced to each tube as an RNA carrier. After the introduction of isopropanol, the specimens underwent an incubation period of 10 minutes at room temperature, followed by centrifugation at a force of 12,000 xg for 10 minutes at a temperature of 4°C. This centrifugation step was performed in order to precipitate the RNA, resulting in its formation into a compact pellet. In order to eliminate any remaining impurities or salts, the RNA pellet underwent a washing procedure involving the use of 75% ethanol. Subsequently, the sample was subjected to centrifugation at a force of 8,000xg for a duration of 10 minutes at a temperature of 4°C. This centrifugation step was performed to ensure the complete removal of ethanol from the RNA pellet. The RNA pellet underwent a brief air-drying process prior to being resuspended in RNase-free water, resulting in the achievement of the ultimate RNA concentration. The assessment of both the quality and quantity of the extracted RNA was conducted by employing a Nanodrop spectrometer. The RNA samples that were obtained were subsequently preserved at a temperature of -80°C in order to maintain their integrity and stability for subsequent analysis.

2.2.5 Purelink™ RNA Mini Kit Extraction

The PureLink™ RNA Micro Kit is a commercially available kit used to isolate total RNA from a variety of samples. It employs a silica-based membrane technique that enables for the purification of RNA while eliminating impurities such as DNA and proteins. This column-based purification procedure was utilised to extract RNA from 3D culture samples due to the lower input of cells.

To extract RNA from 3D culture samples, the samples were homogenized using the given lysis buffer with 2-mercaptoethanol at a ratio of 10 μL 2-mercaptoethanol per 1 mL of lysis buffer. The cell suspensions were directly mixed with 350 μL of lysis buffer. Following the manufacturer's instructions, PureLink™ Carrier RNA was prepared and added to the mixture in the tubes. The tubes were vortexed at high speeds to ensure that the cell pellets were evenly distributed and that the cells were thoroughly lysed. The contents of the tubes were then homogenized by pipetting up and down gently. Homogenized samples were then incubated at room temperature for 5 minutes to allow for full lysis.

Following cell lysis, 350 uL of 70% ethanol was added to the lysates and vortexed to mix. The mixture was then transferred to the PureLink™ RNA Micro Kit spin column, which was inserted in a 2 mL collection tube, and centrifuged for 1 minute at 12,000 xg. The flow-through was discarded, and the column was reinserted into the collection tube.

The PureLink™ RNA Micro spin column was washed with 600 μL of Wash Buffer I and centrifuged at 12,000 × g for 15 seconds at room temperature. Following that, the column was washed twice with 500 μL of Wash Buffer II and centrifuged for 15 seconds each time at 12,000 xg. After, the spin column was centrifuged at 12,000 xg for a further 1 minute to remove any remaining ethanol.

The elution of purified RNA was achieved by introducing 22 uL of RNAse-free water into the central region of the column, followed by a 1-minute incubation period ambient temperature. Subsequently, the column was subjected to centrifugation for a duration of 2 minutes at a force of 12,000 x g in order to facilitate the separation and collection of the RNA molecules into a fresh recovery tube that had been treated to be free of any ribonucleases.

The concentration and purity of the extracted RNA were quantified using a Nanodrop spectrophotometer. Subsequently, the samples were stored at a temperature of -80°C for preservation and subsequent analysis.

2.2.6 cDNA Synthesis

The cDNA synthesis procedure was conducted using the LunaScript RT Supermix kit. This kit was employed to facilitate the conversion of RNA samples into complementary DNA (cDNA). This kit provides an extremely efficient and convenient reverse transcription technique that accurately represents the original RNA transcript levels.

Each sample mixture contained: 4 μL LunaScript RT Supermix, the specified amount of extracted RNA sample required (up to a maximum of 1μg), and nuclease-free water to bring the final reaction volume to 20 μL. The mixtures were prepared in 0.2 mL PCR tubes.

The reaction mixture underwent gentle vortexing and was subsequently subjected to a brief centrifugation step. A thermal cycler was used to carry out the cDNA synthesis reaction for 1 cycle at 25°C for 2 minutes of primer annealing and 55°C for 10 minutes of reverse transcription. To terminate the reverse transcription reaction and assure the stability of the produced cDNA for downstream applications, the reaction was heated to 95°C for 1 minute.

After the run was finished, all cDNA samples were diluted with 80uL of nuclease-free before being stored at -20°C.

2.2.7 Quantitative Polymerase Chain Reaction (qPCR)

The quantification of genes of interest was performed in this study using quantitative polymerase chain reaction. It facilitates the precise measurement of DNA or cDNA levels in real-time.

All qPCR assays were run on a qPCR machine (StepOne Plus model by Applied Biosystem). The reaction was carried out in a total volume of 10 µL. In each qPCR reaction, a standardized mixture was prepared, consisting of 5 microliters (µl) of Luna probe qPCR master mix, 0.5 µl of TaqMan probe, 1 µl of complementary DNA (cDNA) template, and 3.5 µl of molecular grade water. In order to ascertain the presence of any potential contamination, negative controls were incorporated into the experimental design. These negative controls consisted of molecular grade water, which served as a substitute for the cDNA samples. The cycling conditions employed for the polymerase chain reaction (PCR) were as follows: an initial denaturation step at a temperature of 95°C for a duration of 1 minute, followed by a series of 40 cycles of denaturation at the same temperature (95°C) for a duration of 15 seconds each. The annealing and extension steps were carried out at a temperature of 60°C for a duration of 30 seconds. The raw qPCR data was subjected to analysis using the ΔΔCt method (Livak & Schmittgen, 2001). The normalization of the target gene(s) expression levels was performed by referencing them to the expression levels of two reference genes (B2M and HPRT1). B2M and HPRT1 were selected as reference genes due to their established status as housekeeping genes, characterized by their consistent expression levels across diverse experimental conditions and tissues. This inherent stability renders them invaluable for the normalization of gene expression data,

ensuring the accuracy of quantitative analyses (Eisenberg & Levanon, 2013; Vandesompele et al., 2002). This approach was adopted to account for any potential variations arising from differences in cDNA loading and reverse transcription efficiency. The qPCR experiments were performed in duplicate at a minimum to ensure the reproducibility of the obtained results. The findings were presented in the form of fold change. quantitative polymerase chain reaction data was subjected to statistical analysis utilizing the GraphPad Prism software.

2.2.8 Processing Whole Blood Samples

2.2.8.1 *Isolation of PBMCs from Whole Blood*

The isolation of peripheral blood mononuclear cells (PBMCs) was performed utilised anonymous donor buffy coats, obtained from the Irish Blood Transfusion Service, Dublin, Ireland. The PBMC isolation process was carried out in a sterile atmosphere, with all equipment and reagents pre-warmed to room temperature. PBMCs were isolated from whole blood using density gradient centrifugation and Ficoll-Paque.

Briefly, buffy coats where mixed 1:1 with HBSS and were then layered on top of Ficoll-Paque PLUS in sterile 50 mL falcon tubes. The tubes were centrifuged at 400 g for 25 minutes at room temperature with the brake switched off. Following centrifugation, the PBMCs formed a distinct layer between the plasma and the Ficoll-Paque, which was carefully removed using a sterile Pasteur pipette and transferred to a new 50 mL centrifuge tube. The volume was adjusted with HBSS. The separated PBMCs were washed twice with HBSS to eliminate any leftover Ficoll-Paque and other impurities. During each wash step, the samples were then centrifuged at a speed of $300 \times g$ for 5 minutes. The centrifuge brakes were activated and set at a level of 9 to ensure proper separation and sedimentation of the components. After centrifugation, the supernatant was carefully removed without damaging the PBMC pellet, and the PBMCs were

resuspended in RPMI medium (containing 10% FBS and Penicillin-Streptomycin). The viability of isolated PBMCs was determined using the trypan blue exclusion test as described.

2.2.8.2 *Isolation of NK Cells from PBMCs*

Natural killer (NK) cells were isolated from freshly isolated PBMCs using a manual magnetic separation process based on the recognition and isolation of specific surface markers (MojoSort™ Human NK Cell Isolation Kit was used). PBMCs from peripheral blood were resuspended in flow buffer and deposited in 15 mL falcon tubes. The PBMCs were treated with a cocktail of biotin-conjugated antibodies that were specially tailored to target non-NK cell surface markers. After that, the cells were incubated for 15 minutes. After incubation, the tubes were washed with flow buffer and centrifuged for 5 minutes at 300 xg. Afterwards, the supernatants were removed, the cells were vortexed, and streptavidin-coated magnetic beads were added to the cell mixture for an additional 15 minutes of incubation on ice. Following that, the cells were washed again in flow buffer at 300 g for 5 minutes. After discarding supernatants and vortexing to resuspend the cell solution, the tubes were put on a magnetic separation column, and unlabelled NK cells that did not bind to the magnetic beads were collected in the flow-through fraction.

The unlabelled NK cell flow-through was collected and centrifuged at 300 g for 5 minutes at 4°C to produce the pellet. The trypan blue exclusion test was used to examine the viability of isolated NK cells as described.

2.2.9 Flow Cytometry

In this study, flow cytometry analyses were conducted using two distinct flow cytometers: the BD Accuri™ C6 and the Attune NxT. Specific details regarding the staining protocols and antibodies employed can be found in the respective study designs. For all cell washing and resuspension steps, a flow buffer was utilized, which was prepared by mixing HBSS with 0.5% BSA and 1 Mm EDTA. All samples were prepared in 5 mL polystyrene round bottom tubes, commonly referred to as flow tubes. To facilitate compensation adjustments, controls were prepared for CD56, CD3, and CD16 using compatible compensation beads.

2.2.10 Statistical Analysis

The data sets were subjected to statistical analysis using GraphPad Prism. The specific statistical test used for each figure is indicated in the corresponding legend. Normality tests were conducted on the data within each group to assess their distribution characteristics. The datasets were analyzed using parametric statistical tests, assuming a normal distribution. Data that did not exhibit a normal distribution underwent analysis using non-parametric statistical tests. In the analyses, symbols *, **, ***, and **** represent p-values of 0.05, 0.01, 0.001, and 0.0001, respectively. When analyzing matched samples, an appropriate paired data analysis method was employed.

Chapter 3 Liver Expression of TGF-α and The Response of Hepatocytes

3.1 Introduction

The human liver is a complex organ with diverse cell populations that play crucial roles in metabolism, detoxification, and immune responses (Kubes et al., 2018). Understanding the gene expression patterns within individual liver-resident cell types can provide valuable insights into the liver's physiological and pathological processes. One such gene of interest is *TGFA*, which encodes for the epidermal growth factor (EGF) ligand transforming growth factor alpha (TGF-α). TGF-α is known to have significant implications for cell proliferation, differentiation, and tissue repair (Michalopoulos, 2010).

Hepatocytes, the predominant cell type in the liver, show varying levels of *TGFA* expression, which might reflect their role in tissue regeneration and maintenance (Fausto & Campbell, 2003). Additionally, non-parenchymal cells such as Kupffer cells, endothelial cells, lymphoid cells, and stellate cells also contribute to the overall TGFA expression profile in the liver (Bissell et al., 1995; Schwabe et al., 2020).

Understanding the behavior of hepatocytes in response to TGF-α holds immense significance due to the central role of the liver in maintaining systemic equilibrium (Michalopoulos & DeFrances, 1997). The liver's regenerative capacity and the balance between hepatocyte proliferation and apoptosis are intricately regulated by growth factors, with TGF-α emerging as a pivotal player (Forbes et al., 2015). While gene knockout studies have implicated TGF-α in liver regeneration, the response of hepatocytes to TGF-α stimulation have not been exhaustively characterized.

Cell culture has been a cornerstone technique in the field of biology and biomedical research for decades (Griffith & Swartz, 2006). Two primary systems have emerged as the mainstays of cell culture research: two-dimensional (2D) and three-dimensional (3D) culture systems

(Hutmacher, 2010). The use of a 2D in vitro cell culture system is a conventional approach involving a flat support structure to facilitate the growth of cells in a monolayer. The system is well-established in the history of research, dating back to the early 1900s, where it has been predominantly used in the co-culturing of diverse cell types (Vinci et al., 2012).

However, as the understanding of the concept of the cell microenvironment has advanced, it has become clear to researchers that the physiological state and activity of cells in 2D culture environments do not entirely align with those of cells in vivo (Bissell et al., 1982; Weaver et al., 1997) This discrepancy can be attributed to differences in factors such as tissue structure, biological signals, physiology, and cell-matrix interactions within the growth environment. In fact, the interaction between cells and their ECM plays a crucial role in regulating cellular processes such as growth, proliferation, and function, and this interaction is absent in 2D culture environments, highlighting the importance of studying cellular behavior in 3D systems (Tiniakos et al., 2010).

Furthermore, discrepancies between the outcomes of 2D cell experiments and those derived from animal and clinical experiments have been observed. Therefore, over the course of the last decade, researchers have focused their efforts on creating diverse 3D culture methodologies in order to establish a culture environment that more accurately mimics the in vivo environment for cells (Schwabe et al., 2020).

A 3D cell culture is an in vitro system that enables the growth and interaction of biological cells with their surrounding environment in three dimensions (Griffith & Swartz, 2006). As opposed to the conventional 2D cell culture systems, 3D cell cultures provide a more physiologically relevant environment for in vitro cell growth by allowing cells to proliferate in all directions, thereby closely resembling their in vivo growth pattern (Ravi et al., 2015)

Various 3D platforms are employed to facilitate the growth of cells into 3D cellular structures such as spheroids or organoids. These include scaffold systems, such as hydrogel matrices and solid scaffolds, as well as scaffold-free systems, such as low-adhesion plates, hanging drop plates, rotary cell culture, and nanoparticle facilitated magnetic levitation (Hirschhaeuser et al., 2010). Spheroids are 3D cellular structures that are generated in vitro (outside of a living organism) through the aggregation of cells. These structures closely mimic the architecture and microenvironment of tissues found in living organisms (Fennema et al., 2013). Unlike traditional cell cultures, where cells are typically grown in a flat, 2D monolayer on a petri dish, spheroids offer a more physiologically relevant model for studying cell behavior, interactions, and responses to stimuli (Lee et al., 2007).

Spheroids can be formed from a variety of cell types, including cancer cells, stem cells, or differentiated cells, depending on the research objectives (Vinci et al., 2012) They are typically formed by culturing cells in a non-adherent environment, such as a suspension culture, where they self-assemble into compact, spherical structures. They can be used to study various cellular processes, including proliferation, differentiation, apoptosis (cell death), and responses to drugs or other treatments (Weigelt et al., 2010) hence the reason for employing them in this study. Spheroids have gained significant importance in fields like cancer research, drug development, and regenerative medicine due to their ability to mimic tissue-like structures.

Organoids are more complex 3D structures that closely mimic the architecture and functionality of specific organs or tissues found in living organisms (Duval et al., 2017; Haycock, 2011) They are typically generated from stem cells or organ-specific progenitor cells (Takebayashi-Suzuki & Suzuki, 2020). Organoids can self-organize and differentiate into various cell types, recapitulating the cellular diversity and functionality of the organ they are derived from.

Organoids are powerful tools for studying organ development, disease modelling, and drug screening (Haycock, 2011) They have been generated for a wide range of organs, including the brain, liver, kidney, intestine, and more. Organoids have played a crucial role in advancing our understanding of organ-specific biology and have the potential to revolutionize drug discovery and personalized medicine. By analyzing the response of hepatocytes within the context of 2D and 3D cultures, this study aims to unravel insights into the impact of TGF-α on liver cellular behavior and functional outcomes.

3.2 Methods

3.2.1 Preparation of 2D Cell Culture Medium

HepG2 cells were seeded at a concentration of 2.5×10^4 cells per well, while Huh7 cells were seeded at a concentration of 8×10^3 cells per well. Informed by the outcomes illustrated in figures 3.4 and 3.5, our seeding strategy for HepG2 and Huh7 cells was carefully determined. Figure 3.4 demonstrated the response of HepG2 cells under varying seeding concentrations, guiding our choice of 2.5×10^4 cells/well. This concentration was selected to strike a balance: ensuring ample cells for robust data while preventing over confluency.

Conversely, the results depicted in figure 3.5 for Huh7 cells revealed their distinct growth rate in comparison to HepG2 cells. Huh7 cells appeared to have a faster proliferation rate at lower concentrations compared to HepG2 cells. As a result, we opted for a lower seeding concentration of 8×10^3 cells/well for Huh7 cells. Adapting the seeding concentration for Huh7 cells was crucial to maintaining a comparable confluency level for both cell lines throughout the experimental timeline. The adjusted seeding concentration accounts for the disparate growth kinetics of Huh7 cells, fostering healthy growth and division during the course of our experiment.

The 2D culture setups were done using 96-well plates in final volumes of 100 μL per well for each cell type. Recombinant TGF-α was obtained and diluted to varying concentrations: 0.5 ng/mL, 1 ng/mL, 5 ng/mL, and 10 ng/mL using the culture medium. After the cells were allowed to adhere for 24 hours, the culture medium was replaced with 100 μL media with the respective TGF- a concentration. Control wells without TGF-α treatment were also included. Cell proliferation was assessed over the course of 72 hours by imaging and WST-1 assay.

3.2.2 Preparation of 3D Cell Culture Medium

HepG2 cells, initially maintained in DMEM, were mixed with Happy Cell ASM in a 15 mL centrifuge tube. The final volume of the culture was adjusted to 1 mL.

The selection of ASM Happy cell media was predicated upon its known ability to promote spheroid formation and maintain hepatocyte phenotype in three-dimensional cultures (Koledova, 2017). Its composition, containing essential nutrients and factors supporting cell viability and function, was deemed suitable for fostering the growth and behavior of HepG2 spheroids during the experimental timeframe. Compared to hanging drop or non-adherent plates technologies for spheroid production, the ASM Happy Cell media generates a large number of spheroids, rather than just a single spheroid (Koledova, 2017), and the higher cell numbers makes it more suitable for downstream molecular and cellular analysis.

The initial concentration of HepG2 cells used for the 3D culture was 2.5 x 10^5 cells/mL (Figure 3.1A). As shown in the representative image (Figure 3.1B) this concentration was used in order to generate 3D spheroid structures while preventing them from becoming too crowded, which can lead to nutrient depletion and altered cellular behavior.

The tubes containing the 3D cell culture was incubated for 72 hours in a humidified incubator set at 37°C and 5% CO2, allowing the cells to form multicellular spheroids within the culture medium.

Following the 72-hour incubation period, the contents of the 3D culture falcon tube were transferred to a 96-well plate. Each well received 200μL of the culture, containing approximately 5×10^4 cells. The cells were then subjected to treatment with varying concentrations of recombinant TGF-α (0.5 ng/mL, 1 ng/mL, 5 ng/mL, and 10 ng/mL while a control group received no treatment). The 96-well plate was then subjected to an additional 72-hour incubation period and proliferation was assessed using WST-1 proliferation assay according to the manufacturer's instructions. Plate was read using a microplate reader. See figure 3.1 below for 3D culture setup
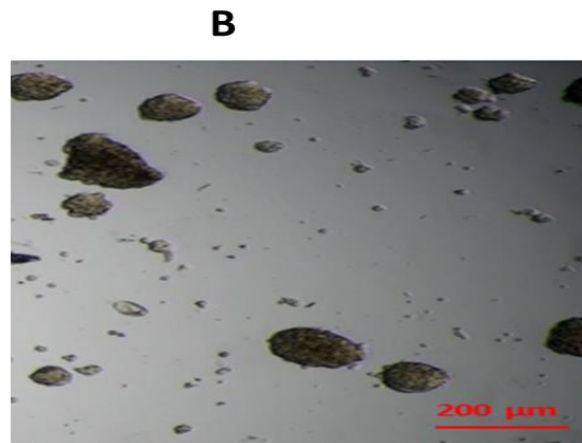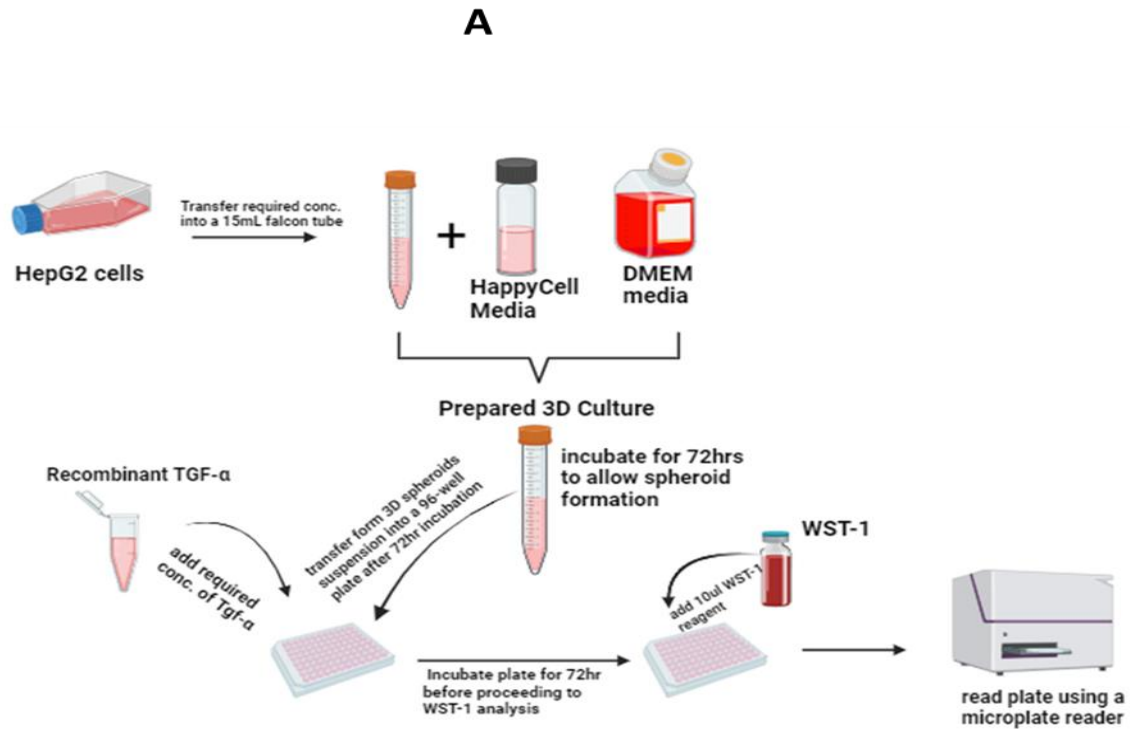
Figure 3. 1: Experimental setup for 3D culture system

This figure illustrates the experimental workflow employed in setting up a 3D culture system using Happy Cell ASM media. **(A)** represents the 3D culture setup. **(B)** Representative image of a formed 3D HepG2 spheroid.

3.2.3 qPCR Analyses

Quantitative polymerase chain reaction analysis was conducted to quantify the gene expression levels of target and reference genes. Primers specific to the genes of interest, including *G6PD*, *MYC*, *ALB*, *AFP*, *HIF1A*, *VEGFA*, *SREBF1*, and *EGFR*. From literature, all the above stated genes are thought to have the potential to be regulated by TGF-α hence the reason why we are examining them. The genes were selected according to their functions in metabolic processes, cellular signaling, differentiation of hepatocytes, and cell survival, as categorized in Figure 3.1. Reference genes *B2M* and *HPRT1*, were used for the qPCR reactions. Real-time PCR amplification was carried out in a thermal cycler, and the fluorescence emitted during amplification was monitored. The threshold cycle (Ct) values were determined for each gene.
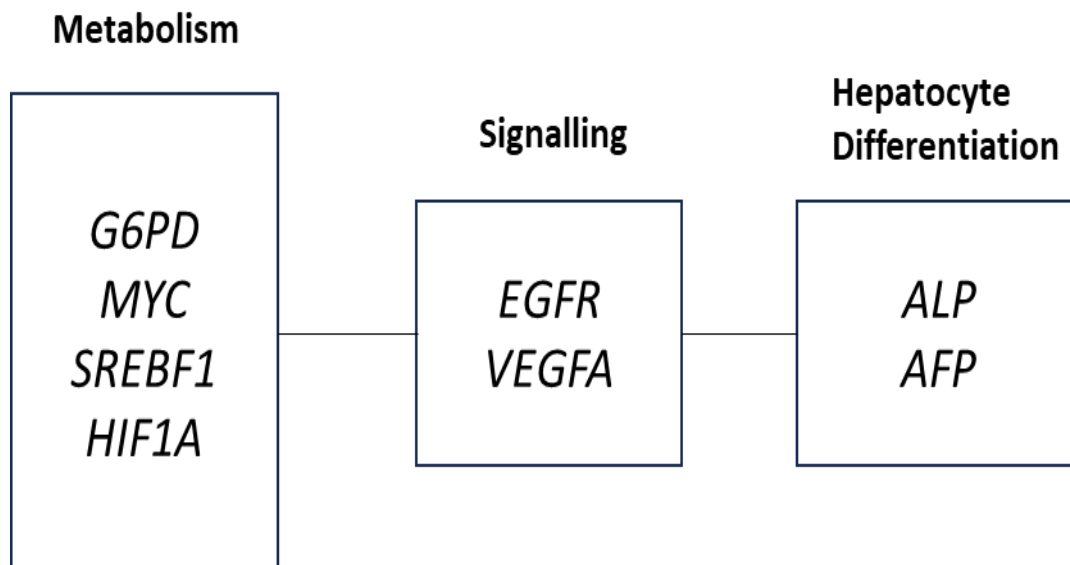

Figure 3. 2 *TGFA*-regulated genes

This figure shows *TGFA*-regulated genes classified based on their respective functions in cellular metabolism, signalling pathways, and differentiation of hepatocytes.

3.3 Results

3.3.1 Dynamics of Hepatocyte Cell Proliferation and Confluency Evaluation (HepG2 and Huh7) Across Different Time Points and Concentrations.

An experiment was conducted to evaluate the proliferation and confluency of two distinct types of hepatocyte cell lines, namely HepG2 cells and Huh7 cells, over a period of 72 hours. Various concentrations of cells were introduced into a 12-well plate and monitored over time. The primary aim was to observe how cell confluency changed over time and to investigate the impact of different cell concentrations on coverage. The ultimate objective was to identify the optimal cell concentrations for subsequent studies.

The experiment employed four different cell concentrations: 8×10^4 cells/mL, 16×10^4 cells/mL, 24×10^4 cells/mL, and 32×10^4 cells/mL. Photographs of the cell culture plate were taken at specific time intervals of 24, 48, and 72 hours. The level of cell confluency was then quantified using ImageJ software. The results indicated that cell confluency and proliferation both HepG2 and Huh7 increased with both higher concentration and longer incubation time. The data derived from the images also revealed a clear correlation between cell concentration, time, and coverage for both cell lines.
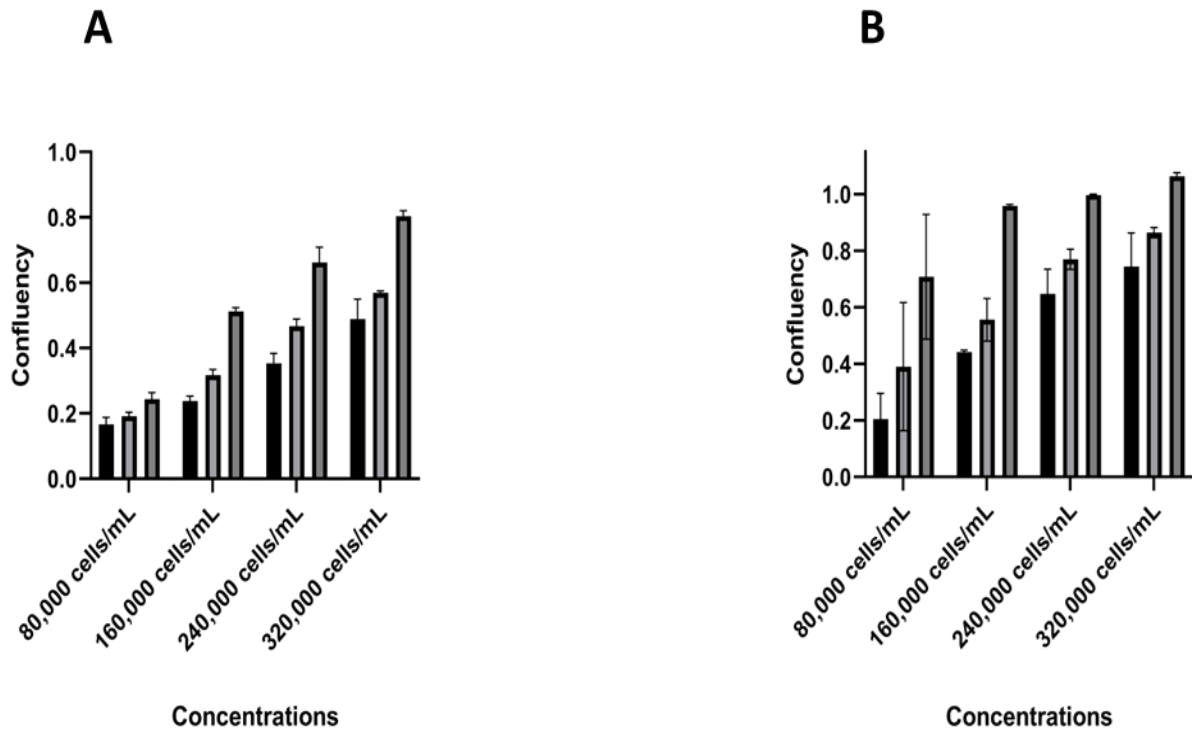
Figure 3. 3: Cell Proliferation Dynamics of HepG2 and Huh7 Cells Under Differing Concentrations over time

An experimental investigation conducted to evaluate temporal changes in cell confluence and the impact of different cell concentrations on the proliferation of hepatocyte cell lines, specifically HepG2 (A) and Huh7 (B). The study involved four distinct cell concentrations: $8x10^4$ cells/mL, $16x10^4$ cells/mL, $24x10^4$ cells/mL, and $32x10^4$ cells/mL. Cellular confluence quantification was performed using ImageJ software, generating significant data. The findings unveiled a clear correlation between cell concentration, exposure duration, and confluence for both cell lines. Data points represent means with standard deviation. For Huh7, n=2; for HepG2, n=3.
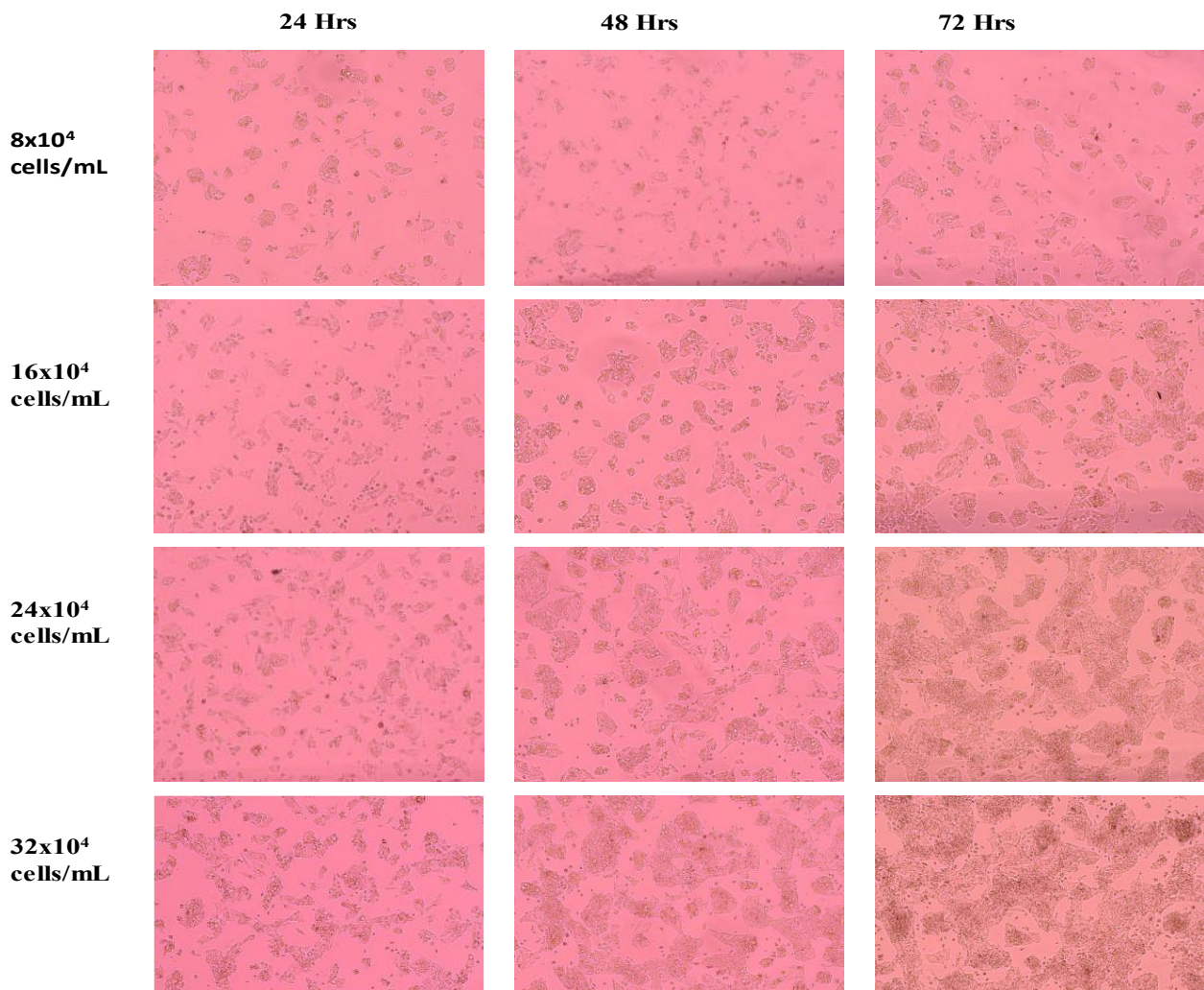
Figure 3. 4: Cell Proliferation Dynamics of HepG2 Cells Under Differing Concentrations over time: Insights from Microscopic Analysis

Microscopic images illustrating the distinct variations in the proliferation of HepG2 cells at different concentrations (8×10^4 cells/mL, 16×10^4 cells/mL, 24×10^4 cells/mL, and 32×10^4 cells/mL) over a 72-hour period. These visuals substantiate the link between cell concentration and proliferation dynamics, further reinforcing the correlation highlighted in figure 3.3A. This correlation elucidates the relationship between cell concentration, exposure duration, and confluence in HepG2, as analyzed through ImageJ.
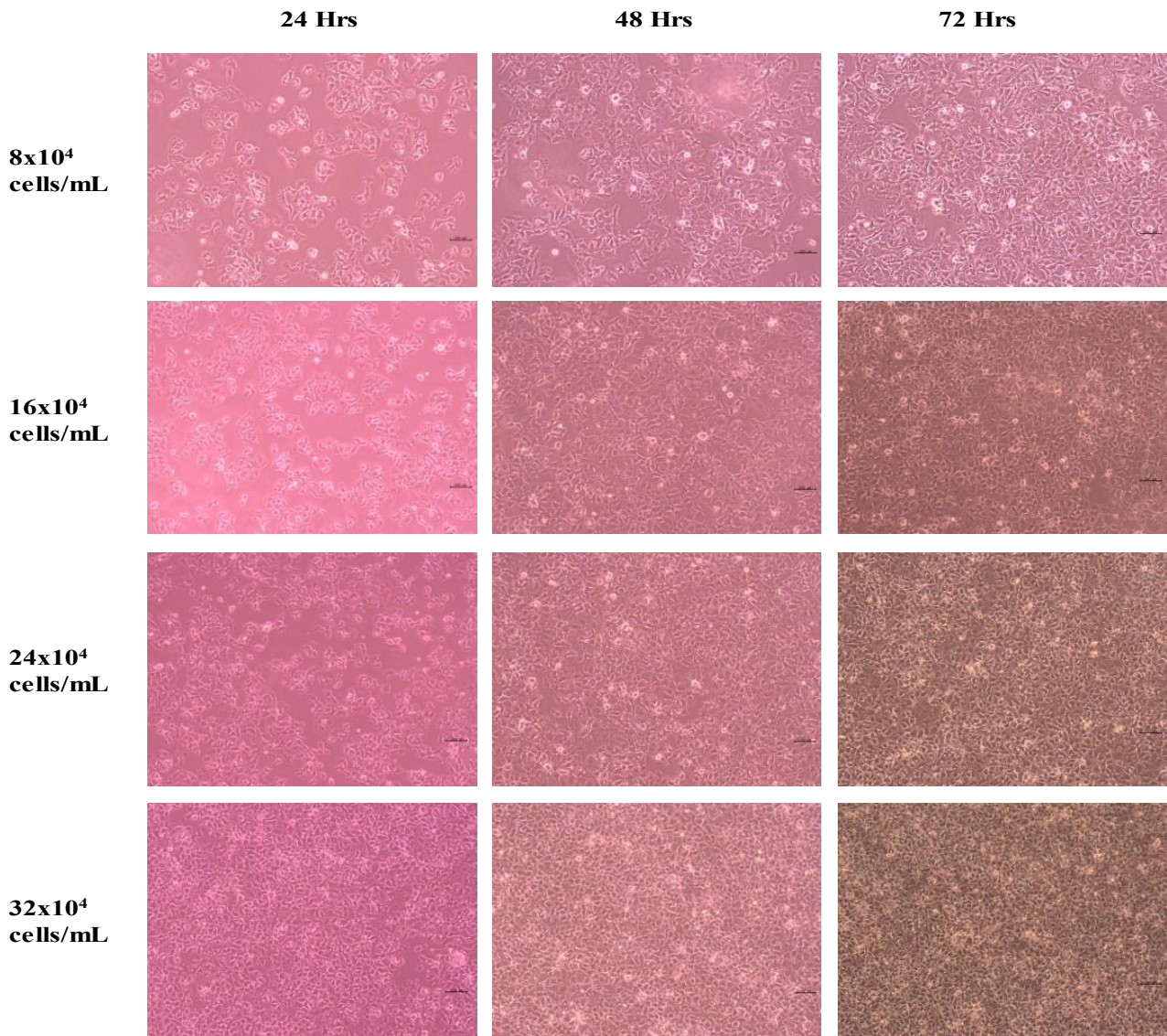
Figure 3. 5: Cell Proliferation Dynamics of Huh7 Cells Under Differing Concentrations over time: Insights from Microscopic Analysis

Microscopic images illustrating the distinct variations in the proliferation of Huh7 cells at different concentrations (8×10^4 cells/mL, 16×10^4 cells/mL, 24×10^4 cells/mL, and 32×10^4 cells/mL) over a 72-hour period. These visuals substantiate the link between cell concentration and proliferation dynamics, further reinforcing the correlation highlighted in figure 3.3B. This correlation elucidates the relationship between cell concentration, exposure duration, and confluence in Huh7, as analyzed through ImageJ.

3.3.2 Proliferative response of hepatocytes in 2D following treatment with TGF-α.

The current study aimed to assess the impact of recombinant TGF-α treatment on the proliferation of HepG2 and Huh7 cells within a 2D culture system. Various concentrations of TGF-α (0.5ng/mL, 1ng/mL, 5ng/mL, and 10ng/mL) were employed to determine its effects on cell growth, compared to control groups that did not receive TGF-α treatment (0ng/mL). The experiment utilized a 72-hour monitoring period, with observations and imaging conducted at 24, 48, and 72-hour intervals. A WST-1 proliferation analysis was performed after 72 hours to evaluate the cellular proliferation in the wells subsequent to the administration of TGF-α treatment.

The results obtained from this study provide important insights into the influence of recombinant TGF-α on HepG2 and Huh7 cell proliferation. Notably, the examination of the collected data revealed a lack of significant alteration in the proliferation rates of both cell types following treatment with recombinant TGF-α compared to their respective control groups (Figure 3.4). These findings suggest that within the parameters of this study, TGF-α did not exert a noticeable impact on the proliferation dynamics of HepG2 and Huh7 cells in 2D cell culture.
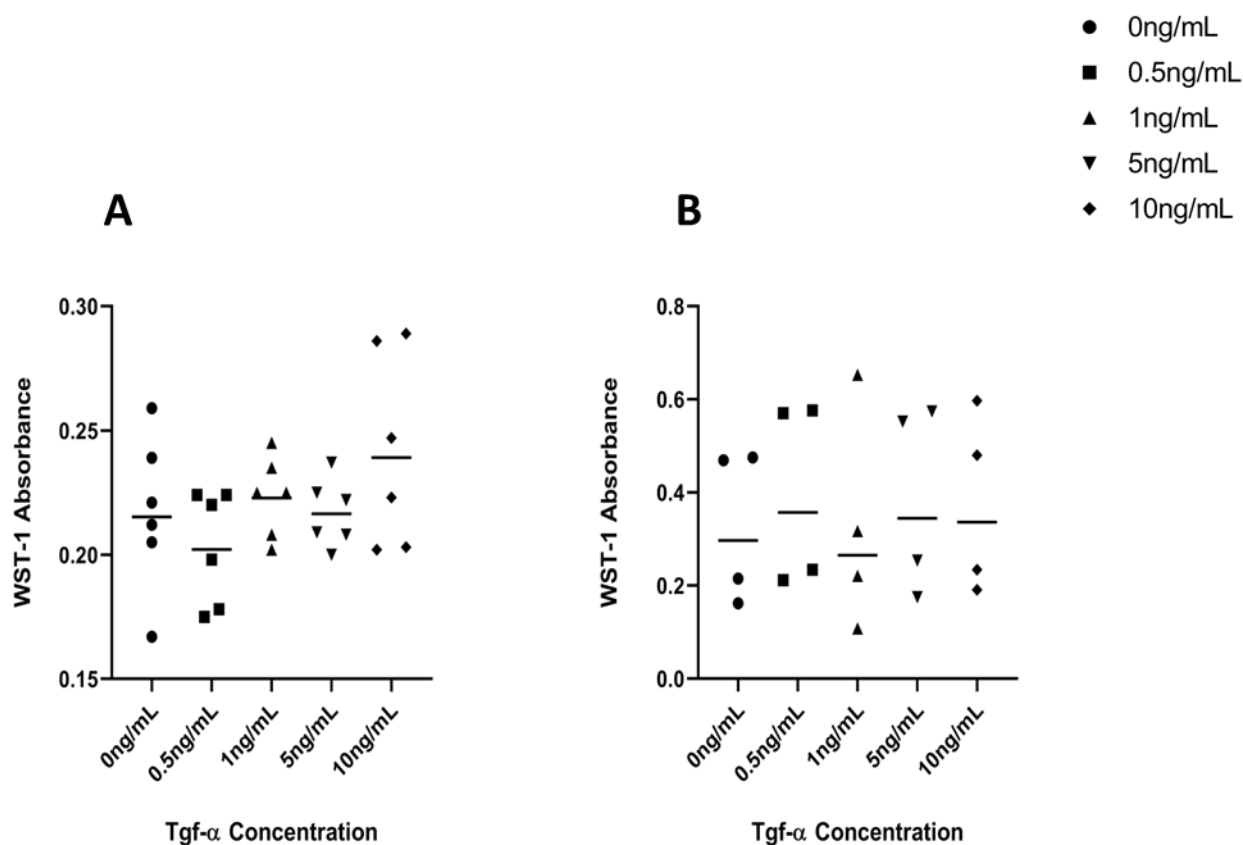
Figure 3. 6: Impact of Recombinant TGF-α on HepG2 and Huh7 Cell Proliferation in 2D Culture System.

The impact of recombinant TGF-α treatment on the proliferation of HepG2 (A) and Huh7 (B) cells was investigated using a 2D culture system. Various concentrations of TGF-α (0.5 ng/mL, 1 ng/mL, 5 ng/mL, and 10 ng/mL) were administered to assess their effects on cell growth, with untreated control groups (0 ng/mL) for comparison. The experiment was conducted over a 72-hour period. After the treatment, a WST-1 proliferation analysis was conducted to assess cell proliferation rates. The HepG2 sample group consisted of n=6 replicates, while the Huh7 groups consisted of n=4 replicates. Geometric means were used to represent data points. Statistical analysis involved RM One-way ANOVA with Geisser-Greenhouse correction, followed by Dunnett's multiple comparison test. Significance levels are denoted as *, p<0.05; **, p<0.01.

3.3.3 Proliferative response of hepatocytes in 3D

We examined the influence of recombinant TGF-α on the proliferation of hepatocytes by employing a 3D culture approach. Specifically, we cultured HepG2 cells in Happy Cell ASM 3D culture medium to form 3D spheroids. These HepG2 spheroids were then exposed to various concentrations of recombinant TGF-α (0.5ng/mL, 1ng/mL, 5ng/mL, and 10ng/mL) and monitored over a 72-hour period. When we assessed cell proliferation at the 72-hour mark using the WST-1 assay, we observed a noteworthy increase in HepG2 cell growth following treatment with TGF-α at concentrations of 5ng/mL and 10ng/mL, as compared to the untreated control group (Figure 3.5A).

To gain further insight into this proliferation trend, we conducted an analysis based on the quantification of 3D spheroids. Our observations showed a significant increase in cell proliferation specifically at the 5ng/mL TGF-α concentration (Figure 3.5B). These findings strongly imply that the 3D culture system offers a more pertinent model for evaluating the influence of TGF-α signaling on hepatocyte proliferation.
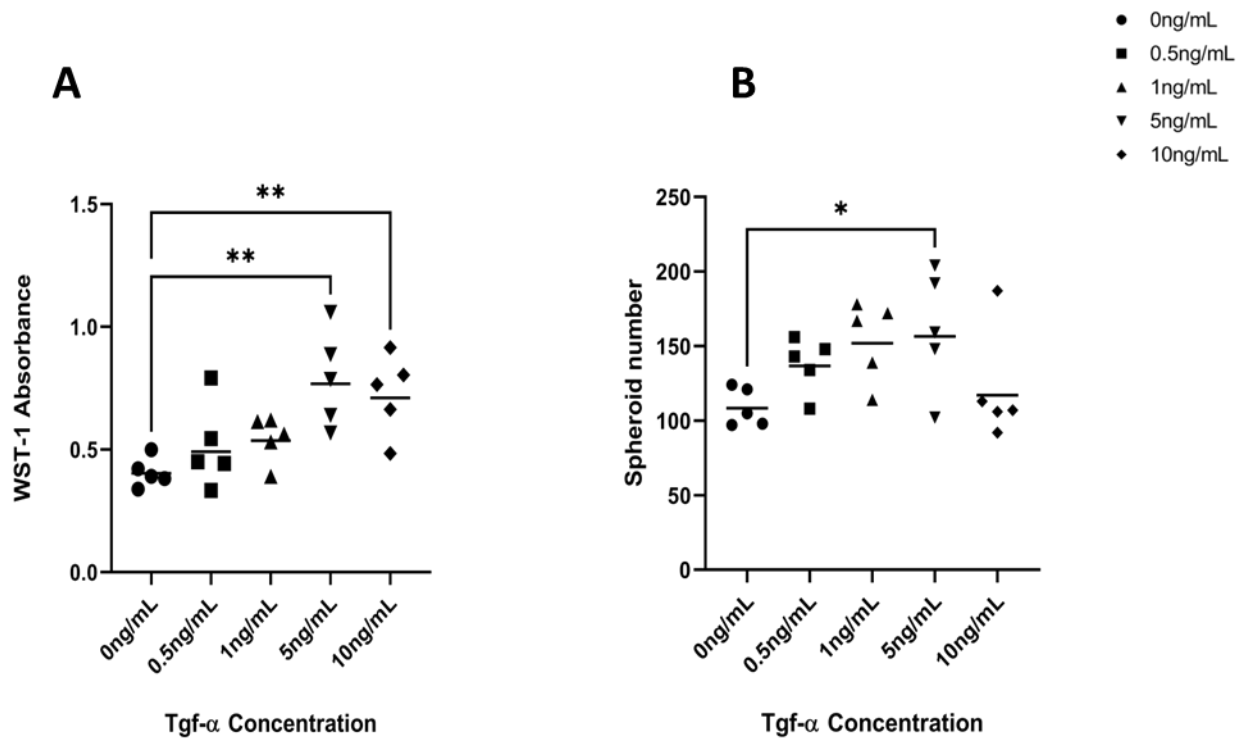
Figure 3. 7: Impact of Recombinant TGF-α on Hepatocyte Proliferation in 3D Culture Systems

This figure illustrates the impact of varying concentrations of recombinant TGF-α (0.5 ng/mL, 1 ng/mL, 5 ng/mL, and 10 ng/mL) on the proliferation of HepG2 cells in a 3D culture system over a 72-hour period. Two distinct analyses were conducted**: Graph A** shows the assessment of cell proliferation using Absorbance values from the WST-1 proliferation assay, while **Graph B** displays the results based on spheroid counts. The experiment involved five replicates (n=5), and data points are represented as geometric means. Data analysis was carried out employing RM One-way ANOVA with Geisser-Greenhouse correction and Dunnett's multiple comparison test. Significance levels are denoted as follows: *, $p<0.05$; **, $p<0.01$.

3.3.4 Transcriptional response of hepatocytes in 2D

3.3.4.1 *HepG2 vs Huh7 response at 4hrs*

The quantification of TGF-α regulated genes associated with metabolism, signaling, hepatocyte differentiation, and cell survival was performed using real-time PCR following the administration of recombinant TGF-α. The following genes were evaluated: *G6PD*, *MYC*, *ALB*, *AFP, HIF1A, VEGFA, SREBF1*, and *EGFR*. *B2M* and *HPRT1* were employed as reference genes. The comparative analysis of gene expression was conducted using 2D culture models between two distinct types of hepatocyte cell lines (HepG2 and Huh7 cells) and quantified in terms of fold change.

Recombinant TGF-α was used to stimulate HepG2 and Huh7 cells individually for 4 hours, with concentrations of 0.5ng/ml and 10ng/ml compared to a control group of 0ng/ml. Each cell type was seeded at a concentration of 2.5×10^5 cells/mL into three distinct wells in a 12-well plate, followed by a 24-hour incubation. After media extraction and substitution, TGF-α concentrations were introduced, and a 4-hour stimulation period was applied. RNA extraction using the TRIzol method was followed by cDNA synthesis and qPCR analysis.

In Huh7 cells, qPCR analysis revealed a significant upregulation in the expression of the *ALB* gene after exposure to 0.5ng/ml TGF-α treatment (Figure 3.6E). This upregulation was suppressed with 10ng/ml TGF-α treatment. Conversely, HepG2 cells showed a reduction in *ALB* expression at 10ng/ml TGF-α (Figure 3.7E), relative to 0.5ng/ml.

No significant change was observed in the expression of the *AFP* gene in either HepG2 (Figure 3.7A) or Huh7 cells following stimulation (Figure 3.6A). *HIF1A* expression increased significantly in Huh7 cells at 10ng/ml TGF-α (Figure 3.6B). In HepG2 cells, *HIF1A* expression remained unchanged at both TGF-α doses (Figure 3.7B).

The *MYC* gene exhibited significant upregulation in Huh7 cells after 0.5ng/ml TGF-α treatment (Figure 3.6D), with no such increase in HepG2 cells (Figure 3.7D). However, both cell lines showed downregulation of *MYC* expression at 10ng/ml TGF-α (Figure 3.6D and Figure 3.7D).

SREBF1 was downregulated in HepG2 cells with 10ng/ml TGF-α (Figure 3.7G), while no significant alteration was detected in Huh7 cells (Figure 3.6G). The expression of *G6PD* remained unchanged in both cell types upon TGF-α stimulation.

Moreover, upregulation of *VEGFA* and *EGFR* genes was observed in HepG2 cells. *VEGFA* exhibited upregulation at 0.5ng/ml TGF-α treatment (Fig 3.7H), while *EGFR* exhibited upregulation at both 0.5ng/ml and 10ng/ml TGF-α (Fig 3.7C). No significant changes were observed in the expression of *VEGFA* and *EGFR* in Huh7 cells.
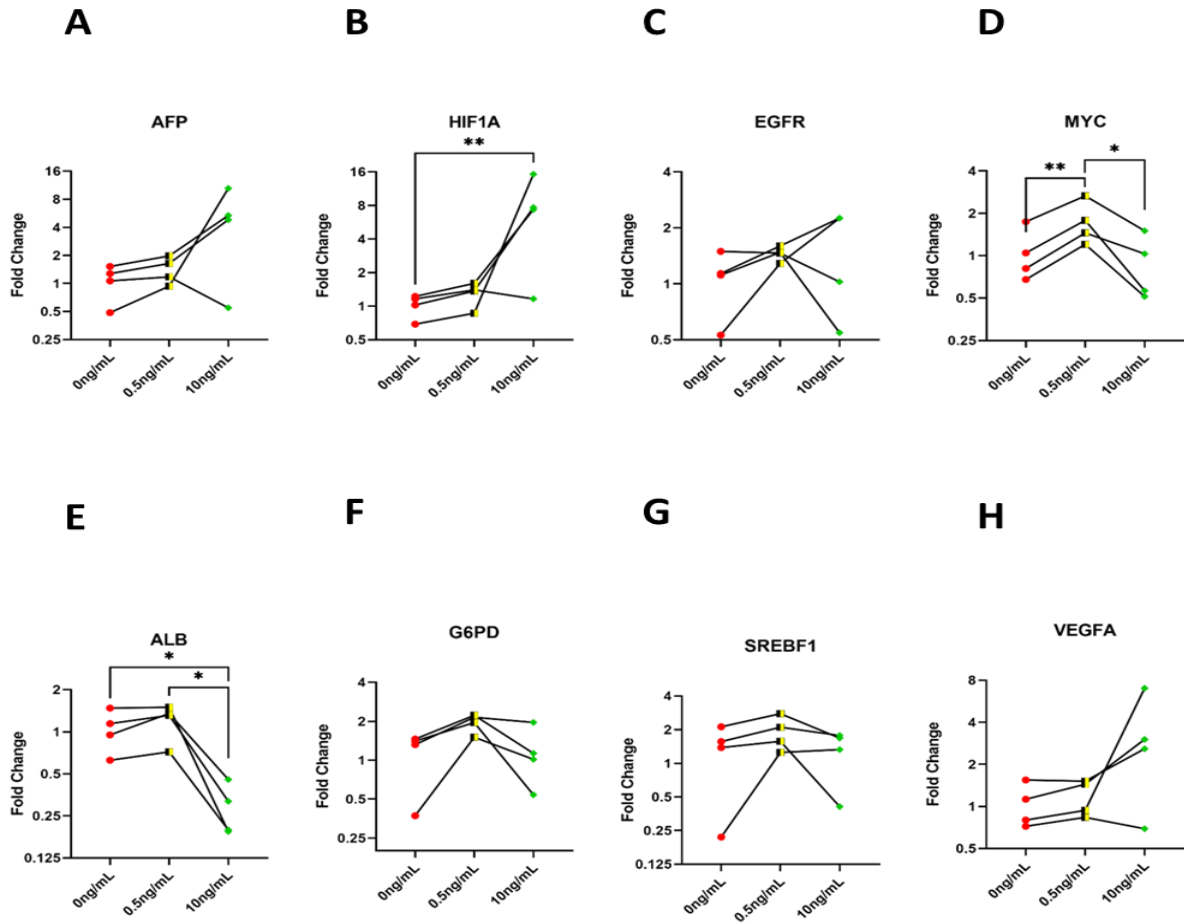
Figure 3. 8: Differential Expression of TGF-α-regulated Genes in Huh7 Cells Upon TGF-α Stimulation at 4 hours.

The impact of recombinant TGF-α administration on the expression of TGFA-regulated genes was assessed using real-time PCR. Genes associated with diverse functions including metabolism, cellular signaling, hepatocyte differentiation, and cell viability were examined. Reference genes B2M and HPRT1 were utilized for normalization. The analysis was performed on 2D cultured hepatocyte cell lines (huh7 cells), and fold change was used to quantify gene expression. Stimulation with two concentrations of recombinant TGF-α (0.5ng/ml and 10ng/ml) was compared against a control group (0ng/ml) after a 4-hour exposure period. Each treatment condition included four biological replicates. Data points are represented as geometric means. Statistical analysis employed Friedman test with Dunn's multiple comparison. Significance levels are indicated as *, $p<0.05$; **, $p<0.01$.

3.3.4.2 *HepG2 response at 4 hours vs 24 hours*

The study aimed to investigate the effects of TGF-α treatment on the expression of *TGFA*-regulated genes in HepG2 cells using 2D culture models. The genes of interest included *G6PD, MYC, ALB, AFP, HIF1A, VEGFA, SREBF1,* and *EGFR,* alongside reference genes *B2M* and *HPRT1.*

The experimental setup involved seeding HepG2 cells at a concentration of 2.5x10^5 cells/mL into three wells in a 12-well plate, followed by a 24-hour incubation. After media replacement, TGF-α was introduced into the wells at concentrations of 0.5ng/mL and 10 ng/mL, with another well with a control of no treatment. Incubation durations were 4 hours and 24 hours. RNA was extracted using the TRIzol method, and cDNA synthesis was followed by qPCR analysis.

The qPCR analysis revealed significant downregulation of *MYC, ALB,* and *SREBF1,* and genes at 10 ng/mL after 4 hours (Figure 3.7D, Figure 3.7E and Figure 3.7G). *ALB* and *SREBF1* remained significantly reduced at 24 hours (Figure 3.8E and Figure 3.8G). *MYC,* however, showed no change after 24 hours (Figure 3.8D). *AFP* gene downregulation at 10 ng/mL was observed only after 24 hours (Figure 3.8A).

EGFR gene exhibited significant upregulation at both 4 hours (Figure 3.7C) and 24 hours (Figure 3.8C) for 0.5 ng/mL and 10 ng/mL TGF-α. *VEGFA* gene showed initial upregulation at 10 ng/mL after 4 hours (Figure 3.7G), but not at 24 hours (Figure 3.8G). No changes were observed for *G6PD* and *HIF1A* genes after TGF-α treatment in both time points.
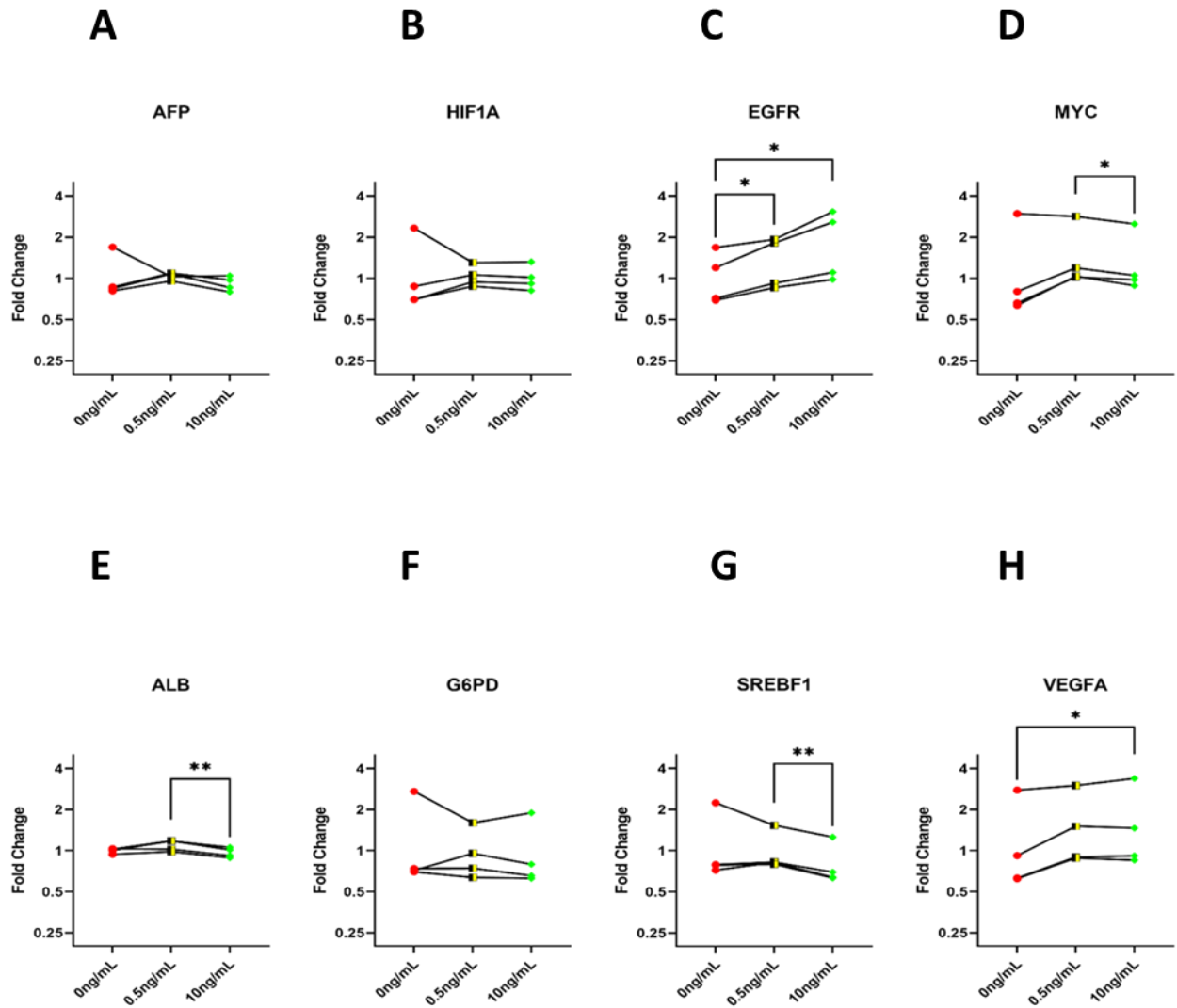
Figure 3. 9 Expression of TGFA-regulated genes in HepG2 cells following TGF-α treatment at 4 hours.

The impact of TGF-α treatment on gene expression in HepG2 cells was investigated using 2D culture models. The expression levels of *TGFA*-regulated genes (*G6PD, MYC, ALB, AFP, HIF1A, VEGFA, SREBF1,* and *EGFR*) were evaluated following treatment with two concentrations of TGF-α (0.5 ng/ml and 10 ng/ml) for 4 hours, compared to an untreated control group (0 ng/ml). Quantitative polymerase chain reaction analysis was performed to assess fold changes in gene expression. Each experimental group had n=4 samples. Data points are represented as geometric means. Statistical analysis employed Friedman test with Dunn's multiple comparison. Significance levels are indicated as *, $p<0.05$; **, $p<0.01$.
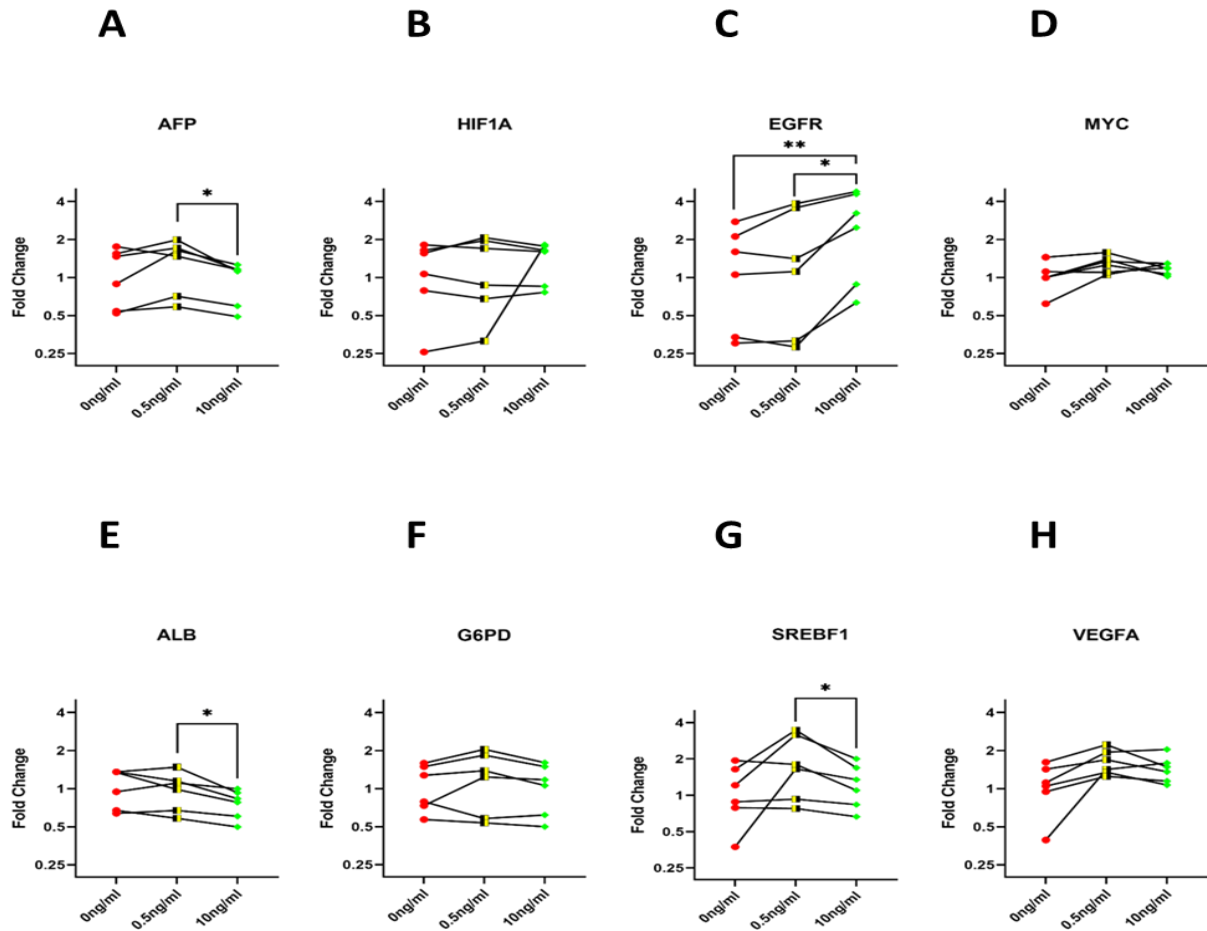
Figure 3. 10: Expression of TGFA-regulated genes in HepG2 cells following TGF-α treatment at 24 hours.

The impact of TGF-α treatment on *TGFA*-regulated gene expression in HepG2 cells within 2D culture models after a 24-hour stimulation period was assessed. HepG2 cells were subjected to varying concentrations of TGF-α (0.5 ng/mL and 10 ng/mL), and their gene expression profiles were analyzed. Genes of interest (*G6PD, MYC, ALB, AFP, HIF1A, VEGFA, SREBF1*, and *EGFR*). Each experimental group consisted of n=6 samples, and data points are represented as geometric means. Statistical analysis was carried out using the Friedman test with Dunn's multiple comparison. Significance levels were denoted as follows: *, $p < 0.05$; **, $p < 0.01$.

3.3.5 Transcriptional response of hepatocytes in 3D (4 hours vs 24 hours)

The results obtained from the investigation into the response of HepG2 cells to TGF-α stimulation in 3D models provided valuable insights into gene expression dynamics of the target genes under varying conditions. The experiment involved creating 3D spheroids using Happy Cell ASM 3D culture media, followed by treatment with two different dosages of TGF-α (0.5ng/ml and 10ng/ml) for stimulation periods of 4 hours and 24 hours. RNA extraction using the PureLink RNA extraction kit was performed on each sample after stimulation, followed by cDNA synthesis and qPCR testing to assess gene expression changes. Fold changes were used to quantify gene expression alterations.

Following 24 hours of stimulation with 0.5ng/ml TGF-α, a significant increase in *MYC* gene expression was observed (Fig. 3.10D). However, no significant change in *MYC* expression was observed after 4 hours of TGF-α stimulation (Figure 3.9D). *G6PD* gene expression showed a similar pattern, with a significant increase after 24 hours of stimulation with 0.5ng/ml TGF-α (Figure 3.10F), but no significant change after 4 hours (Figure 3.9A).

VEGFA gene showed a significant elevation in expression at 4 hours following stimulation with 0.5ng/ml TGF-α (Figure 3.9H), while this increase was not sustained after 24 hours of stimulation (Figure 3.10H).

Conversely, the genes *ALB, AFP, HIFIA, SREBF1,* and *EGFR* within the 3D culture model did not exhibit significant changes in response to TGF-α stimulation at either the 4-hour or 24-hour time points when compared to the untreated control.
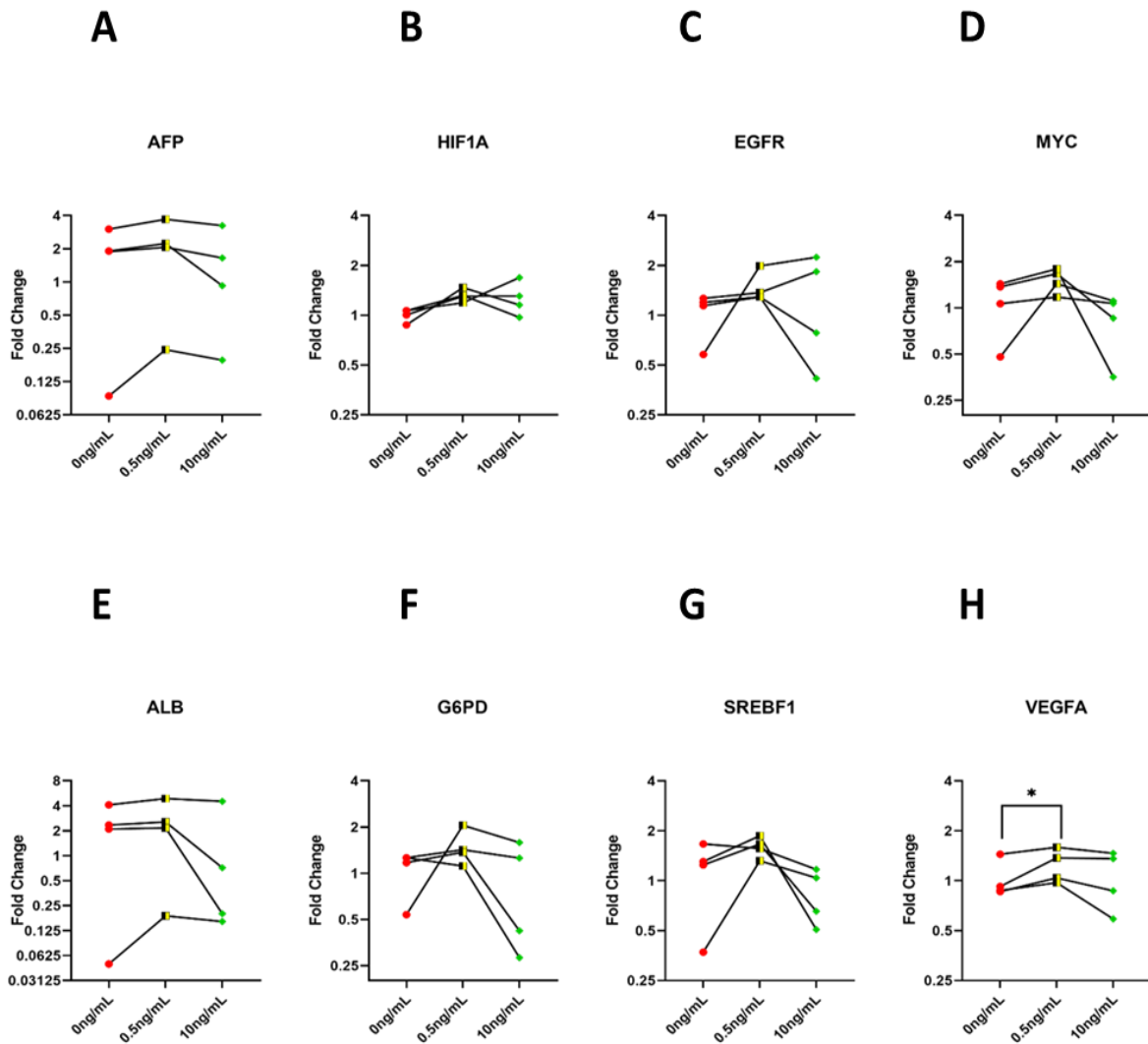
Figure 3. 11: Gene Expression Dynamics in HepG2 Cells Responding to TGF-α Stimulation at 4 hours in 3D Models.

The response of HepG2 cells to TGF-α stimulation in 3D models. HepG2 cells were cultured in 3D spheroids using Happy Cell ASM 3D culture media and treated with two different dosages of TGF-α (0.5ng/ml and 10ng/ml) for a stimulation period of 4 hours. qPCR analyses were conducted to evaluate changes in gene expression. Fold changes were utilized to quantify alterations in gene expression levels. Each experimental group comprised n=4 samples, and data points are represented as geometric means. Statistical analysis was performed using the Friedman test with Dunn's multiple comparison. Significance levels were indicated as follows: *, $p < 0.05$; **, $p < 0.01$.
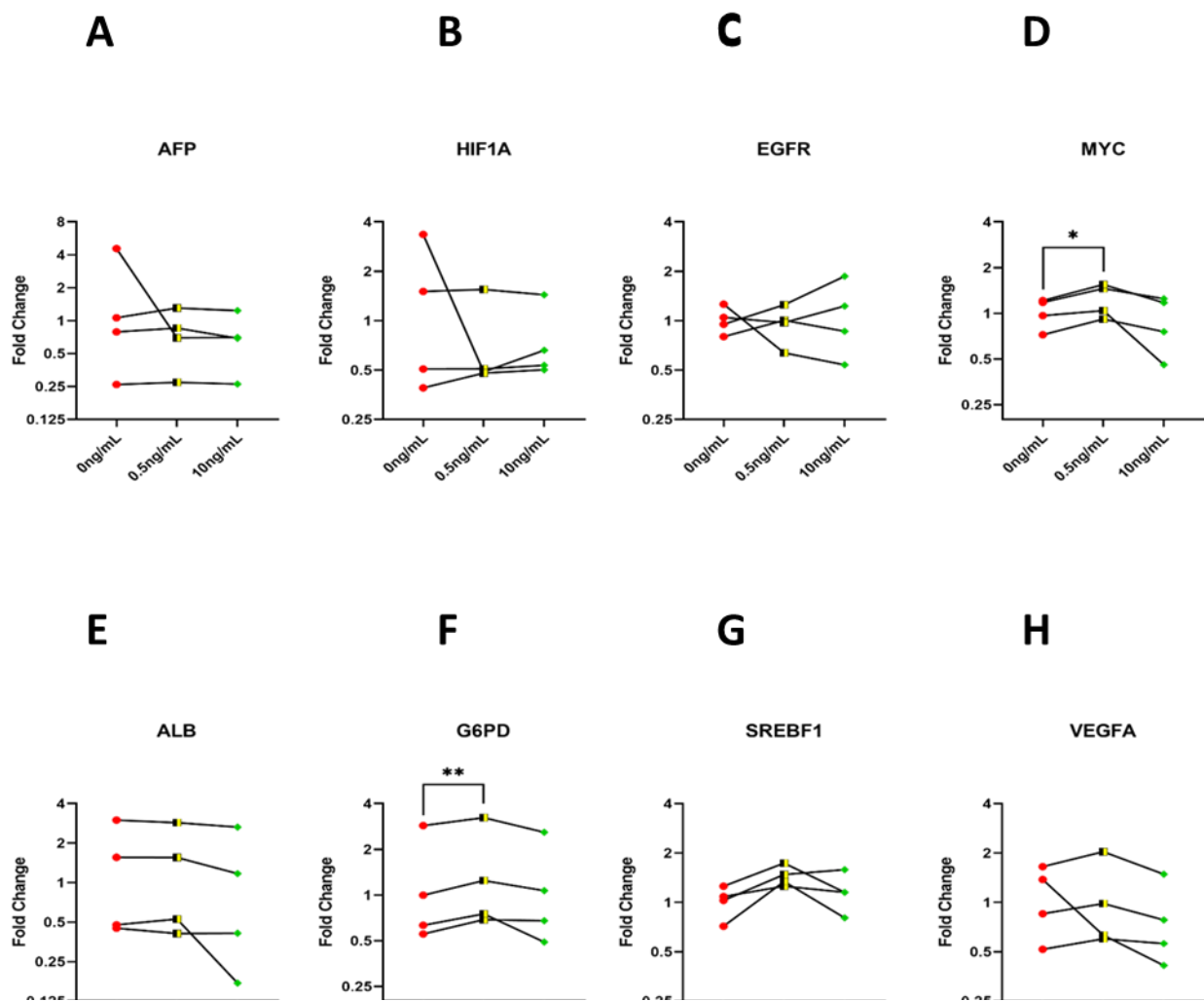
Figure 3. 12: Gene Expression Dynamics in HepG2 Cells Responding to TGF-α Stimulation at 24 hours in 3D Models.

The response of HepG2 cells to TGF-α stimulation in 3D models. HepG2 cells were cultured in 3D spheroids using Happy Cell ASM 3D culture media and treated with two different dosages of TGF-α (0.5ng/ml and 10ng/ml) for a stimulation period of 24 hours. qPCR analyses were conducted to evaluate changes in gene expression. Fold changes were utilized to quantify alterations in gene expression levels. Each experimental group comprised n=4 samples, and data points are represented as geometric means. Statistical analysis was performed using the Friedman test with Dunn's multiple comparison. Significance levels were indicated as follows: *, $p < 0.05$; **, $p < 0.01$

3.4 DISCUSSION

The results from this Chapter demonstrate the impact of cell concentration and culture context on hepatocyte proliferation dynamics and gene expression in response to TGF-α stimulation. Higher cell concentrations and 3D culture environments promote proliferation, emphasizing the importance of considering cellular context as demonstrated in the results above.

As seen in the results above, the expression of particular target genes (*G6PD, MYC, ALB, AFP, HIF1A, VEGFA, SREBF1, EGFR*) were analysed. The reason for choosing these genes was to gain a comprehensive understanding of how TGF-α prompts responses in hepatocytes at the molecular level. They represent various critical cellular functions related to metabolism, growth, differentiation, and response to environmental signals.

Genes crucial for metabolic regulation were targeted to understand the molecular responses of hepatocytes to TGF-α. *G6PD* (Glucose-6-Phosphate Dehydrogenase) was selected due to its pivotal role in the pentose phosphate pathway, impacting cellular energy and redox balance. Analyzing *G6PD* expression aided in understanding the metabolic alterations induced by TGF-α in hepatocytes (Richardson & O'Malley, 2022). Similarly, *MYC*, a proto-oncogene which is known to be a master regulator of metabolism, holds pivotal control over cell growth and proliferation. Monitoring *MYC* expression provided insights into the impact of TGF-α on cell cycle progression and hepatocyte proliferation, offering implications for liver regeneration (Dang, 2012). *SREBF1* (Sterol Regulatory Element-Binding Transcription Factor 1) was chosen owing to its involvement in lipid metabolism, offering insights into how TGF-α affects lipid homeostasis during hepatocyte regeneration (Peng et al., 2016). Additionally, *HIF1A* (Hypoxia-Inducible Factor 1 Alpha) played a crucial role in regulating cellular responses to hypoxia. Analyzing *HIF1A* expression provided insights into how TGF-α influences

hepatocyte responses to changes in oxygen levels, crucial for liver regeneration (Semenza, 2011).

Genes associated with cell signaling pathways were targeted to understand their interplay in TGF-α-induced responses. *EGFR* (Epidermal Growth Factor Receptor) was chosen for its role as a TGF-α receptor and its significance in cell proliferation and survival. Monitoring *EGFR* expression provided insights into the autocrine effects of TGF-α on hepatocytes during liver regeneration (Yarden & Sliwkowski, 2001). Similarly, *VEGFA* (Vascular Endothelial Growth Factor A), involved in angiogenesis and vascularization, offered insights into how TGF-α might influence liver tissue vascularization, a critical aspect of successful regeneration (Carmeliet, 2005).

To comprehend the effects of TGF-α on hepatocyte differentiation and function, genes associated with these processes were selected. *ALB* (Albumin), a major protein synthesized by hepatocytes crucial for maintaining osmotic balance, was targeted. Analyzing *ALB* expression provided insights into hepatocyte function and protein synthesis following TGF-α treatment (Kuten Pella et al., 2022). Additionally, *AFP* (Alpha-Fetoprotein), serving as a marker for liver development and hepatocellular carcinoma, aided in assessing hepatocyte differentiation and the potential effects of TGF-α on liver regeneration (Ashry et al., 2018).

To ensure accurate qPCR data, reference genes *B2M* (Beta-2-Microglobulin) and *HPRT1* (Hypoxanthine Phosphoribosyltransferase 1) were chosen. These genes are commonly used due to their stability in expression under various conditions, serving as crucial internal controls for normalizing gene expression data (Bustin et al., 2009).

The study reveals differential gene expression responses between Huh7 and HepG2 cells, highlighting the complex and cell-specific nature of TGF-α signalling pathways. Notably, *ALB, MYC, SREBF1, G6PD, HIF1A, VEGFA*, and *EGFR* exhibit distinct responses, suggesting their

involvement in various cellular processes. Temporal analysis within 2D culture and 3D spheroid models uncovers early and prolonged responses, with genes like *ALB, SREBF1*, and *MYC* showing lasting effects. Overall, these findings provide valuable insights into hepatocyte biology, TGF-α signalling, and potential implications for liver regeneration and disease.

The exploration of proliferation dynamics in HepG2 and Huh7 cell lines sheds light on the influence of cell concentration and duration on hepatocyte proliferation. It has been observed that higher cell concentrations can potentially enhance proliferation by facilitating increased paracrine signalling and improved nutrient availability (Metallo & Vander , 2013). Additionally, cell-cell interactions and the achievement of an optimal cell density, as noted in studies by (Barretina et al., 2012) and contribute to this process. Nonetheless, it is important to acknowledge that the utilization of a 2D culture system simplifies the complexity encountered in an in vivo environment.

Interestingly, 2D assessment of hepatocyte proliferative response yielded no significant results. The lack of discernible alteration in cell proliferation with both HepG2 and Huh7 cells doesn't necessarily indicate a lack of biological response. The absence of a detectable response could possibly be due to limitations of the 2D system that might affect TGF-α responsiveness. The sensitivity of the WST-1 assay in 2D cell culture at 72 hours may also mask subtle responses.

However, transitioning to a 3D culture system, emulating in vivo conditions, yielded different results. The significant increase in HepG2 cell proliferation following TGF-α treatment at 5ng/mL and 10ng/mL highlights the importance of culture context. The 3D environment's cellular and extracellular matrix interactions reveal TGF-α's stimulatory effect on hepatocyte proliferation. The 2D vs. 3D disparity underscores 2D limitations in representing complex behaviors and responses.

The investigation into the transcriptional responses of hepatocytes to TGF-α stimulation offers a comprehensive understanding of the intricate interplay between TGF-α signalling and gene expression. The study delves into the complex landscape of gene regulation by examining differential responses between two hepatocyte cell lines, Huh7 and HepG2, both stimulated with TGF-α. This exploration uncovers a series of dynamic gene expression patterns that shed light on the multifaceted roles of specific genes in mediating cellular responses to TGF-α, while also emphasizing the importance of considering the unique characteristics of each cell line.

The consistent alterations in gene expression patterns observed in response to TGF-α treatment in Huh7 and HepG2 cells underscore the significance of divergent regulatory pathways operating within HCC cell lines. This exploration reveals distinct molecular mechanisms at play, thereby deepening our comprehension of various facets of hepatocyte biology and hepatocellular carcinoma.

One notable observation involves the differential regulation of *ALB* expression in Huh7 and HepG2 cells. At a low concentration of TGF-α (0.5 ng/ml), Huh7 cells exhibit a significant upregulation of *ALB*, which suggests its involvement in hepatocyte differentiation (Schreiber et al., 1986). However, this upregulation is reversed at higher TGF-α concentrations (10 ng/ml), indicating a dose-dependent effect. In contrast, HepG2 cells display distinct downregulation of *ALB* at 10 ng/ml TGF-α, highlighting the dissimilar regulatory mechanisms between these cell lines. This finding underscores the importance of precise TGF-α dosage in modulating hepatocyte differentiation and emphasizes the potential clinical relevance of fine-tuning TGF-α therapy in liver-related disorders.

Additionally, the disparate expression of *HIF1A* in response to TGF-α treatment is noteworthy. Huh7 cells show an increase in *HIF1A* expression, suggesting its potential involvement in hypoxia-related responses (Schreiber et al., 1986). This response is conspicuously absent in

HepG2 cells, indicating a cell-specific regulation of *HIF1A*. Understanding these differences may provide insights into the variable hypoxic responses observed in liver tumors and could potentially inform tailored therapeutic approaches.

Another intriguing aspect is the fluctuation in *MYC* expression in Huh7 cells at different TGF-α concentrations, hinting at potential metabolic shifts (Shachaf et al., 2004). In contrast, the response of *MYC* in HepG2 cells is negligible. This discrepancy underscores the cell-specific regulation of metabolic processes and suggests that therapeutic strategies targeting *MYC* in liver cancer may need to consider the specific cellular context.

The downregulation of *SREBF1* in HepG2 cells is a significant finding that points towards potential impacts on lipid metabolism and cellular growth regulation (Goldstein et al., 2006). Given the pivotal role of lipid metabolism in liver diseases, these observations warrant further investigation to understand their broader implications for hepatocellular carcinoma treatment.

Lastly, the upregulation of *VEGFA* and epidermal growth *EGFR* in HepG2 cells suggests the involvement of TGF-α in angiogenesis and cell proliferation, critical processes in tumor growth and progression (Yarden & Sliwkowski, 2001). These findings underscore the potential of targeting these pathways as part of a comprehensive therapeutic strategy in liver cancer.

The consistent changes in gene expression between Huh7 and HepG2 cells treated with TGF-α reveal intricate and cell-specific regulatory mechanisms. These observations provide valuable insights into hepatocyte differentiation, hypoxia-related responses, metabolic shifts, lipid metabolism, and cellular growth, with potential implications for the development of targeted therapies in hepatocellular carcinoma.

The observed distinct reactions of Huh7 and HepG2 cell lines upon TGF-α stimulation highlight the crucial role of cellular context in signaling pathways. TGF-α's actions are cell-

specific, indicating its reliance on the particular cellular environment (Derynck,1990). The impact of microenvironmental factors, including paracrine signaling and cell-cell interactions, on proliferation dynamics signifies their significant contribution to cellular behaviors.

The differential expression of genes like *ALB, MYC, SREBF1*, and others following TGF-α stimulation highlights potential targets for therapeutic interventions in liver-related disorders. Notably, the disparity between outcomes in 2D and 3D cultures highlights the necessity for careful selection of culture models to accurately depict cellular behaviors (Metallo & Vander , 2013), thereby emphasizing the importance of culture dimensionality in cellular studies.

Examining the dose-dependent effects of TGF-α on gene regulation, such as the contrasting regulation of *ALB* at varying concentrations, emphasizes the need for precise dosing strategies in modulating cellular responses (Schreiber et al., 1986). These insights provide valuable information for tailored therapeutic approaches, stressing the significance of considering cell-specific responses in treatment strategies.

Extending the study to different time points within 2D culture, significant insights emerge regarding the early and prolonged responses of HepG2 cells to TGF-α stimulation. Noteworthy downregulation of ALB, SREBF1, and *MYC* genes after 4 hours of TGF-α treatment suggests their potential involvement in the initial cellular response to TGF-α signalling. The persistence of reduced *ALB* and *SREBF1* expression after 24 hours underscores the lasting impact of TGF-α on these genes. Conversely, *MYC* expression remains unaltered at 24 hours, indicating temporal specificity. *EGFR's* consistent upregulation at both time points highlights its central role in mediating cellular responses to TGF-α. The initial increase in *VEGFA* expression implies its early involvement in processes such as angiogenesis. The lack of sustained upregulation after 24 hours suggests a transient role. The unchanged expression levels of *G6PD*

and *HIF1A* point toward their indirect relationship with TGF-α signalling under the conditions tested.

In a 3D spheroid model, the study delves into the dynamic gene expression changes of HepG2 cells in response to TGF-α stimulation. The upregulation of *MYC* expression after 24 hours of prolonged TGF-α treatment suggests its potential role in mediating cellular responses, aligning with previous studies. *G6PD*'s upregulation after 24 hours also hints at its involvement in adaptive metabolic responses triggered by prolonged TGF-α stimulation. Notably, the genes *ALB, AFP, HIF1A, SREBF1*, and *EGFR* do not exhibit significant changes in response to TGF-α stimulation, indicating their potential insensitivity to short-term or prolonged exposure in the context of the 3D spheroid model.

The significance of this observed difference between 2D and 3D HepG2 cultures is that it highlights that the cellular environment, specifically the dimensionality of the culture, can have a substantial impact on how genes are regulated in response to TGF-α. This insight is crucial for researchers studying the behavior of HepG2 cells and potentially other cell types in different experimental settings, and it underscores the importance of choosing an appropriate culture model for specific research objectives.

In summary, this study has provided multifaceted insights into the regulatory effects of TGF-α on hepatocyte proliferation and gene expression. The shift from 2D to 3D culture highlighted the importance of considering cellular context, revealing contrasting proliferation dynamics. The divergent gene expression responses highlight the context-dependent nature of TGF-α signalling pathways (Duval et al., 2017; Ravi et al., 2015).The findings contribute to our understanding of cellular responses to TGF-α and its potential implications in liver regeneration and disease contexts, as well as a deeper understanding of hepatocyte biology.

Future research may delve into the underlying molecular mechanisms governing these responses, potentially revealing new avenues for therapeutic interventions targeting hepatocyte growth and differentiation. Additionally, further research to explore the proliferative response of hepatocytes to different TGF-α concentrations at different time points could reveal interesting findings.

Chapter 4   Investigating TGF-α Production by NK Cells and Their Interplay with Hepatocytes: A 3D Coculture Approach

4.1 Introduction

Liver regeneration is a complex and highly orchestrated process essential for maintaining liver function and homeostasis (Michalopoulos & Bhushan, 2020) Upon injury or partial hepatectomy, the liver exhibits remarkable regenerative capacity, primarily driven by hepatocyte proliferation. NK cells, traditionally recognized for their role in immune surveillance and elimination of virally infected or tumor cells, have emerged as key players in tissue regeneration and repair (Vivier et al., 2011). During liver injury, the immune response is activated, leading to the recruitment and activation of NK cells in the liver microenvironment (Ali et al., 2021).

These NK cells secrete various cytokines and growth factors that modulate the regenerative process (Streetz et al., 2000). Among them, TGF-α stands out as a potent factor secreted by NK cells that can influence hepatocyte behavior (He & Karin, 2010). TGF-α plays a pivotal role in cell growth, differentiation, and tissue repair. NK cells have been postulated as an important source of TGF-α during liver regeneration (Sun & Gao, 2004).

In the liver, TGF-α acts as a mitogen for hepatocytes and triggers their entry into the cell cycle (Michalopoulos, 2007). TGF-α binds to the epidermal growth factor receptor on hepatocytes, activating downstream signalling cascades that promote cell division and tissue regeneration. This paracrine loop is critical for the initiation and progression of liver regeneration (He & Karin, 2010).

Studies have suggested that NK cells are capable of producing TGF-α in response to liver injury signals (Sun & Gao, 2004) This NK cell-derived TGF-α can act in both autocrine and paracrine manners. Autocrine signalling supports NK cell proliferation and activation, enhancing their

effector functions (Sun & Gao, 2004). Paracrine signalling, on the other hand, stimulates neighbouring hepatocytes to undergo proliferation and contributes to the restoration of liver mass (Sun & Gao, 2004). The interaction between NK cell-derived TGF-α and hepatocyte EGFR activation promotes hepatocyte entry into the cell cycle, cell division, and ultimately liver regeneration (Taub, 2004).

The interplay between NK cells and hepatocytes during liver regeneration is a dynamic and reciprocal process (Ali et al., 2021). NK cells respond to liver injury cues and infiltrate the regenerating tissue, where they establish a microenvironment favorable for hepatocyte proliferation. Concurrently, hepatocytes express factors that attract and activate NK cells, creating a feedback loop that supports tissue repair. Additionally, NK cells can directly interact with hepatocytes through cell-cell contact, further shaping the regenerative milieu (Ali et al., 2021)

The communication between NK cells and hepatocytes extends beyond TGF-α production. NK cells influence the microenvironment through the secretion of various cytokines, such as interferon-gamma (IFN-γ) and tumor necrosis factor-alpha (TNF-α) (Heymann & Tacke, 2016). These cytokines modulate hepatocyte responses to injury, inflammation, and regeneration.

This study seeks to unravel the intricate communication between NK cells and hepatocytes, focusing on the production of TGF-α by NK cells within a 3D coculture model. We hypothesize that NK cells play a role in TGF-α production and, by extension, impact the regenerative capacity of hepatocytes. Furthermore, an intriguing aspect of this investigation is the potential reciprocal relationship: can the coculture with hepatocytes lead to an expansion of NK cell populations producing TGF-α?. Understanding how the microenvironment influences NK cell

proliferation and survival could provide valuable insights into designing strategies for enhancing NK cell-based therapeutic approaches in liver diseases and regenerative medicine.

By examining the interactions between NK cells and HepG2 cells as well as the PBMCs and HepG2 cells in a 3D coculture model, we aim to shed light on the role of TGF-α in liver regeneration and elucidate the influence of NK cells on this process. The findings from this research may contribute to advancing our comprehension of liver biology and could pave the way for innovative strategies to promote tissue repair and regeneration.

4.2 Method

4.2.1 Thawing of PBMCs

A thawing solution was prepared by combining a 200µL aliquot of DNase I stock with 10mL of RPMI Media, which contained 10% FBS and P/S (to achieve a final concentration of 125µg/mL DNase I) . This mixture was placed in a 15mL falcon tube and pre-warmed to 37°C. Cryovials containing PBMCs, each with a concentration of $1x10^7$ cells/mL, were carefully transferred from liquid nitrogen to a 37°C water bath for thawing. Using a Pasteur pipette, 1mL of the pre-warmed thawing solution was added to each cryovial, taking about 30 seconds for this step. The diluted cell suspension was then centrifuged at 300 x g for 5 minutes. Following centrifugation, the pellet was then resuspended in 2.5mL of warm complete RPMI per single cryovial, with the goal of achieving a concentration of $4 x 10^6$ cells/mL. To allow the cells to rest, we transferred the specified volume into two wells of a 12-well cell culture plate. The plate was then incubated at 37°C in an environment with 5% CO2 for 24 hours prior to further analysis.

4.2.2 LPS Stimulation of PBMCs

After allowing the recovered PBMCs to incubate for 24 hours, we transferred them from the 12-well culture plate into appropriately labelled 15 mL Falcon tubes. Following this, we determined the cell count and then subjected the cells in the Falcon tubes to centrifugation at 300 x g for 5 minutes. Cells were then resuspended at 1.5 x 10^6 cells/mL in fresh media (RPMI supplemented with 10% heat inactivated foetal bovine serum and 1X penicillin/streptomycin).

In new 12-well plates, each sample was distributed into three separate wells at a concentration of 1.5 x 10^6 cells/mL per well. The first set of wells remained unstimulated, serving as controls. The second and third sets of wells were stimulated with 1 µg/mL and 5 µg/mL of LPS, respectively. We adjusted the volume in each well to a final measurement of 1 mL. The plates were then placed in an incubator at 37°C with 5% CO2 for the required durations, which were 6 hours and 24 hours.

4.2.3 3D Co-Culture Setup

In the co-culture experiment, we initiated the study by combining freshly isolated NK cells and HepG2 cells at a 1:1 ratio, each having a cell concentration of 1.25 x 10^5 cells/mL.

The methodological choice regarding the NK:Hepatocyte culture ratios in the co-culture experiment was based on several considerations aimed at achieving a balanced interaction between natural killer (NK) cells and HepG2 hepatocyte cells. The decision to combine these cell types at a 1:1 ratio, each having a cell concentration of 1.25 x 10^5 cells/mL, stemmed from the intention to create an environment that reflects a physiological equilibrium between NK cells and hepatocytes within the liver microenvironment. This ratio was chosen to simulate a scenario where both cell types are present in comparable proportions, aiming to mimic a realistic physiological setting relevant to liver regeneration.

The 1:1 ratio was selected after considering previous literature indicating the significance of NK cells in modulating hepatocyte functions during liver regeneration. Additionally, the chosen concentration of 1.25×10^5 cells/mL for each cell type aimed to strike a balance between providing a sufficiently dense culture for meaningful cellular interactions and avoiding overcrowding, which could potentially alter the dynamics of the co-culture system.

By maintaining an equal ratio of NK cells to HepG2 cells at a specified concentration, this experimental design sought to ensure that the interactions between these cell populations were representative of their *in vivo* counterparts, thus facilitating a more accurate assessment of their interplay.

These co-cultures were established in a final volume of 1 mL, utilizing Happy Cell ASM 3D growth media at a 1X concentration. Co-cultures using PBMCs and HepG2 cells were set-up in the same way, maintaining the same cell concentrations and ratio. This was achieved by gently mixing the required quantities of NK cells or PBMCs with HepG2 cells, along with the addition of Happy Cell ASM 3D culture medium in 15 mL falcon tubes. Furthermore, we prepared separate control setups for 3D cultures, consisting of HepG2 cells only, NK cells only, and PBMCs only. In order to ensure the viability of the cells throughout the duration of the experiment, we added interleukin-15 (IL-15) to all tubes at a concentration of 2 ng/mL before initiating the incubation process. Subsequently, all tubes were incubated for a period of 7 days. Following the completion of the 7-day incubation period, the co-cultures and control setups underwent flow analysis to assess their characteristics and interactions.

4.2.4 Extracellular Staining of 3D Coculture Samples for Flow Analysis

Co-culture and control tubes were briefly spun in a centrifuge to pellet the spheroids. From the initial 1 mL volume in each tube, we carefully withdrew 500 µL of supernatant, which was then stored in Eppendorf tubes for subsequent ELISA analysis.

Next, we introduced 10 µL of an inactivation solution (to inactivate the Happy Cell ASM 3D culture medium) into each tube and incubated for 30 minutes. After this period, the tubes underwent a 5-minute centrifugation at 300 x g. Following centrifugation, any remaining supernatant was gently removed from each tube using a P1000 pipette. Subsequently, 550 µL of HBSS was added to the tubes. We gently shook the contents of each tube and then subjected them to another 5-minute centrifugation at 300 x g. Once the second centrifugation cycle was complete, we carefully decanted the HBSS solution from the tubes. 500 µL of trypsin was then added to each tube, followed by a 20-minute incubation period. After this incubation, an equal volume of DMEM was uniformly added to all tubes. The tubes were mixed and subjected to a 5-minute centrifugation. At the end of this step, any remaining supernatants were discarded. To resuspend the cells in each tube, we added 300 µL of flow buffer. The contents of each tube were then transferred into freshly labelled flow tubes.

In each of the flow tubes, we introduced 20 µL of count beads, and then washed cells using flow buffer by centrifuging at 300 xg for 5 minutes. After this wash, we removed the supernatant, and the tubes were gently vortexed to facilitate cell resuspension. Following this, 1 µL of FCR blocking solution was added to all tubes. With the exception of the "Unstained" and "Live/Dead" tubes, 2.5 µL of primary TGF-α antibody was introduced to the other tubes. Cells were incubated for 20-minutes on ice. During this incubation, a master mix was prepared, containing all the remaining antibodies (rat anti-mouse IgM secondary, CD69, CD45, CD3, CD16, CD56, CD14) and a fixable live/dead stain. Details of these antibodies can be found in

chapter 3 (table number to be inserted). After the incubation period, all tubes were washed with flow buffer. Once the washing was complete, we discarded any remaining supernatants and vortexed the tubes to resuspend the cells. The prepared master mix was added to all tubes except the "Unstained" and "Live/Dead" tubes. The "Live/Dead" tube received only the live/dead stain. Subsequently, all tubes underwent an additional 20-minute incubation on ice. During this second incubation period, compensation tubes were prepared. Following the second incubation, both the sample tubes and compensation tubes were wash using flow buffer. The cells were then resuspended in a final volume of either 200 µL or 400 µL of flow buffer, depending on the flow cytometer to be used (Accuri or Attune flow cytometer, respectively). Finally, the prepared samples were acquired on the flow cytometer for analysis.

4.2.5 Intracellular staining of LPS stimulated PBMCs for Flow Analysis

Samples intended for intracellular flow staining analysis were treated with 1X monensin and brefeldin A solution in order to inhibit the export of proteins from the endoplasmic reticulum to the Golgi apparatus, thereby facilitating the accumulation of specific intracellular molecules. The monensin and brefeldin A solution was added prior to the 24-hour stimulation.

Following incubation cell samples were transferred into labelled 5ml flow tubes. Subsequently, a centrifugation at 300xg for 5 minutes was performed to remove the culture media. Cells were washed with flow buffer at 300xg for 5 minutes to ensure complete removal of any remaining media. The resulting cell pellet was gently resuspended in the buffer, and we added 1ul of FcR blocking solution to all tubes to prevent nonspecific antibody binding. Next, we prepared a master mix that included cell surface antibodies (CD69, CD45, CD3, CD16, CD56, CD14) for staining and a fixable live/dead stain. Details of these antibodies can be found in chapter 3 (table number to be inserted). The prepared master mix was then added to each tube, followed

by vortexing and an incubation period of 20-30 minutes at 4°C in the dark to prevent light-induced changes. After this incubation, we performed a wash step using flow buffer at 300xg for 5 minutes. The supernatant was discarded, and each tube was vortexed to resuspend the cell pellet.

To enable intracellular staining, we added 1 mL of Foxp3 Fixation/Permeabilization working solution to each tube, pulse-vortexed, and then incubated for 30 minutes at 4°C while protecting the samples from light. Following this, we added 2 mL of 1X Permeabilization Buffer, and the samples were centrifuged at 300 x g for 5 minutes at room temperature. The supernatant was discarded, and the pellet was gently resuspended by vortexing. We then added 1uL FcR blocking solution to all tubes before adding the primary TGF-α antibody (2.5ul per tube) to the cells. The tubes were then incubated for a minimum of 30 minutes at 4°C, once again in the dark. This incubation excluded the unstained, FMO (fluorescence minus one), and LD (live/dead) tubes. Following the incubation, we repeated the wash step using 2 mL of Permeabilization Buffer at 300 x g for 5 minutes. The supernatant was removed, and the tubes were vortexed to resuspend the cells. To ensure accurate staining, we added 2.5ul of rat anti-mouse IgM secondary antibody for 30 minutes at 4°C, all while protecting the samples from light. During this stage, we also prepared compensation tubes.

After the last incubation, we performed another wash cycle on all tubes, involving centrifugation at 300 x g for 5 minutes using flow buffer. The supernatant was once again discarded, and the tubes were vortexed to ensure proper resuspension of the cell pellets. To conclude the staining procedure, we gently resuspended the cells or beads in 400µL of flow buffer (for Attune NxT) or 200µL of flow buffer (for Accuri) and placed them on ice in the dark. The final step involved acquiring the beads or cells using the flow cytometer.

4.2.6 RNA extraction

All RNA extractions were carried out using PureLink™ RNA Micro Kit according to the protocol outlined in chapter 2.

4.2.7 cDNA synthesis

All cDNA syntheses followed the procedures detailed in chapter 2.

4.2.8 ELISA Analyses

To assess the expression of TGF-α proteins, the Human TGF-α ELISA Kit (catalogue number EHTGFAX10) by Invitrogen and the Human TGF-alpha Quantikine ELISA kit (catalogue number DTGA00) by R&D Systems were used in accordance with the manufacturer's instructions.

4.2.9 qPCR Analyses

To explore the expression levels of *TGFA, ADAM17, CSF2, EGFR, TNF-alpha, VEGFA*, and *MYC,* qPCR analyses were conducted per the protocol outlined in chapter 2.

In our investigation, *ADAM17* emerged as a key focus, given its fundamental role in cleaving and releasing TGF-α from the cell membrane (Yamamoto et al., 2020). This exploration aimed to shed light on the initial stages of TGF-α production and its regulation within PBMCs and liver resident NK cells. Futhermore, *TGFA* gene analysis directly linked gene expression to TGF-α production. By analyzing *TGFA* expression levels, we gained insights into the basal production of TGF-α and its potential modulation under varying stimuli.

EGFR and *VEGFA*, as previously mentioned in chapter 3, were analysed due to their significant roles in cell proliferation and angiogenesis, contributing substantially to the understanding of these critical processes regulated by TGF-α.

CSF2 and *TNF- α* were employed as positive control genes. *CSF2*, also recognized as Colony Stimulating Factor 2, was important in comprehending NK cell growth and differentiation within PBMCs and liver resident NK cells. Investigating CSF2 shed light on how TGF-α might influence NK cell behavior, given their involvement in immune responses (Mitra et al., 2012). *TNF-α,* a pro-inflammatory cytokine associated with liver injury and regeneration (Bourgine et al., 2012), was included in the analysis to explore the interaction between inflammatory responses and the potential regenerative effects induced by TGF-α.
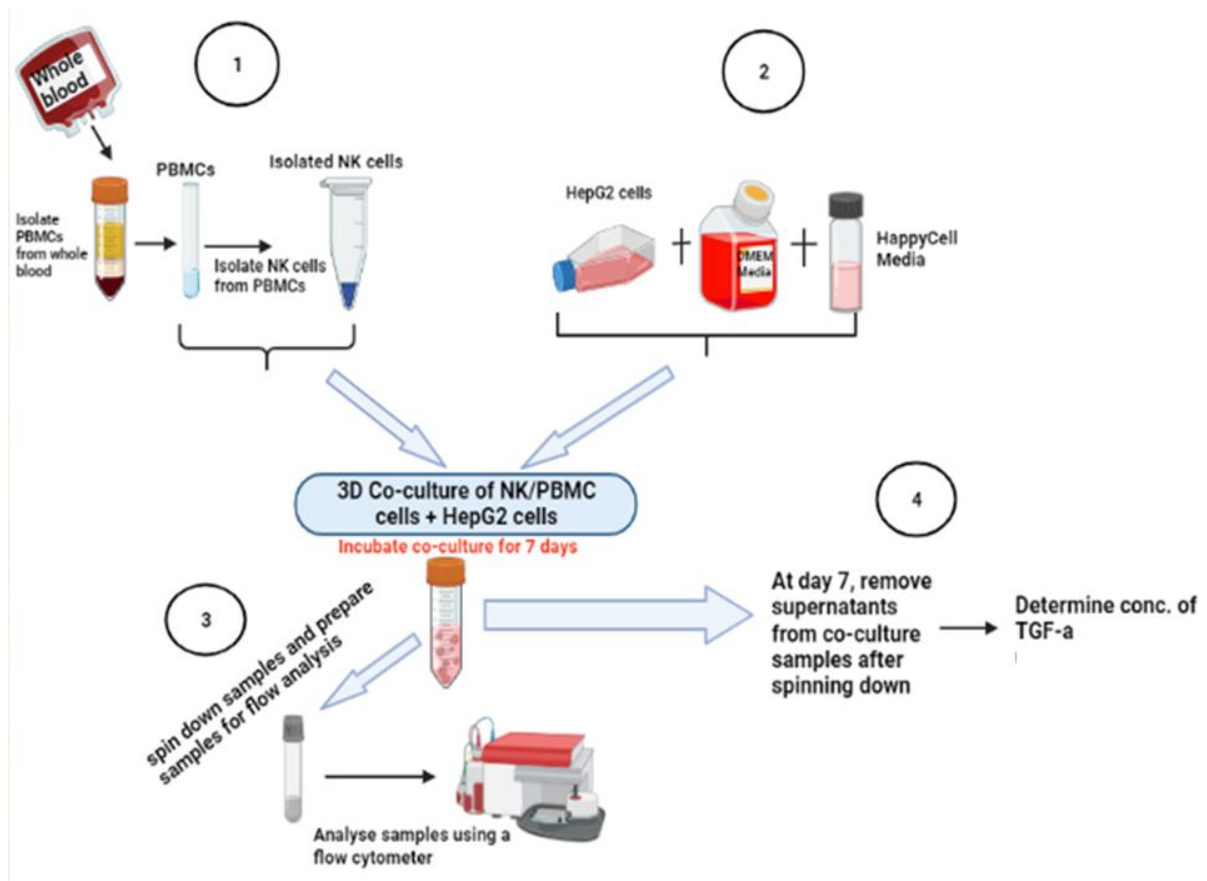
Figure 4. 1: Experimental Workflow for Assessing TGF-α Expression in a 3D Coculture System

Figure 4.1 illustrates the experimental workflow employed to investigate the expression of TGF-α within a 3D coculture system. **Phase 1** encompasses the isolation of PBMCs from whole blood samples, with subsequent isolation of NK cells from the PBMCs via magnetic cell sorting. **Phase 2** involves the cultivation of HepG2 cells with Happy Cell media. **Phase 3** features the coculture of PBMCs and NK cells with the 3D HepG2 culture. Following coculture, TGF-α expression in NK cells and PBMCs is assessed using flow cytometry. In **phase 4**, supernatants from the coculture system are collected and subjected to ELISA analysis to quantify the levels of TGF-α secreted in response to the coculture conditions.

4.3 Results

4.3.1 Confirming expression of *TGFA* gene in purified liver resident NK cells

4.3.1.1 *A Comparative Study of ADAM17, TGFA, and CSF2 Gene Expression in Liver Resident CD56^{Bright} and CD56^{Dim} NK Cell Subsets*

The primary objective of this study was to examine the variances in the expression levels of *ADAM17, TGFA,* and *CSF2* genes within unstimulated liver resident CD56^{Bright} and CD56^{Dim} NK cell subpopulations. Archived cDNA samples from flow sorted liver resident CD56Bright and CD56^{Dim} NK cell subpopulations (>98% purity) were analysed (obtained from the Robinson Lab). The expression levels of *TGFA* and *CSF2* were found to be elevated in the CD56^{Bright} group when compared to the CD56^{Dim} group, as depicted in Figure 4.2B and Figure 4.2C, respectively. In contrast to the observed alterations in *TGFA* and *CSF2* expression, the levels of *ADAM17* remained relatively stable across the CD56^{Bright} and CD56^{Dim} subsets of NK cells, as depicted in Figure 4.1A.
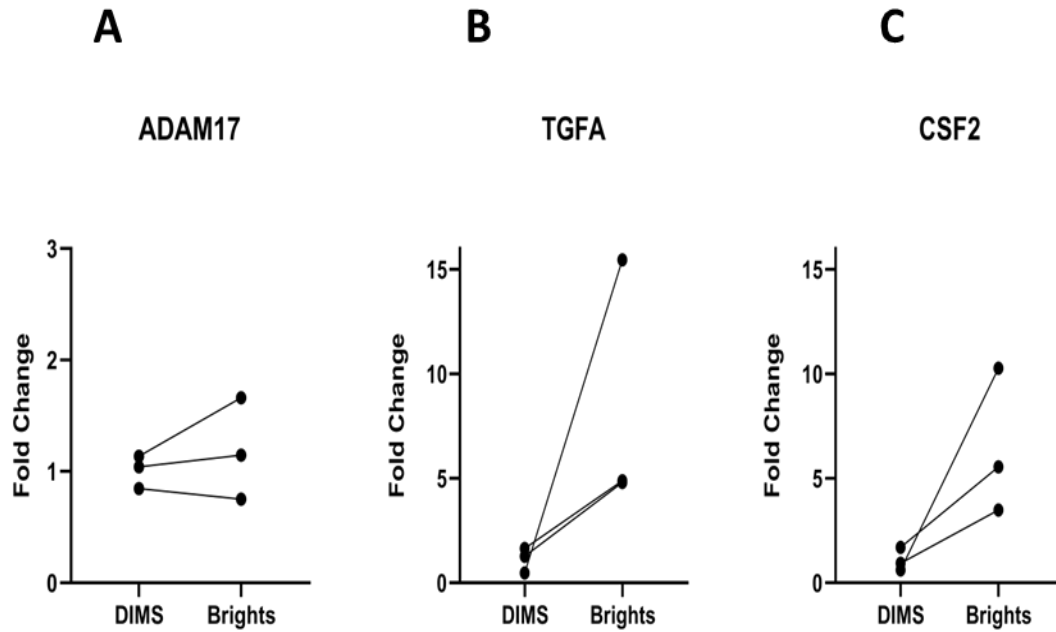
Figure 4. 2: Comparative Analysis of Expression of ADAM17, TGFA, and CSF2 Genes in Unstimulated Liver Resident CD56Brights and CD56Dims NK cell Populations.

Graphs A, B, and C represent the relative expression levels of *ADAM17*, *TGFA*, and *CSF2* genes, respectively, in unstimulated liver resident samples. The CD56Brights and CD56Dims NK cell Populations were compared among control groups (n=3 for each group). The data are presented as fold change, indicating the relative expression level compared to controls.

4.3.1.2 *Gene Expression Profiling in Liver-Resident NK Cell Subsets (CD56^{Bright} and CD56^{Dim}) Following Diverse Stimuli*

To assess if *TGFA* expression could be induced upon activation, we assessed the levels of expression of the *ADAM17*, *TGFA*, and *CSF2* genes within the liver-resident CD56^{Bright} and CD56^{Dim} NK cell populations subsequent to exposure to diverse activation stimuli. Archived cDNA samples from flow sorted liver resident CD56^{Bright} and CD56^{Dim} NK cell subpopulations (>98% purity) that were unstimulated, stimulated with LPS, stimulated with IL2/IL12 or stimulated with PMA and ionomycin (PMA/ION), were analysed (obtained from the Robinson Lab).

Our findings indicated no observable alteration in the expression of *ADAM17* across all sample groups within the CD56^{Bright} NK cell population (Figure 4.3A). In the subset of CD56^{Bright} NK cells, exposure to PMA/ION resulted in a notable increase in the expression of *CSF2* as observed in Figure 4.3C. No noteworthy alteration in the expression of *CSF2* was observed in CD CD56^{Bright} NK cells across all other stimulation groups.

Contrarily, the data revealed no noteworthy alteration in the expression of *CSF2* across all the groups of stimulated samples within the CD56^{Dim} NK cell population (Figure 4.4C).

Upon stimulation with IL-2/IL-12, a noteworthy increase in the expression of *ADAM17* was observed specifically within the CD56^{Dim} NK cell subset (as depicted in Figure 4.4A). In a similar vein, the expression of *ADAM17* exhibited a substantial increase upon exposure to PMA/ION stimulation specifically within the CD56^{Dim} NK cell subset (as depicted in Figure 4.4A).

The expression of *TGFA* was not detected in any of the stimulated sample groups, within both the CD56^{Bright} and CD56^{Dim} populations of NK cells.

Figure 4. 3: Expression Analysis of ADAM17, TGFA, and CSF2 Genes in Liver-Resident CD56Bright NK Cell Population upon Stimulation with LPS, IL2/IL12, and PMA/ION.

Graphs A, B, and C depict the relative expression levels of *ADAM17*, *TGFA*, and *CSF2* genes, respectively, in liver-resident CD56[Bright] NK cell populations under different stimulation conditions. Unstimulated samples served as the control group. The experiment included separate stimulations with LPS, IL2/IL12, and PMA/ION, with each sample group consisting of n=3 replicates.

The data is presented as fold change values relative to the geometric mean expression level. Statistical analysis was performed using the Friedman test to assess overall significance, followed by Dunn's multiple comparisons test. Significance levels are indicated as: * $p<0.05$, ** $p<0.01$, *** $p<0.001$.
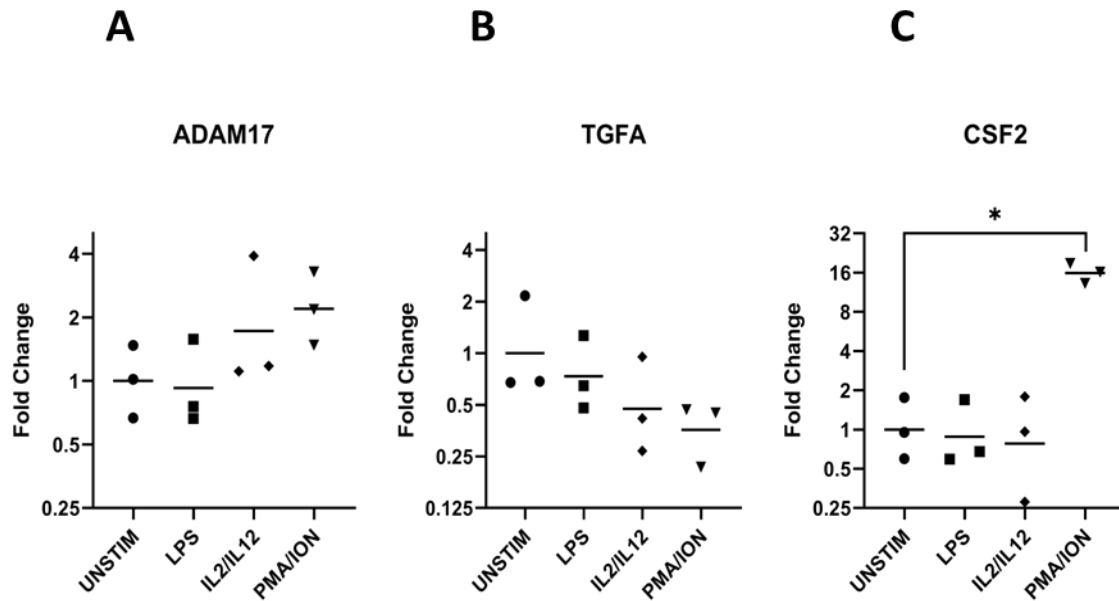
Figure 4. 4: Expression Analysis of ADAM17, TGFA, and CSF2 Genes in Liver-Resident CD56Dim NK cell Populations upon Stimulation with LPS, IL2/IL12, and PMA/ION.

Graphs A, B, and C depict the relative expression levels of *ADAM17*, *TGFA*, and *CSF2* genes, respectively, in liver resident CD56^{Dim} NK cell Populations under different stimulation conditions. Unstimulated samples served as the control group. The experiment included separate stimulations with LPS, IL2/IL12, and PMA/ION, with each sample group consisting of n=3 replicates.

The data is presented as fold change values relative to the geometric mean expression level. Statistical analysis was performed using the Friedman test to assess overall significance, followed by Dunn's multiple comparisons test. Significance levels are indicated as: * $p < 0.05$, ** $p < 0.01$, *** $p < 0.001$.
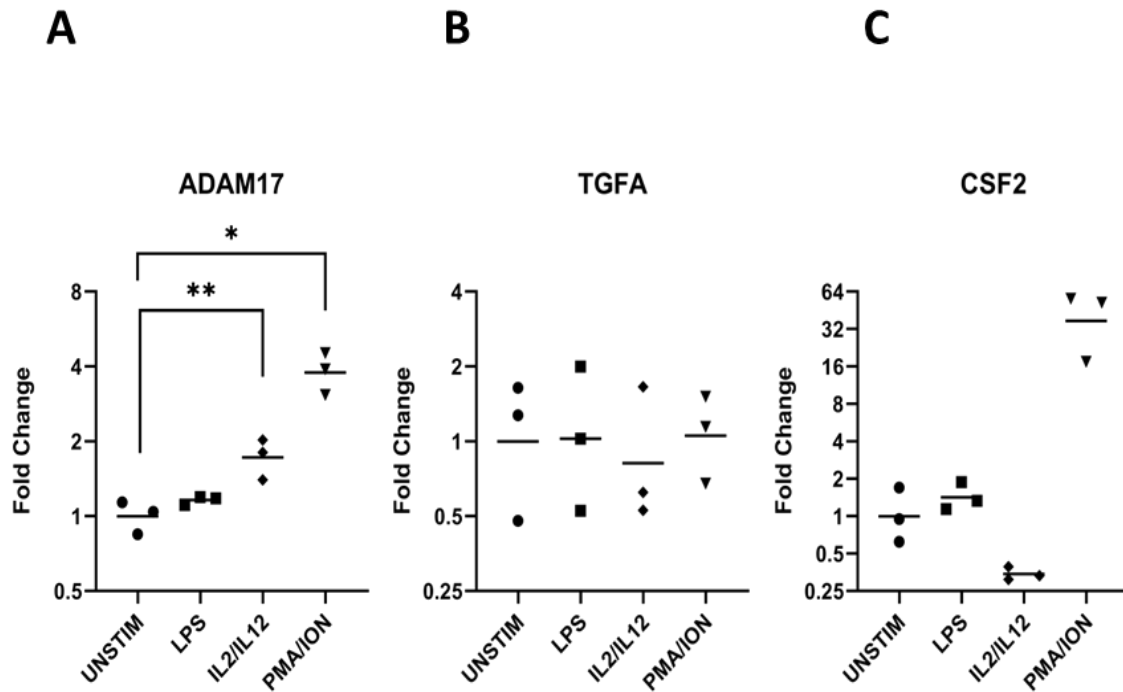
4.3.2 Validating Antibody Staining of TGF-α

4.3.2.1 *Gene Expression Dynamics in PBMCs Upon LPS Stimulation: Insights into ADAM17, TGFA, and CSF2 Regulation*

In order to validate protocols for detecting TGF-α protein expression by flow cytometry we utilised PBMC samples and LPS stimulation, which is known from previous research to induce TGF-α in monocytes (Rossol et al., 2011). We first aimed to elucidate the effects of LPS stimulation on the regulation of gene expression (*ADAM17, TGFA*, and *CSF2*), with specific emphasis on the time intervals of 6 hours and 24 hours.

At the 6-hour time point, the examination of gene expression revealed no discernible alterations in the expression levels of *ADAM17* (Figure 4.5A), *TGFA* (Figure 4.5B), and *CSF2* (Figure 4.5C) genes across the diverse LPS concentrations.

At the 24-hour time point, a notable upregulation in the expression of the *TGFA* gene was detected in both the 1ug/ml and 5ug/ml LPS-stimulated PBMC samples, as compared to the control group (Figure 4.6B). Furthermore, it was observed that the expression of the *CSF2* gene, which serves as a reliable indicator for LPS stimulation, exhibited a substantial increase in the samples treated with a concentration of 5ug/ml LPS after 24 hours (Figure 4.6C). Remarkably, an absence of substantial alterations was observed in the expression of the *ADAM17* gene upon exposure to either concentration of LPS at the 24-hour time interval (Figure 4.6A).
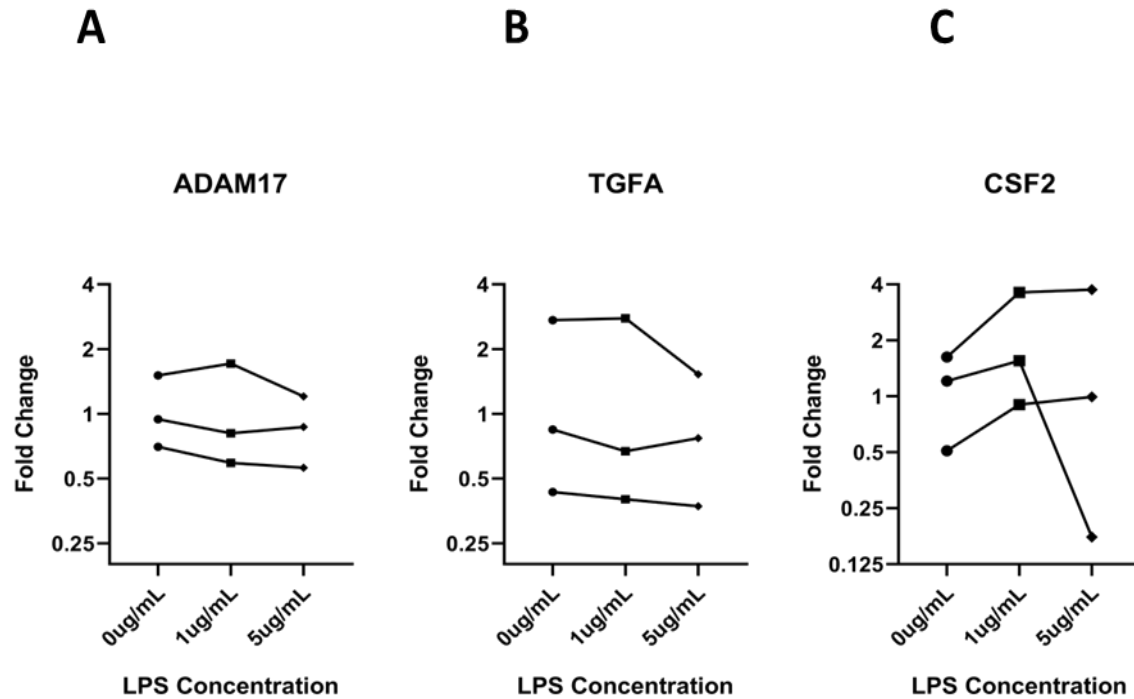
Figure 4. 5: Gene Expression Analysis of ADAM17, TGFA and CSF2 in LPS-Stimulated PBMC Samples at 6 hours.

Gene expression levels of *ADAM17* (A), *TGFA* (B), and *CSF2* (C) were investigated and PBMC samples following stimulation with LPS at concentrations of 1 μg/ml and 5 μg/ml for 6 hours. A control group without LPS stimulation (0 μg/ml) was included. All experimental groups consisted of triplicate samples (n=3). The expression levels are presented as fold changes compared to the control group. Statistical analysis was performed using the Friedman test followed by Dunn's multiple comparisons test.
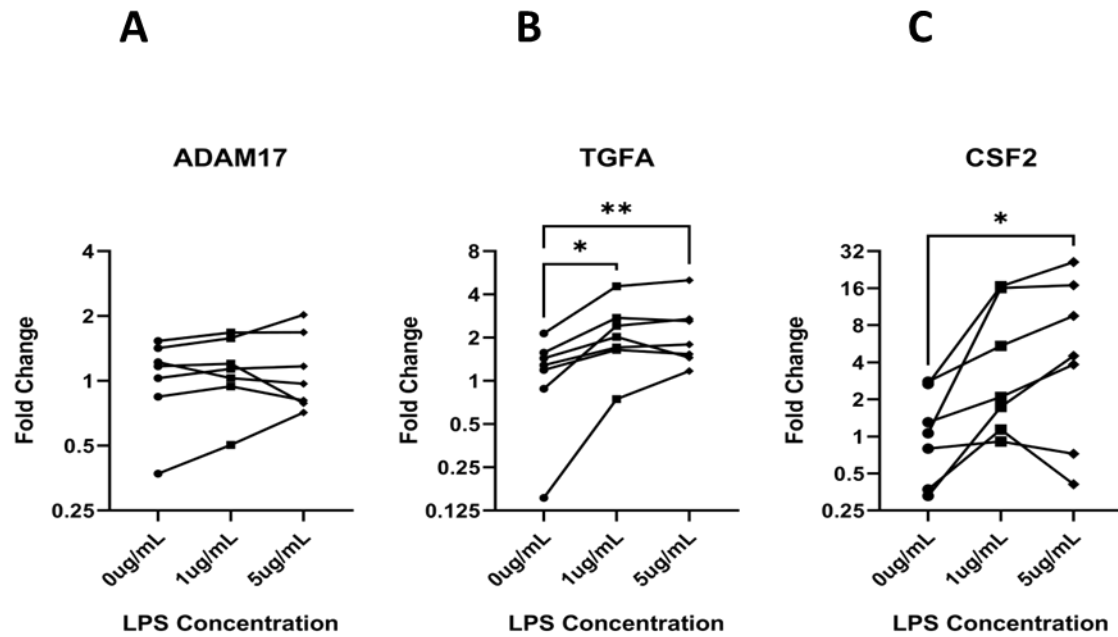
Figure 4. 6: Gene Expression Analysis of ADAM17, TGFA and CSF2 in LPS-Stimulated PBMC Samples at 24 hours.

Gene expression levels of *ADAM17* (A), *TGFA* (B), and *CSF2* (C) were investigated and PBMC samples following stimulation with LPS at concentrations of 1 μg/ml and 5 μg/ml for 24 hours. A control group without LPS stimulation (0 μg/ml) was included. All experimental groups consisted of triplicate samples (n=7). The expression levels are presented as fold changes compared to the control group. Statistical analysis was performed using the Friedman test followed by Dunn's multiple comparisons test (*p<0.05, **p<0.01, ***p<0.001).

4.3.2.2 *Assessing TGF-α Expression in PBMCs After LPS Stimulation: A 24-Hour ELISA Investigation*

In order to validate the up-regulation of the *TGFA* gene observed in PBMCs upon LPS stimulation, we next utilised ELISA to direct measure TGF-α in culture supernatants. After 24 hours of LPS stimulation, both the absorbance readings and assessed concentrations revealed a discernible increase in TGF-α protein levels within the supernatants of the stimulated PBMCs, at both 1 µg/ml and 5 µg/ml LPS concentrations (Figure 4.7).
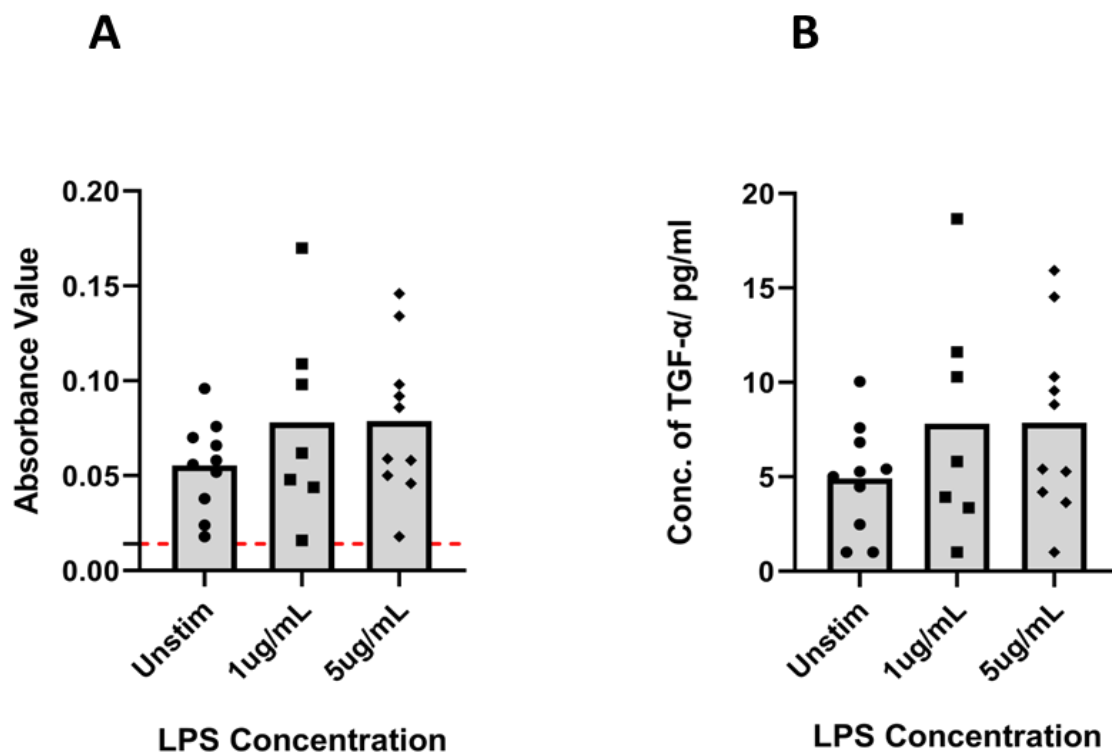
Figure 4. 7: Expression of TGF-α in PBMC Samples following LPS Stimulation for 24 hours.

ELISA analysis was conducted to investigate the expression of TGF-α in PBMC samples following stimulation with LPS. PBMC samples were subjected to stimulations with 1 μg/ml (n=7) and 5 μg/ml (n=10) of LPS for a duration of 24 hours. A control group without LPS stimulation (0 μg/ml, n=10) was included for comparison. **Graph A** depicts absorbance readings. The dashed red lines shown represent the background reading. **Graph B** represents the concentrations of assessed TGF-α across all sample groups. Mean values were plotted as data points. Statistical analysis was performed using an Ordinary one-way ANOVA followed by Dunnett's multiple comparisons test.

4.3.2.3 *Impact of LPS Stimulation on CD69 and TGF-α Expression in NK Cells and Monocytes Cells in PBMCs: A Flow Cytometry Analysis.*

Having confirmed that TGF-α is induced at a transcriptional level and at a protein level in PBMCs upon LPS stimulation, we next assessed the ability of our flow cytometry protocol to detect this up-regulation. We first assessed an extracellular staining protocol for TGF-α and CD69 in NK cells and monocytes cells present within PBMCs stimulated with 5ug/ml LPS stimulation for 24 hours. The MFI values were quantified as measures of TGF-α and CD69 expressions based on the flow gating strategy described in Figure 4.8.

Our results showed a statistically significant augmentation in the expression of the CD69 marker within the NK cell subset (Figure 4.9A). The data presented suggests that the stimulation of LPS had a notable impact on the induction of CD69 expression in NK cells.

In contrast to the observed effects of CD69 in the NK cell subset, the examination of CD69 expression failed to unveil any notable alterations in monocytes cells (Figure 4.9C) after LPS stimulation. No discernible modifications in the expression of TGF-α were observed in either the NK cells (Figure 4.9B) or of myeloid cells populations (Figure 4.9D). The MFI values observed for TGF-α expression in both NK cells and CD14+ monocytes were largely indistinguishable from the FMO control, indicating that specific staining of TGF-α was not present.
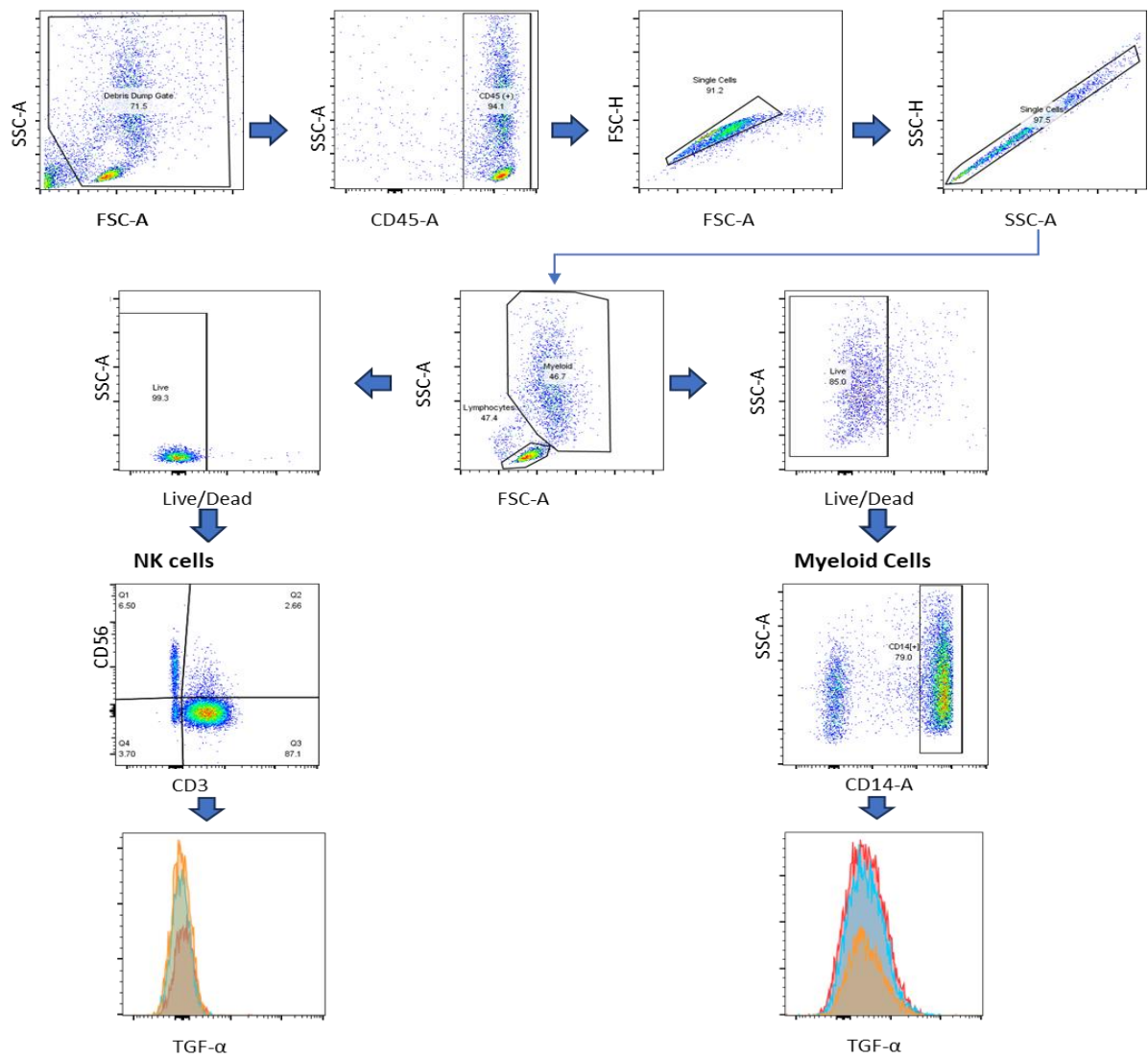
Figure 4. 8: Flow Gating Strategies for TGF-α Quantification in NK Cells and Monocyte Cells within PBMCs

Flow cytometry gating strategies employed to quantify TGF-α expression in NK cells and monocyte cells isolated from PBMCs. Forward scatter (FSC) and side scatter (SSC) profiles were used to identify the PBMC population. Doublet discrimination was applied to exclude cell aggregates and Live cells were gated based on viability staining. Subpopulations of monocyte cells were identified using cell-specific marker CD14. NK cells were distinguished from other lymphocytes using NK cell-specific markers, CD3−CD56+. TGF-α expressions were assessed within the defined NK cell and monocyte cell populations, and median fluorescence intensity were quantified as measures of TGF-α expression.
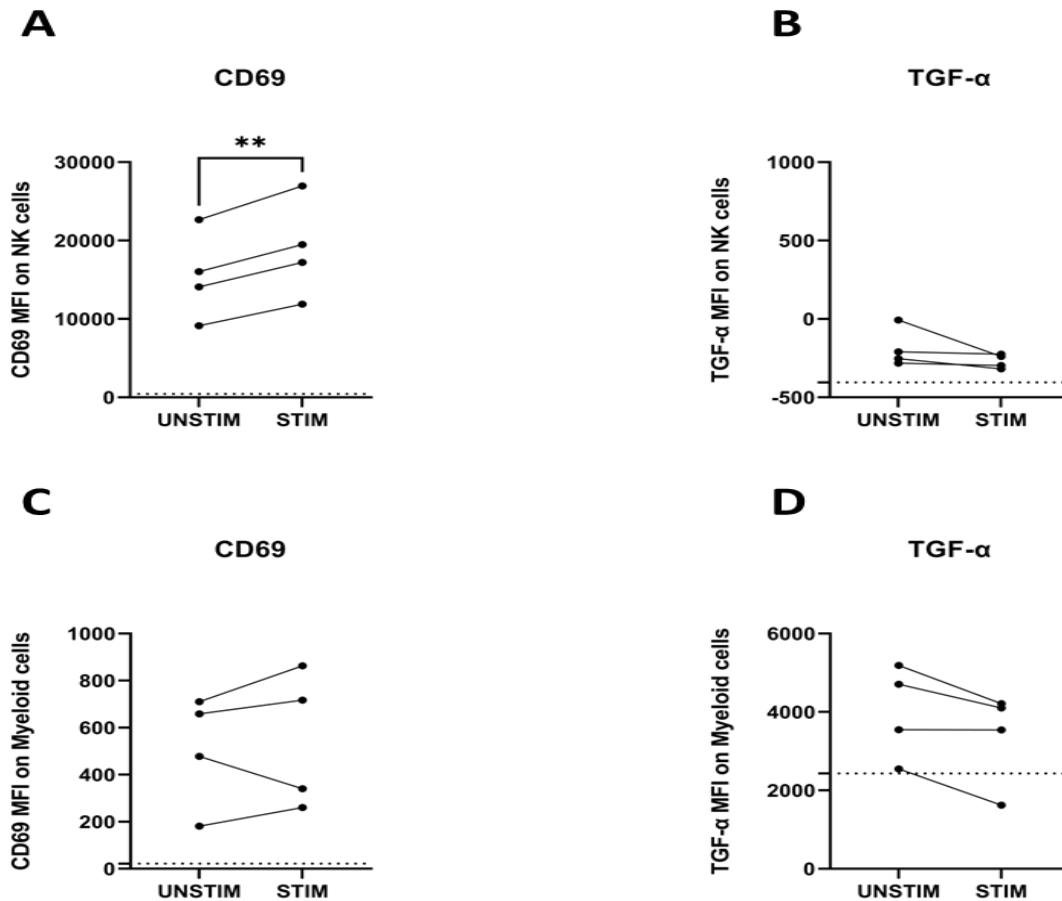
Figure 4. 9: Extracellular Expression of CD69 and TGF-α Markers in LPS-Stimulated PBMC Samples across NK and Monocyte Cell Groups.

The experiment aimed to investigate the extracellular expression of CD69 and TGF-α markers in two distinct PBMC subsets, namely NK cells and monocyte cells, following stimulation with LPS. PBMC samples were stimulated with LPS at a concentration of 5ug/ml for 24 hours, while unstimulated samples were utilized as controls. Extracellular staining was performed to assess the expression of the markers utilizing flow cytometry.

Graphs A and B depict the expression profiles of CD69 and TGF-α, respectively, in NK cells. Graphs C and D illustrate the corresponding expression patterns of CD69 and TGF-α in monocyte cells. MFI values used for data representation. The horizontal dashes evident in each graph represent FMO values, with FMO CD69 values utilized for Graphs A and C, and FMO TGF-α values for Graphs B and D. All experimental groups consisted of n=4 samples each. Statistical analysis was conducted using a paired t-test (*p<0.05, **p<0.01, ***p<0.001).

4.3.2.4 *Intracellular TGF-α Expression in PBMCs after LPS Stimulation: Lack of Significant Alterations in NK and Monocyte Cell Populations*

Given the absence of observable TGF-α expression on the cell surface of PBMCs subjected to LPS stimulation, we proceeded to examine whether intracellular expression of TGF-α was detectable. There was no detectable change in the expression of TGF-α within both the NK cells (Figure 4.10A) and the CD14+ monocytes (Figure 4.10B), LPS stimulation. Similar to the extracellular staining protocol, the MFI values observed for TGF-α expression in both NK cells and CD14+ monocytes were largely indistinguishable from the FMO control, indicating that specific staining of TGF-α was not present.
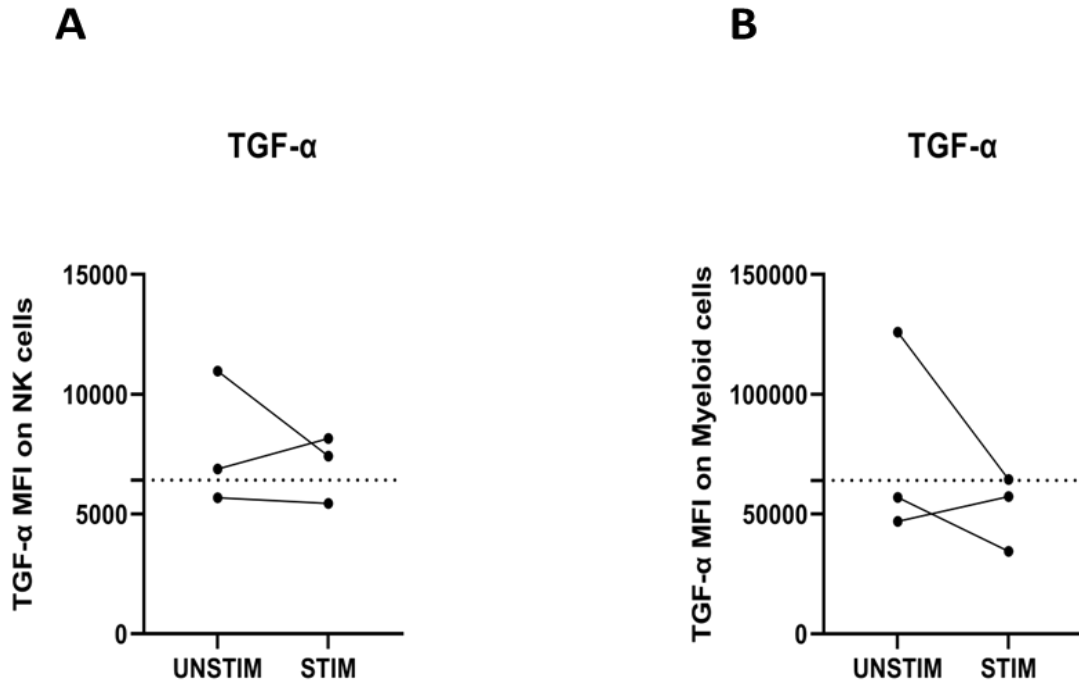
Figure 4. 10: Intracellular Expression of TGF-α in LPS-Stimulated PBMC Samples across NK and Myeloid Cell Groups.

Intracellular expression of TGF-α was investigated in PBMC samples stimulated with LPS at a concentration of 5 μg/ml for 24 hours. Unstimulated samples served as controls. Flow cytometry analysis was utilized to detect TGF-α expression in NK cells (Graph A) and Myeloid cells (Graph B). MFI values of intracellular TGF-α were used for data representation, with FMO TGF-α values indicated by dashed lines on each graph. All sample groups were composed of n=3 replicates. Statistical significance was assessed using paired t-test analysis.

4.3.3 3D Co-Culture to Determine if NK Cells Induce TGF-α

4.3.3.1 *Comparative Analysis of NK Cell Expansion in 3D Coculture Models: NK-HepG2 vs. PBMC-HepG2*

Previous research in the Robinson Lab described the expansion of NK cell populations upon co-culture with hepatocyte cell lines (Jameson et al., 2021). We initially assessed two different co-culture models to replicate this previous observation: NK-HepG2 coculture (n=3) and PBMC-HepG2 coculture (n=3). The flow cytometric gating strategy as described in Figure 4.11 was used to identify and quantify NK cell populations within the co-culture systems.

The examination of the NK cell populations subsequent to a 7-day period of co-culture revealed that in the NK-HepG2 coculture, a slight decrease in the percentage NK cells was observed (Figure 4.12A). In contrast the PBMC-HepG2 coculture exhibited an obvious expansion in the percentage of NK cells (Figure 4.12B).
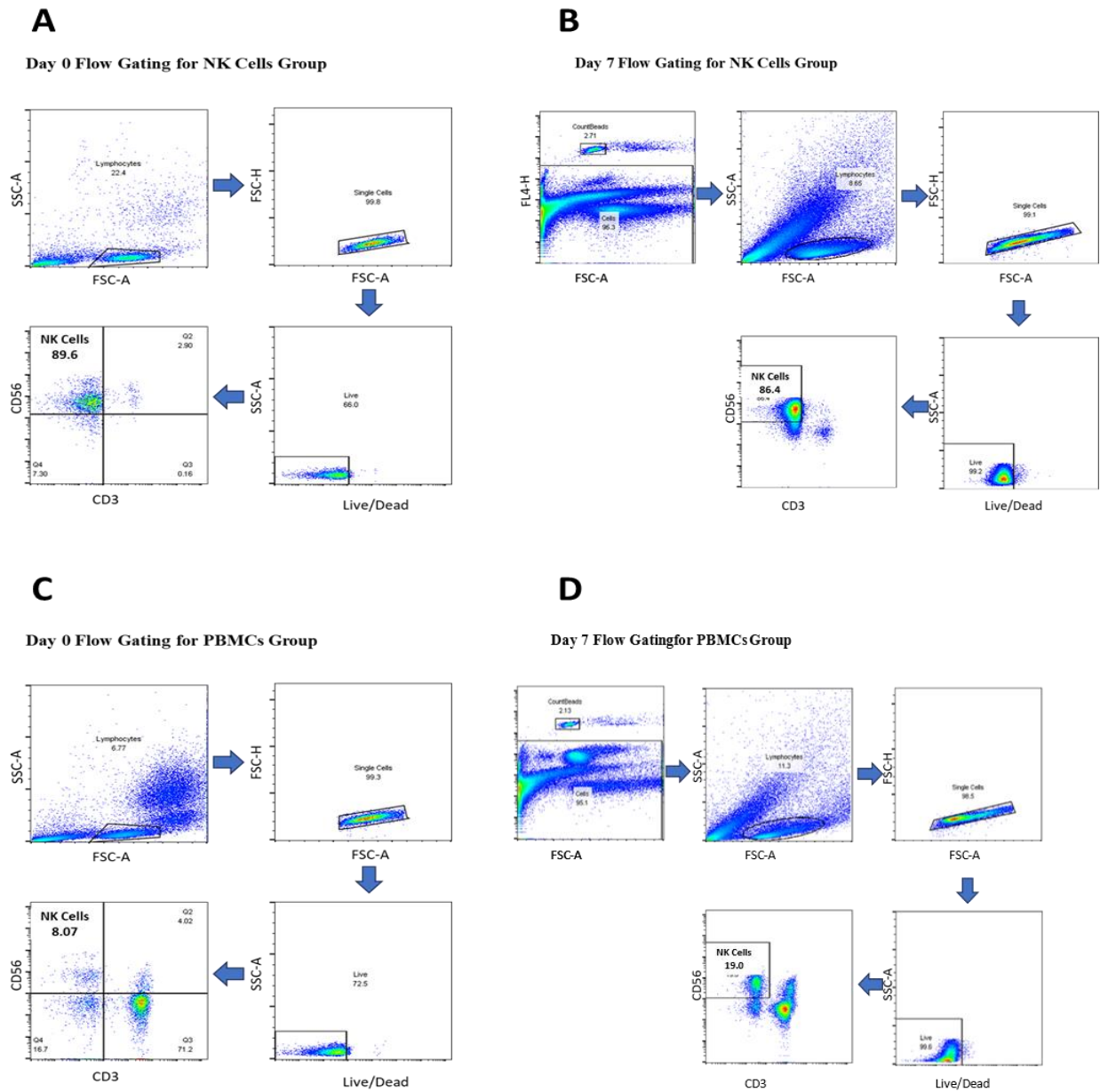
Figure 4. 11: Flow Gating Strategies for NK Cell Quantification in 3D co-culture

Representative flow cytometry gating strategies employed for the quantification of NK cell numbers in 3D cocultures of NK cells group and PBMCs group at both day 0 and day 7 timepoints using one sample in each group. (A) gating strategy for NK cells at day 0 in the NK group, (B) gating strategy for NK cells at day 7 in the NK group, (C) gating strategy for PBMCs at day 0 in the PBMC group, (D) gating strategy for PBMCs at day 7 in the PBMC group. The lymphocytes were gated using FSC/SSC scatter. The NK cells were identified as CD3−CD56+ cells.
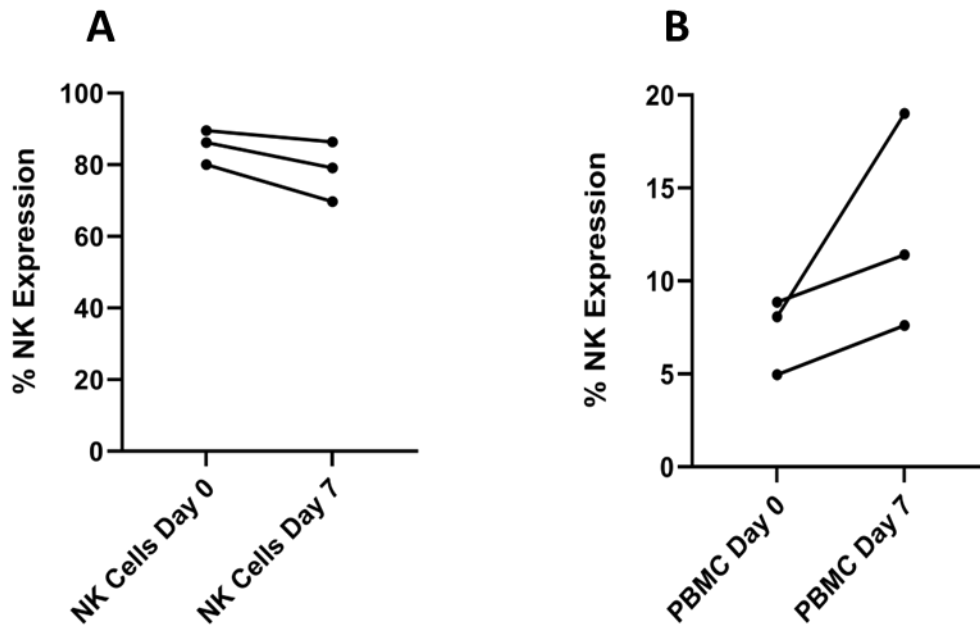
Figure 4. 12: Comparison of %NK Expression in 3D Co-culture Models

To investigate changes in NK cell populations, two distinct 3D co-culture systems were employed: NK-HepG2 and PBMC-HepG2. **(A)** Graph A illustrates the %NK expression within the NK-HepG2 3D co-culture over a 7-day period, spanning from Day 0 to Day 7. **(B)** Graph B depicts the %NK expression in the PBMC-HepG2 3D co-culture over the same time frame. Notably, a marked increase in %NK expression was observed within the PBMC-HepG2 3D co-culture group. The experiment was performed in triplicate (n=3) for all groups.

4.3.3.2 *Expression of TGF-α Is Undetectable in 3D Co-Culture Supernatants.*

Having replicated the previous observation that NK cells expand within PBMC and hepatocyte co-culture systems we next assessed the expression of TGF-α in supernatants. Supernatants were collected from NK-HepG2 co-culture experiments, PBMC-HepG2 co-culture experiments, HepG2 control spheroids, NK cell controls, and PBMC controls. The quantification of TGF-α levels was carried out employing ELISA techniques.

Our analysis revealed consistent levels of TGF-α expression across all sample groups, as both absorbance values (Figure 4.13A) and assessed concentrations (Figure 4.13B) indicated no statistically significant alterations. It is noteworthy that the measured TGF-α concentrations in supernatants consistently fell below the lowest ELISA standard concentration of 15.6 pg/ml. This is in marked contrast to previous experiments utilising LPS stimulated PBMC samples, where TGF-α expression is detectable.
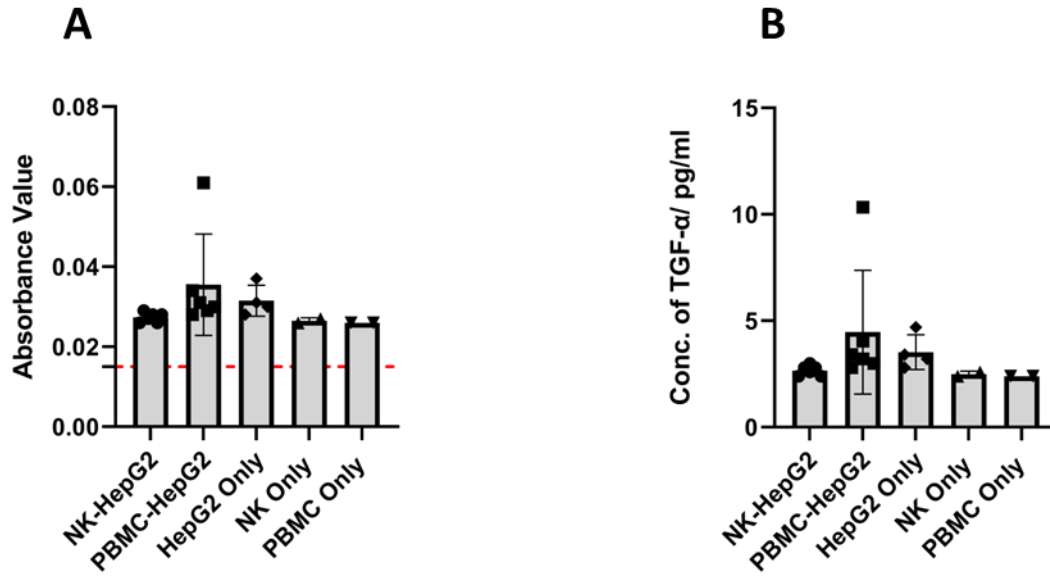
Figure 4. 13: ELISA Analysis of TGF-α Expression in 3D Co-culture and Monoculture Systems.

Graphs depicting the results of ELISA analysis investigating the expression of TGF-α in various 3D culture samples. The experiment involved the following groups: NK-HepG2 coculture (n=6), PBMC-HepG2 coculture (n=6), HepG2 only (n=4), NK only (n=2), and PBMC only (n=2). Graph A illustrates the absorbance readings obtained from the ELISA analysis across the different cell groups. The dashed red lines shown represent the background reading. Graph B presents the concentrations of assessed TGF-α in the respective sample groups. The data points in both graphs are represented as the mean values along with standard deviations. The analysis employed an Ordinary one-way ANOVA followed by Tukey's multiple comparisons test for statistical analysis.

4.3.3.3 *Gene Expression Profiling in 3D Co-Cultures Reveals A Lack of TGFA Upregulation.*

Results from the ELISA experiments on 3D co-culture supernatants suggested that co-culture with NK cells does not result in detectable TGF-α. To confirm we observation we delved into the gene expression profiles of key genes, namely *TNFA, MYC, VEGFA, ADAM17*, *TGFA*, and *EGFR*. 3D co-cultures of PBMCs and HepG2 cells were incubated for a duration of five days and the RNA was extracted. HepG2-only samples served as controls for the experiment.

Notably, we observed an increase in *TNFA* expression within the PBMC co-culture samples in comparison with the control group (Figure 4.14A), consistent with the idea that the addition of immune cells (PBMCs) results in the detection of genes associated with immune cells. The expression levels of *MYC, VEGFA, ADAM17*, *TGFA*, and *EGFR* remained unchanged in the PBMC-HepG2 co-culture. Our findings imply that under the specific co-culture conditions used in this study, there is no discernible upregulation of *TGFA*. These genes appear to demonstrate a level of resilience or insensitivity, as they remained unaltered in their expression levels, showing no statistically significant shifts.
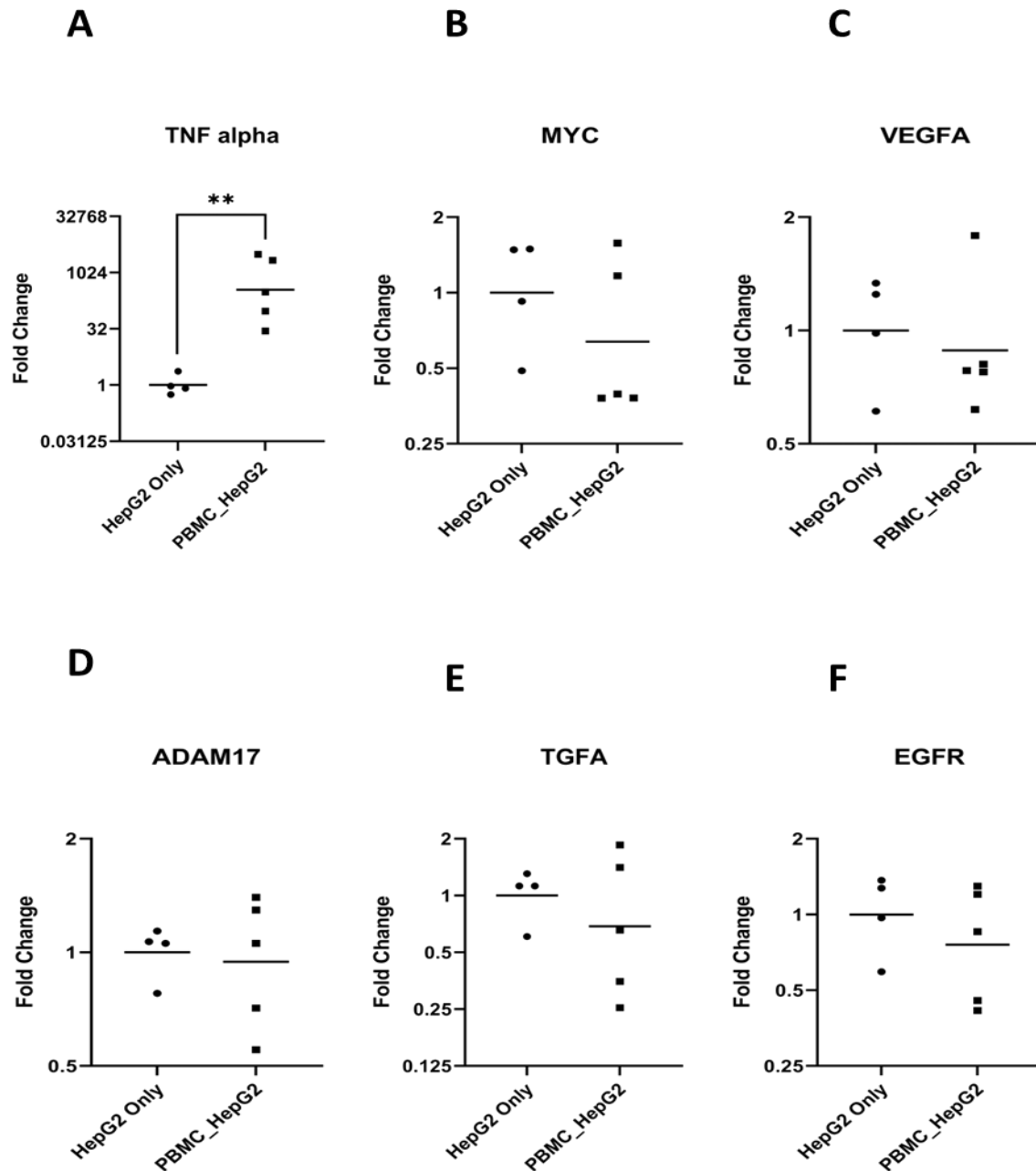
Figure 4. 14: Gene Expression Analysis in 3D Cultures of PBMC-HepG2 Coculture and HepG2 Monoculture.

Graphs depict the fold change in gene expression of **(A)** *TNFA*, **(B)** *MYC*, **(C)** *VEGFA*, **(D)** *ADAM17*, **(E)** *TGFA*, and **(F)** *EGFR* in 3D culture samples comprising PBMC-HepG2 coculture and HepG2 monoculture. Incubation period was 5 days, and HepG2 monoculture samples served as controls. The PBMC-HepG2 coculture group consisted of n=4 samples, while the HepG2 monoculture group comprised n=5 samples. Statistical significance between groups was determined by paired t-test (*p < 0.05, **p < 0.01, *** p<0.001).

4.4 DISCUSSION

The results from this chapter have illuminated the regulation and expression of TGF-α in NK cell populations. We have confirmed the expression of *TGFA* in liver-resident NK cell populations at a transcriptional level. Moving on from here we have utilised LPS stimulation of PBMCs to validate experimental techniques for the detection of TGF-α. We utilised these techniques to demonstrate that while PBMC and hepatocyte co-culture induces expansion of NK cell populations, there is no upregulation of TGF-α protein or the *TGFA* gene during this co-culture protocol. These results underscore the complexity of the interactions between hepatocytes and immune cell populations, emphasizing the need to consider temporal, cell-specific, and contextual factors when studying gene expression and immune regulation.

The results obtained from our comparative analysis of gene expression patterns in unstimulated liver resident CD56^{Bright} and CD56^{Dim} NK cell populations shed light on the potential functional differences between these subsets within the liver's microenvironment. The elevated levels of *TGFA* and *CSF2* gene expression observed in CD56^{Bright} NK cells raise intriguing possibilities regarding the unique roles these genes may play within this specific subset. Given TGF-α's established functions in immune regulation and cell proliferation, as well as *CSF2*'s well-documented involvement in coordinating immune responses, it is plausible that these genes could act as key drivers of distinct immune activities within the liver's microenvironment (Mitra et al., 2012). Conversely, the unchanged expression levels of *ADAM17* across both CD56^{Bright} and CD56^{Dim} NK cell subsets hint at its conserved importance in NK cell function, irrespective of the CD56 phenotype.

Building upon these insights, our investigation delved deeper into the functional diversity exhibited by distinct subsets of NK cells and their responsiveness to various activating signals.

Of particular significance is the substantial upregulation of *CSF2* expression exclusively within the CD56[Bright] NK cell population following PMA/ION stimulation. This noteworthy observation may be attributed to the cytokine-producing nature of CD56[Bright] NK cells (Cooper et al., 2001), potentially driving the induction of *CSF2*. This discovery holds particular significance in the context of the liver microenvironment, as it suggests a potential functional role for *CSF2* in modulating CD56[Bright] NK cell activities. The findings suggest that there is a potential connection between *CSF2* processes related to tissue regeneration. *CSF2* may play a crucial role in cells involved in tissue repair, inflammation, or immune modulation. This indicates that *CSF2* might have specialized functions in these contexts, potentially aiding in the regeneration of the liver. However, more in-depth research is needed to fully understand and specify the precise role of *CSF2* in these cells during the process of regeneration.

The significant upregulation of *ADAM17* in both IL-2/IL-12 and PMA/ION stimulated samples suggests its involvement in the response of CD56[Dim] NK cells to distinct activating signals (Romee & Miller, 2015; Yamamoto et al., 2020). The IL-2/IL-12 pathway is well-established for its role in augmenting NK cell cytotoxicity and effector functions (Cooper et al., 2001; Vivier et al., 2008) The observed upregulation of *ADAM17* in this context may imply its participation in cytokine receptor signalling, potentially influencing downstream responses to IL-2/IL-12. Likewise, the heightened expression of *ADAM17* upon PMA/ION stimulation hints at its role in downstream signalling pathways activated by these potent activators (Black et al., 1997; Yamamoto et al., 2020)

Intriguingly, the expression of *ADAM17* remained unaltered across all examined sample groups within the CD56[Bright] NK cell population, shedding light on potential disparities in the regulatory networks governing *ADAM17* expression between CD56[Bright] and CD56[Dim] NK cells (Yamamoto et al., 2020). This divergence in *ADAM17* expression may be linked to the distinct

functional roles attributed to these two NK cell subsets. CD56^{Bright} cells are conventionally associated with cytokine production and regulatory functions, as opposed to direct cytotoxicity (Cooper et al., 2001; Vivier et al., 2008)

The absence of *TGFA* expression within all stimulated sample groups, in both CD56^{Bright} and CD56^{Dim} NK cell populations, suggests that *TGFA* may not play a primary role in the immediate transcriptional response of liver-resident NK cells to the tested stimuli. Nonetheless, it is imperative to recognize that the lack of detectable *TGFA* expression does not preclude its potential involvement in other contexts or under distinct stimulatory conditions. Subsequent investigations are imperative to ascertain whether *TGFA* may exert an influence in specialized scenarios or if its expression is elicited by stimuli not examined in this study.

Transitioning from the realm of liver-resident NK cells to a broader perspective, our attention shifts towards LPS-stimulated PBMCs. The study of these peripheral blood mononuclear cells imparts valuable insights into the intricate interplay between LPS stimulation and the dynamics of gene expression within PBMCs. The absence of significant changes in gene expression observed at the 6-hour time point suggests that the initial immune response may not have had a substantial impact on the transcriptional activity of the *ADAM17*, *TGFA*, and *CSF2* genes, possibly due to the timing of the transcriptional response.

This observation aligns with the concept that certain cellular responses, particularly those entailing gene expression changes, may necessitate an extended period to manifest fully (Medzhitov & Janeway, 2000).

The contrasting observations at the 24-hour time point underscore the temporal dynamics inherent to immune responses. The evident upregulation of *TGFA* expression implies its potential multifaceted involvement in the delayed immune response initiated by LPS, particularly at the transcriptional level within PBMCs. This surge in *TGFA* expression also

hints at its presumed pivotal role as a central orchestrator in various immune-related processes, including but not limited to inflammation and cell proliferation (Dranoff, 2004). The delayed response observed may suggest that certain genes may partake in the resolution or modulation of the immune reaction, rather than its initial triggering phase. Furthermore, the increase in *CSF2* gene expression, especially in response to LPS, reaffirms its status as a reliable indicator of successful immune activation (Sielska et al., 2020).

However, the unaltered *ADAM17* gene expression suggests that *ADAM17* may not be directly implicated in the gene expression changes under the experimental conditions. This emphasizes the gene-specific responses to LPS and highlights the complexity of cellular reactions to immune stimuli. This finding prompts further exploration into the potential involvement of *ADAM17* in other facets of the immune response or different experimental contexts. The findings from this investigation of LPS-stimulated PBMCs suggest PBMCs' capacity to mount a robust immune response when stimulated by LPS and contribute significantly to our comprehension of the intricate regulatory mechanisms governing gene expression in response to LPS stimulation. The results indicate that *ADAM17*, *TGFA*, and *CSF2* exhibit divergent expression patterns in PBMCs across varying time intervals and LPS concentrations. This diversity in responses stresses the imperative need for a comprehensive approach when investigating immune responses, taking into account multiple contributing factors influencing gene expression modulation.

Expanding upon our gene expression analysis, we turn our attention to the assessment of TGF-α protein expression in PBMCs in response to LPS stimulation using ELISA techniques. The substantial augmentation in TGF-α expression observed following 24 hours of stimulation signifies a time-dependent regulatory response to LPS exposure. This observation suggests that

the prolonged exposure to LPS has induced a noteworthy upregulation in TGF-α production within PBMCs.

To further enhance our insight into TGF-α expression dynamics, we employed flow cytometry analysis to delve deeper into the immune cell behaviors during LPS stimulation.

The flow cytometry analysis has yielded valuable insights into the response of NK cells and monocytes to LPS stimulation, particularly in relation to the expression of TGF-α. However, our observations concerning TGF-α expression have raised significant concerns regarding the functionality of the antibodies employed in our experimental setup. In contrast to the expected increase in CD69 expression in NK cells following LPS stimulation, our data indicate no discernible changes in the expression of TGF-α in either NK cells or monocytes. This deviation from the anticipated response is noteworthy, considering the established role of TGF-α in immunoregulation and its documented production by various immune cell types, including monocytes (Derynck et al., 2001).

The MFI values for TGF-α closely resembling those of the FMO control strongly suggest that the antibodies used to detect TGF-α may not be efficiently binding to the target in our samples. This raises a critical concern regarding the reliability of our measurements of TGF-α. Several factors could potentially contribute to this observation.

First and foremost, the antibodies themselves may not be functioning optimally within our experimental system. Antibody performance can be influenced by various factors, including batch variability, storage conditions, and sensitivity to the specific tissue or cellular milieu (Baker, 2015; Bradbury & Plückthun, 2015).

Furthermore, it is crucial to take into account the cellular context and timing of TGF-α expression. TGF-α production often constitutes a rapid and transient response to specific

stimuli. The choice of a 24-hour time point for our analysis may not align with the peak expression of TGF-α in our system. Conducting additional experiments at different time points may better capture the dynamic changes in TGF-α expression.

This observation may also suggest that this cytokine might not be directly influenced by LPS stimulation at the extracellular level within the assessed timeframe. Also, the lack of detectable expression of TGF-α could suggest that their relevance in these stimulated systems is limited, or their expression occurs at levels below the sensitivity of the assay used. Such a revelation prompts questions into the specific signalling pathways and molecular components implicated in the initial phases of LPS-induced immune activation.

Based on our findings from the extracellular staining flow analysis, we hypothesized that it is possible that TGF-α was being produced intracellularly but had not yet been released into the extracellular environment. Therefore, we redirected our focus towards evaluating the intracellular expression of TGF-α within our LPS-stimulated PBMCs. Intriguingly, the outcomes of this investigation also revealed absence of significant TGF-α expression within both NK and myeloid cell subpopulations. This discovery bears significance, especially considering the well-established roles of TGF-α in cellular responses and immune regulation. The observation that LPS stimulation did not induce discernible alterations in TGF-α expression via flow analysis, whether at the cell surface or intracellularly, suggests that TGF-α may not be closely associated with the early immune responses triggered by LPS. However, it is essential to acknowledge that TGF-α might still exert its influence in later phases of the immune response or under specialized conditions not encompassed within the scope of our study. These findings align with prior research emphasizing the complicated and context-dependent control of TGF-α expression within immune cells (Blasband et al., 1990).

It is worth noting that the intracellular staining approach used in this study provides a snapshot of TGF-α expression at a specific time point (24 hours) following LPS stimulation. The relatively short 24-hour incubation period may not have been sufficient to induce substantial changes in TGF-α expression. Alternative time points or additional stimuli could potentially trigger alterations in TGF-α expression that remained unexplored in the current experimental design. Moreover, the absence of significant changes in the FMO TGF-α control group highlights the specificity of our staining and analysis methodology. This control group serves as a crucial benchmark for accurately quantifying TGF-α expression levels and distinguishing them from background fluorescence or nonspecific staining (Zlotnik & Yoshie, 2000).

Transitioning to the use of 3D culture systems for investigating the potential induction of TGF-α by NK cells in co-culture with HepG2 cells, the results of the flow cytometric analysis conducted to assess the NK cell populations in 3D coculture systems provide valuable insights into the dynamics of NK cell behavior in these environments. Significantly, the percentage frequency of viable NK cell expression data unveiled a distinctive pattern between the two co-culture models. The reduced percentage of NK cell expression observed in the NK-HepG2 cocultures is probably a result of the initial high percentage entering the NK-HepG2 co-culture. Since the percentage is already quite elevated, further increase is unlikely.

Conversely, the augmentation in % NK cell expression within the PBMC-HepG2 coculture raises intriguing questions regarding the interplay between various cell types. This hints at a conceivable role played by PBMC-derived cells, including diverse immune cell subsets, in influencing the dynamic shifts within the NK cell population. This observed increase suggests a possible complex crosstalk occurring between NK cells and other immune cell constituents within the coculture milieu.

However, our examination of TGF-α expression via ELISA in 3D coculture samples revealed no noticeable expression of TGF-α, with concentrations consistently falling below the detection threshold of the ELISA assay. This implies that TGF-α may exist at levels lower than quantifiable by the ELISA assay under the experimental conditions examined in this study.

Our gene expression analysis however yielded a noteworthy finding that merits attention. Specifically, there was a substantial upregulation of *TNFA* in PBMC-HepG2 co-culture samples as compared to the control group consisting of HepG2 cells alone. TNF-α's role as a proinflammatory cytokine is well-documented, and its heightened expression in the coculture setup suggests that the interaction between PBMCs and HepG2 cells may have induced an immune-related response, leading to *TNFA* upregulation. This finding validates the functionality of the coculture system and the responsiveness of PBMCs to the 3D environment. The observed *TNFA* upregulation serves as a positive control for the coculture setup's ability to induce a distinct gene expression response. In contrast, the absence of significant changes in the expression of *MYC, VEGFA*, *ADAM17*, *TGFA*, and *EGFR* genes suggest that these particular growth-related and metalloproteinase genes may not markedly influenced by the coculture environment within the 5-day incubation period. These results could be due to the complexity of the interactions within the coculture system, which might require longer incubation periods or the presence of additional factors to induce substantial changes in expression. While these genes are implicated in various cellular processes including cell proliferation, angiogenesis, growth factor signalling, and epidermal growth factor receptor activity, their response might be influenced by factors beyond the current experimental conditions (Bourgine et al., 2012; Hanahan & Weinberg, 2011).

In summary, our findings provide valuable insights into the interplay of genes and immune responses in liver-resident NK cells and LPS-stimulated PBMCs. These results underscore the

need for a comprehensive approach, considering various factors influencing gene expression modulation, to gain a complete understanding of immune regulation in different cellular contexts. Additionally, our investigation into TGF-α expression dynamics using flow cytometry and ELISA techniques offers critical insights into the challenges and considerations in antibody-based assays. The absence of detectable TGF-α expression prompts intriguing questions about its role in early immune responses, emphasizing the importance of further research to elucidate its functions in different contexts and under various stimuli.

Chapter 5   General Discussion and Conclusion

Liver regeneration is a remarkable biological phenomenon vital for sustaining liver function and responding to injuries or diseases (Michalopoulos, 2007). In this study we focus on the potential involvement of NK cell-derived TGF-α in liver regeneration. TGF-α, a multifunctional cytokine, is a pivotal player in promoting hepatocyte proliferation and orchestrating complex signalling pathways within the liver microenvironment (Fausto, 2004). Our research highlights the influence of TGF-α on hepatocyte cell line proliferation in both 2D and 3D cell culture models and identifies that while liver-resident NK cells express TGF-α, co-culture with hepatocytes is insufficient to induce TGF-α in peripheral blood NK cells.

In Chapter 3, we conducted a comprehensive examination of the impact of recombinant TGF-α on hepatocyte cell lines (HepG2 and Huh-7), using both 2D and 3D in vitro models. Our study yielded several vital observations. Notably, exposure to recombinant TGF-α in the 3D culture system led to a significant increase in HepG2 cell proliferation, suggesting a critical role for TGF-α in promoting hepatocyte proliferation within a 3D microenvironment. Examination of TGF-α-regulated genes revealed distinctive expression patterns in 2D and 3D models. Specifically, the upregulation of *EGFR* and *VEGFA* genes in 2D models and upregulation of *MYC*, *VEGFA*, and *G6PD* genes in 3D models provided valuable insights into the context-dependent nature of TGF-α signalling. This discovery holds significant implications for the broader research community particularly in the field of biology as it emphasizes the importance of considering the cellular environment when investigating TGF-α effects. For drug development, this means recognizing that certain drugs may be more effective in 2D settings, while others might work better in 3D environments. The findings also highlight the need for advancements in 3D cell culture techniques to better mimic real-world cellular conditions. Given the complexity of TGF-α signalling, adopting a systems biology approach to explore how different genes interact in these varying contexts could provide deeper insights.

Furthermore, these insights might have far-reaching implications in disease research, particularly in understanding the role of TGF-α in various diseases, including cancer.

Our gene expression analysis in this study offers valuable insights into the distinct responses of 2D and 3D models to recombinant TGF-α stimulation. In 2D models, we observed the upregulation of *EGFR* and *VEGFA* genes, suggesting TGF-α's activation of the *EGFR* pathway and stimulation of *VEGFA* expression. These findings align with previous research highlighting the pivotal roles of *EGFR* and *VEGFA* in hepatocyte proliferation and angiogenesis (Shibuya, 2006; Zhang et al., 2018). *EGFR*, has been extensively studied for its involvement in hepatocyte proliferation, serving as a key regulator of cell growth and division(Yarden & Sliwkowski, 2001b). On the other hand, *VEGFA* is renowned for its potent pro-angiogenic properties, orchestrating the formation of new blood vessels, an indispensable process for tissue vascularization and repair (Carmeliet & Jain, 2011).

In contrast, the 3D models exhibited upregulation of *MYC*, *VEGFA*, and *G6PD* genes. Of particular interest is the upregulation of *MYC*, a well-known metabolic master regulator and proto-oncogene associated with cell cycle progression and proliferation (Dang, 2012). The upregulation of *MYC* is particularly intriguing, as it hints at a potential molecular mechanism through which TGF-α exerts its effects. By promoting increased MYC expression, TGF-α may be altering the metabolic landscape of the treated cells, influencing their energy utilization, and promoting cell division and growth in the 3D culture.

Additionally, the upregulation of *VEGFA* in the 3D models suggests the potential angiogenic effects of TGF-α in this more complex cellular context. The increased expression of G6PD, an enzyme involved in glucose metabolism, in the 3D models may indicate enhanced energy production to support heightened cellular activity (Dang, 2012). Surprisingly, our results revealed a lack of *EGFR* upregulation in the 3D culture.

Several factors may contribute this. One plausible explanation is the microenvironmental disparities between the two culture systems. In 3D cultures, cells are in closer proximity and experience different nutrient and oxygen gradients compared to 2D cultures (Fennema et al., 2013). These altered conditions can influence cellular behavior and gene expression patterns, potentially leading to the observed discrepancy in *EGFR* expression. Furthermore, the distinct cell-ECM interactions in 3D cultures could play a pivotal role in modulating *EGFR* expression. The composition and mechanical properties of the ECM are known to impact cell signalling and behavior (Bissell & Barcellos-Hoff, 1987). Variations in ECM components between 2D and 3D cultures might have contributed to the differential *EGFR* expression.

Cell morphology and polarity are also likely contributors to the observed differences. Cells in 3D cultures often exhibit different morphologies and may adopt altered polarity compared to their counterparts in 2D cultures (Nelson & Bissell, 2006). These morphological changes can influence intracellular signalling pathways, potentially affecting *EGFR* expression.

Moreover, the differentiation state of cells in 3D cultures could be distinct from that of cells in 2D cultures. The 3D environment may promote a different differentiation state, which can have downstream effects on gene expression (Fischbach et al., 2007). This phenotypic shift may account for the lack of *EGFR* upregulation in the 3D culture.

Concerning potential signalling pathways activated in response to TGF-α in the 3D model, it is well-established that *EGFR* signals through the TGF-α/EGFR pathway, as documented in previous studies (Busser et al., 2011). Additionally, the PI3K/AKT and MAPK/ERK pathways, which are commonly associated with TGF-α signalling, play pivotal roles in liver regeneration and the activation of hepatocytes (Komposch & Sibilia, 2015; Singh & Harris, 2005). Our experimental data supports the presumption that these pathways are indeed activated when our 3D cultures are treated with recombinant TGF-α. Future research endeavors could explore the

extent of signalling occurring through these pathways in response to TGF-α stimulation and its relevance to liver regeneration.

The *in vitro* systems utilised in our studies presents a potential limitation due to its potential absence of biological context (Bissell & Radisky, 2001). When utilizing recombinant TGF-α, an artificial element is introduced, devoid of the regulatory mechanisms and multifaceted interactions that are inherent in the in vivo liver microenvironment (Derynck & Budi, 2019). In vivo, TGF-α is synthesized by various cell types and is subjected to localised post-translational regulation, including release via cell surface proteases (Derynck, 1990; Derynck et al., 1984). This post-translational regulation influences TGF-α availability and activity (Derynck & Budi, 2019). Controlled cell culture environments lack these complex regulatory mechanisms, resulting in a simplified and potentially less physiologically relevant scenario (Kapałczyńska et al., 2018; Koledova, 2017). This absence of biological context can significantly impact the interpretation of our experimental results, as it fails to replicate the dynamic and context-dependent fluctuations of TGF-α levels experienced by cells in vivo.

Furthermore, it is imperative to consider that the biological activity of TGF-α in vivo is regulated by its precise temporal and spatial distribution, a phenomenon crucially modulated throughout processes such as embryonic development, tissue regeneration, and the progression of pathological conditions (Derynck & Zhang, 2003; Massagué, 2012). In opposition, when employing recombinant TGF-α in cell culture experiments, a static exposure to a constant and probably supra-physiological concentration is commonly applied. This shift from the dynamic and context-dependent fluctuations of TGF-α levels observed in vivo may potentially give rise to variances in cellular responses, potentially confounding the physiological significance of our research findings.

Another inherent limitation of our study pertains to the choice of hepatocyte cell lines, specifically HepG2 and Huh-7, used in our investigative approach. Although these cell lines offer practical advantages for conducting in vitro experiments, it is crucial to acknowledge their constraints in adequately capturing the full spectrum of cell types and intercellular dynamics found within the liver (Bissell & Guzelian, 1980; Godoy et al., 2013). Hepatocyte cell lines, in essence, serve as simple models that lack the multicellular architecture inherent to the liver's in vivo context.

In the native liver tissue, hepatocytes engage in complex interactions with an array of non-parenchymal cells, including Kupffer cells, stellate cells, and endothelial cells, all of which exert profound influences on liver physiology and pathology (Krenkel & Tacke, 2017; Seki & Schwabe, 2015). The omission of these complex intercellular exchanges and the simplified nature of hepatocyte cell lines utilized in our investigation might impose potential constraints on the direct extrapolation of our research findings to the in vivo milieu. Hence, it is essential to interpret our results within the context of these limitations.

In Chapter 4, we shifted our focus to the expression of TGF-α within liver resident NK cells. At the transcriptional level, we confirmed TGF-α expression in these liver-resident NK cells, specifically noting a significant increase in the expression of the TGFA gene within the CD56[Bright] subset of liver-resident NK cells. This finding holds significant implications for the liver microenvironment, as it suggests that CD56[Bright] NK cells have the potential to contribute to the local TGF-α milieu within the liver. This is particularly significant given the strategic positioning of liver-resident NK cells within the hepatic tissue, where they interact with other liver-resident cells, such as hepatocytes and Kupffer cells. Through these interactions, they may modulate the production and availability of TGF-α within the liver microenvironment, aligning

with previous research in the field (Jameson et al., 2021) that emphasizes the importance of immune cell involvement in liver regeneration processes.

Our study also focused on the production of TGF-α by PBMCs following stimulation with LPS as well as the production of TGF-α by NK cells using 3D coculture.

Upon exposure to LPS, we observed a significant upregulation in the expression of the TGFA gene in PBMCs. This pronounced increase in TGFA gene expression can be attributed to the robust immune response triggered by LPS, a well-known endotoxin that activates the innate immune system and initiates a series of intracellular signalling cascades (Akira et al., 2006)

Additionally, it's important to consider the liver's significant role in LPS. The liver functions as a vital organ in the body's detoxification process, efficiently removing harmful substances, including LPS, from circulation (Abdel-Haq et al., 2019). Within the liver environment, a substantial concentration of LPS may exist, which is capable of inducing the expression of TGF-α. Hence, the stimulation by LPS likely led to the activation of NK cells and other immune cell subsets within PBMCs, thereby causing the transcriptional upregulation of *TGFA* (Banchereau & Pascual, 2006), as we observed. This observation raises the possibility that our in vitro coculture systems may have lacked a sufficient presence of LPS, potentially explaining why we did not observe comparable levels of TGF-α signals as seen in the physiological liver context.

The involvement of NK cells in TGF-α production highlights their pivotal role as potent immune responders. NK cells are recognized for their capacity to secrete cytokines and growth factors like TGF-α in response to infectious or inflammatory stimuli (Cooper, Fehniger, & Caligiuri, 2001). Hence, the observed elevation in TGFA expression suggests the involvement and significance of NK cells in mounting an immune response and potentially contributing to liver regeneration (Notas et al., 2009; Terunuma et al., 2008).

Contrary to our expectations, co-culturing PBMCs or PBMC-derived NK cells with HepG2 cells did not yield detectable TGF-α expression, despite an observed increase in the proportion of NK cells within the PBMC populations. This unexpected outcome raises intriguing questions regarding the complex interactions between immune cells and hepatocytes in the context of TGF-α production. Further investigations are warranted to elucidate the mechanisms responsible for the suppression of TGF-α expression in this co-culture setting.

One critical consideration is the source of NK cells used in the study. In this research, NK cells were derived from PBMCs, which are a commonly used model in immunology research. However, PBMC-derived NK cells may not fully represent the behavior of liver-resident NK cells. Liver-resident NK cells are a distinct subset adapted to the hepatic microenvironment and constantly exposed to various hepatic cell populations (Gao et al., 2009). These differences in phenotype and function, including higher expression levels of activating receptors like NKp46, NKp44, and CD69, may affect their ability to interact with target cells and induce the production of cytokines like TGF-α. Liver resident NK cells were not used in this case which is a possible limitation.

Furthermore, the microenvironment in which the 3D coculture took place is a crucial factor to consider. Liver-resident NK cells are strategically positioned within the liver tissue, allowing them to interact closely with other hepatic cell populations, including hepatocytes, Kupffer cells, and hepatic stellate cells. These interactions are known to be critical for various aspects of NK cell function, including cytokine production (Notas et al., 2009). TGF-α induction, in particular, could be influenced by the crosstalk between liver-resident NK cells and these neighboring cells. In the 3D coculture study, NK cells were cocultured with HepG2 cells, commonly used as a model for studying liver-related immune responses. However, the absence of other hepatic cell populations in this coculture model may have limited the ability of NK

cells to induce TGF-α production. Interactions between NK cells and hepatocytes, for example, have been shown to modulate cytokine secretion in the liver and contribute to its regulation (Jeong et al., 2006). HepG2 cells may not fully replicate the behavior of primary hepatocytes or interact with NK cells in the same way. This interaction could be a critical factor for TGF-α induction. The absence of these crucial cellular interactions in the 3D coculture system might have limited the ability of NK cells to induce TGF-α production.

An alternative hypothesis may pertain to the phenomenon of NK cell exhaustion, a well-documented occurrence in diverse immune responses (Wherry & Kurachi, 2015; Wu et al., 2016). Prolonged and continuous interactions between NK cells and HepG2 cells could potentially induce a state of functional exhaustion in NK cells, a state characterized by a gradual loss of their cytotoxic and cytokine-producing capabilities, including a reduced capacity to produce transforming growth factor alpha (TGF-α) and other critical cytokines (Björkström et al., 2010; Sun et al., 2014).

The process of NK cell exhaustion typically ensues from chronic stimulation (Wherry & Kurachi, 2015). In this particular context, the persistent presence of HepG2 cells may continually activate NK cells, leading to a state of diminished responsiveness over time. Given that NK cells are perpetually engaged in surveilling against cancerous cells such as HepG2, this prolonged exposure could conceivably overtax their functional capacity.

Moreover, the tumor microenvironment shaped by HepG2 cells might also contribute significantly to NK cell exhaustion (Wu et al., 2016). Cancer cells are known to release inhibitory factors such as transforming growth factor-beta (TGF-β) and interleukin-10 (IL-10) as part of their immune evasion strategies (Shimasaki et al., 2020; Wu et al., 2016). These factors have the direct capability to suppress NK cell function and thereby exacerbate their exhaustion. Furthermore, within the tumor microenvironment, the dysregulation of signalling

pathways within NK cells can further impede their ability to produce cytokines, including TGF-α (Shimasaki et al., 2020).

From our study, it is still unclear what the exact mechanisms are governing NK cell transcription and secretion of TGF-α. Further research is needed to elucidate the regulatory pathways involved in TGF-α production by NK cells, both in the liver and in peripheral blood. Also, investigating the potential expression of TGF-α in other liver cell populations is necessary, as these other cell types may also contribute to TGF-α production and play essential roles in the regenerative process. Exploring the crosstalk between liver resident NK cells, TGF-α, and other liver cell populations could provide a more holistic understanding of the complex dynamics involved in liver regeneration.

This investigation provides valuable insights into TGF-α, elucidating its synthesis within hepatocytes and NK cells, as well as its function in hepatocyte proliferation and potential roles in liver regeneration. However, it is imperative to recognize several limitations.

Primarily, the study heavily relies on in vitro models employing recombinant TGF-α, which lack the intricate regulatory mechanisms inherent in the liver's original environment. The simplified 2D and 3D cell cultures may oversimplify the complex interactions observed *in vivo*, diminishing the physiological significance of the findings. Additionally, the use of HepG2 and Huh-7 cell lines may inadequately represents the diverse cell types and interactions within the liver, notably lacking non-parenchymal cells.

Moreover, the study employs NK cells derived from peripheral blood, potentially not fully mirroring the behavior of liver-resident NK cells crucial in the liver microenvironment. The static exposure of recombinant TGF-α in cell culture experiments contrasts with the dynamic regulation of TGF-α *in vivo*, potentially confounding the physiological relevance of the results.

Prolonged interactions between NK cells and HepG2 cells might induce NK cell exhaustion, diminishing their capacity to produce TGF-α.

The 3D coculture system lacks essential interactions between liver-resident NK cells and other hepatic cell populations, such as Kupffer cells and hepatic stellate cells, potentially influencing TGF-α production. The study acknowledges the necessity for further research to comprehend the regulatory pathways involved in TGF-α production by NK cells in the liver microenvironment. Overall, while providing valuable insights, the study's limitations necessitate caution in interpreting and applying the findings to liver regeneration in a more complex and dynamic *in vivo* setting.

In summary, our investigation into the role of TGF-α in liver regeneration has yielded crucial insights, highlighting the elaborate nature of this biological process. While we have observed the upregulation of *TGFA* gene expression and an increase in TGF-α protein levels following LPS stimulation, the inability to detect TGF-α in co-cultures with HepG2 cells underscores the complex nature of immune responses in the liver microenvironment. However, we have identified potential factors contributing to this observation, such as the choice of NK cell source and limitations in our model. These findings provide a solid foundation for future research endeavors aimed at uncovering the precise mechanisms governing TGF-α regulation in liver regeneration. Furthermore, this study has contributed to our comprehension of liver regeneration, yet there remains much to be explored. By addressing the identified limitations and incorporating more physiologically relevant elements into our experimental design, we can further deepen our knowledge of liver biology and contribute to the development of innovative therapeutic strategies for liver-related pathologies.

Moreover, this research has broader clinical implications. Understanding TGF-α's influence on hepatocyte proliferation and gene expression patterns can guide the development of novel

therapeutic approaches for liver regeneration and liver-related diseases. However, it is imperative to acknowledge the necessity for future studies that bridge the gap between in vitro and in vivo findings, potentially through the utilization of animal models or more sophisticated 3D culture systems. In conclusion, our research has furnished valuable insights into the role of TGF-α in liver regeneration, underlining its context-dependent effects. While providing a solid foundation, our study opens the door to further exploration of the multifaceted immune responses in liver regeneration and underscores the importance of understanding the cellular and molecular mechanisms at play in this critical process. We hope our findings contribute to future research works and the development of future novel therapeutic strategies that harness the power of TGF-α and immune cells to promote liver regeneration and tissue repair, ultimately benefiting patients in need of liver repair and regeneration therapies.

5.1 Future Recommendations

To comprehensively address the hypothesis on TGF-α production in hepatocytes and NK cells and its role in liver regeneration, a diverse approach integrating various methodologies is crucial. Future research investigations should consider the factors below:

Shifting from controlled *in vitro* setups to more complex *in vivo* studies using animal models mirroring human liver physiology is key to understanding TGF-α dynamics within the liver's complex environment. Also, Improving coculture models by developing advanced 3D systems that replicate liver cell interactions will provide a more accurate representation of TGF-α dynamics and its impact on hepatocyte behavior and regeneration. Furthermore, understanding TGF-α-mediated signaling pathways like PI3K/AKT, MAPK/ERK, and EGFR in different environments is essential for deciphering its context-specific nature.

Overcoming limitations in current experimental models by using primary hepatocytes and including liver-resident NK cells will offer more relevant insights into TGF-α's role in liver regeneration. Exploring factors influencing TGF-α suppression in coculture settings, such as NK cell exhaustion or tumor microenvironments, will clarify complex immunological interactions affecting TGF-α expression. Bridging experimental findings with clinical relevance is fundamental. Connecting laboratory discoveries with real-world applications could unveil potential therapeutic strategies for liver regeneration and diseases, potentially involving the modulation of TGF-α's effects on hepatocytes.

Finally, further investigation into molecular differences between Huh7 and HepG2 cells in response to varying TGF-α concentrations holds promise for targeted therapeutic strategies. Exploring these differences in proliferation and gene expression responses could guide more effective treatments.

REFERENCES

Abbafati, C., Abbas, K. M., Abbasi-Kangevari, M., Abd-Allah, F., Abdelalim, A., Abdollahi, M., Abdollahpour, I., Abegaz, K. H., Abolhassani, H., Aboyans, V., Abreu, L. G., Abrigo, M. R. M., Abualhasan, A., Abu-Raddad, L. J., Abushouk, A. I., Adabi, M., Adekanmbi, V., Adeoye, A. M., Adetokunboh, O. Amini, S. (2020). Global burden of 369 diseases and injuries in 204 countries and territories, 1990-2019: a systematic analysis for the Global Burden of Disease Study 2019. *Lancet (London, England)*, *396*(10258), 1204–1222. https://doi.org/10.1016/S0140-6736(20)30925-9

Abdel-Haq, R., Schlachetzki, J. C. M., Glass, C. K., & Mazmanian, S. K. (2019). Microbiome-microglia connections via the gut-brain axis. *The Journal of Experimental Medicine*, *216*(1), 41–59. https://doi.org/10.1084/JEM.20180794

Abu Rmilah, A., Zhou, W., Nelson, E., Lin, L., Amiot, B., & Nyberg, S. L. (2019a). Understanding the marvels behind liver regeneration. *Wiley Interdisciplinary Reviews. Developmental Biology*, *8*(3). https://doi.org/10.1002/WDEV.340

Abu Rmilah, A., Zhou, W., Nelson, E., Lin, L., Amiot, B., & Nyberg, S. L. (2019b). Understanding the marvels behind liver regeneration. *Wiley Interdisciplinary Reviews. Developmental Biology*, *8*(3). https://doi.org/10.1002/WDEV.340

Addante, A., Roncero, C., Almalé, L., Lazcanoiturburu, N., García-Álvaro, M., Fernández, M., Sanz, J., Hammad, S., Nwosu, Z. C., Lee, S. J., Fabregat, I., Dooley, S., ten Dijke, P., Herrera, B., & Sánchez, A. (2018). Bone morphogenetic protein 9 as a key regulator of liver progenitor cells in DDC-induced cholestatic liver injury. *Liver International*, *38*(9), 1664–1675. https://doi.org/10.1111/LIV.13879

Akira, S., Uematsu, S., & Takeuchi, O. (2006). Pathogen Recognition and Innate Immunity. *Cell*, *124*(4), 783–801. https://doi.org/10.1016/J.CELL.2006.02.015

Ali, S., Haque, N., Azhar, Z., Saeinasab, M., & Sefat, F. (2021). Regenerative Medicine of Liver: Promises, Advances and Challenges. *Biomimetics*, *6*(4). https://doi.org/10.3390/BIOMIMETICS6040062

Alvarez-Sola, G., Uriarte, I., Latasa, M. U., Jimenez, M., Barcena-Varela, M., Santamaría, E., Urtasun, R., Rodriguez-Ortigosa, C., Prieto, J., Berraondo, P., Fernandez-Barrena, M. G., Berasain, C., & Avila, M. A. (2018). Bile acids, FGF15/19 and liver regeneration: From mechanisms to clinical applications. *Biochimica et Biophysica Acta. Molecular Basis of Disease*, *1864*(4 Pt B), 1326–1334. https://doi.org/10.1016/J.BBADIS.2017.06.025

Araújo, T. G., De Oliveira, A. G., Tobar, N., Saad, M. J. A., Moreira, L. R., Reis, E. R., Nicola, E. M. D., De Jorge, G. L., Dos Tártaro, R. R., Boin, I. F. S. F., & Teixeira, A. R. F. (2013). Liver regeneration following partial hepatectomy is improved by enhancing the HGF/Met axis and Akt and Erk pathways after low-power laser irradiation in rats. *Lasers in Medical Science*, *28*(6), 1511–1517. https://doi.org/10.1007/S10103-013-1264-Y

Ashry, S., Ahmed, S., Salem, H., & Wahdan, M. (2018). Alpha fetoprotein: A prognostic marker for early detection of liver regeneration in acute paracetamol toxicity. QJM: An International Journal of Medicine, 111. https://doi.org/10.1093/qjmed/hcy200.056Asrani, S. K., Devarbhavi,

H., Eaton, J., & Kamath, P. S. (2019). Burden of liver diseases in the world. *Journal of Hepatology*, *70*(1), 151–171. https://doi.org/10.1016/J.JHEP.2018.09.014

Avraham, R., & Yarden, Y. (2011). Feedback regulation of EGFR signalling: decision making by early and delayed loops. *Nature Reviews. Molecular Cell Biology*, *12*(2), 104–117. https://doi.org/10.1038/NRM3048

Bacon, B. R., Adams, P. C., Kowdley, K. V., Powell, L. W., & Tavill, A. S. (2011). Diagnosis and management of hemochromatosis: 2011 practice guideline by the American Association for the Study of Liver Diseases. *Hepatology (Baltimore, Md.)*, *54*(1), 328–343. https://doi.org/10.1002/HEP.24330

Baker, M. (2015). Blame it on the antibodies. *Nature*, *521*(7552), 274–276. https://doi.org/10.1038/521274A

Banchereau, J., & Pascual, V. (2006). Type I interferon in systemic lupus erythematosus and other autoimmune diseases. *Immunity*, *25*(3), 383–392. https://doi.org/10.1016/J.IMMUNI.2006.08.010

Barretina, J., Caponigro, G., Stransky, N., Venkatesan, K., Margolin, A. A., Kim, S., Wilson, C. J., Lehár, J., Kryukov, G. V., Sonkin, D., Reddy, A., Liu, M., Murray, L., Berger, M. F., Monahan, J. E., Morais, P., Meltzer, J., Korejwa, A., Jané-Valbuena, J., … Garraway, L. A. (2012). The Cancer Cell Line Encyclopedia enables predictive modelling of anticancer drug sensitivity. *Nature*, *483*(7391), 603–607. https://doi.org/10.1038/NATURE11003

Bataller, R., & Brenner, D. A. (2005). Liver fibrosis. *The Journal of Clinical Investigation*, *115*(2), 209–218. https://doi.org/10.1172/JCI24282

Berasain, C., & Avila, M. A. (2014). The EGFR signalling system in the liver: from hepatoprotection to hepatocarcinogenesis. *Journal of Gastroenterology*, *49*(1), 9–23. https://doi.org/10.1007/S00535-013-0907-X

Bernal, W., Jalan, R., Quaglia, A., Simpson, K., Wendon, J., & Burroughs, A. (2015). Acute-on-chronic liver failure. *The Lancet*, *386*(10003), 1576–1587. https://doi.org/10.1016/S0140-6736(15)00309-8

Bhat, M., Pasini, E., Baciu, C., Angeli, M., Humar, A., Macparland, S., Feld, J., & McGilvray, I. (2019). The basis of liver regeneration: A systems biology approach. *Annals of Hepatology*, *18*(3), 422–428. https://doi.org/10.1016/J.AOHEP.2018.07.003

Bilzer, M., Roggel, F., & Gerbes, A. L. (2006). Role of Kupffer cells in host defense and liver disease. *Liver International : Official Journal of the International Association for the Study of the Liver*, *26*(10), 1175–1186. https://doi.org/10.1111/J.1478-3231.2006.01342.X

Bissell, D. M., & Guzelian, P. S. (1980). Phenotypic stability of adult rat hepatocytes in primary monolayer culture. *Annals of the New York Academy of Sciences*, *349*(1), 85–98. https://doi.org/10.1111/J.1749-6632.1980.TB29518.X

Bissell, D. M., Wang, S. S., Jarnagin, W. R., & Roll, F. J. (1995). Cell-specific expression of transforming growth factor-beta in rat liver. Evidence for autocrine regulation of hepatocyte

proliferation. *The Journal of Clinical Investigation*, *96*(1), 447–455. https://doi.org/10.1172/JCI118055

Bissell, M. J., & Barcellos-Hoff, M. H. (1987). The influence of extracellular matrix on gene expression: is structure the message? *Journal of Cell Science. Supplement*, *8*(SUPPL. 8), 327–343. https://doi.org/10.1242/JCS.1987.SUPPLEMENT_8.18

Bissell, M. J., Hall, H. G., & Parry, G. (1982). How does the extracellular matrix direct gene expression? *Journal of Theoretical Biology*, *99*(1), 31–68. https://doi.org/10.1016/0022-5193(82)90388-5

Bissell, M. J., & Radisky, D. (2001). Putting tumours in context. *Nature Reviews Cancer 2001 1:1*, *1*(1), 46–54. https://doi.org/10.1038/35094059

Björkström, N. K., Riese, P., Heuts, F., Andersson, S., Fauriat, C., Ivarsson, M. A., Björklund, A. T., Flodström-Tullberg, M., Michaëlsson, J., Rottenberg, M. E., Guzmán, C. A., Ljunggren, H. G., & Malmberg, K. J. (2010). Expression patterns of NKG2A, KIR, and CD57 define a process of CD56dim NK-cell differentiation uncoupled from NK-cell education. *Blood*, *116*(19), 3853–3864. https://doi.org/10.1182/BLOOD-2010-04-281675

Black, R. A., Rauch, C. T., Kozlosky, C. J., Peschon, J. J., Slack, J. L., Wolfson, M. F., Castner, B. J., Stocking, K. L., Reddy, P., Srinivasan, S., Nelson, N., Boiani, N., Schooley, K. A., Gerhart, M., Davis, R., Fitzner, J. N., Johnson, R. S., Paxton, R. J., March, C. J., & Cerretti, D. P. (1997). A metalloproteinase disintegrin that releases tumour-necrosis factor-alpha from cells. *Nature*, *385*(6618), 729–733. https://doi.org/10.1038/385729a0

Blasband, A. J., Gilligan, D. M., Winchell, L. F., Wong, S. T., Luetteke, N. C., Rogers, K. T., & Lee, D. C. (1990). Expression of the TGFα integral membrane precursor induces transformation of NRK cells. *Oncogene*, *5*(8), 1213–1221.

Borowiak, M., Garratt, A. N., Wüstefeld, T., Strehle, M., Trautwein, C., & Birchmeier, C. (2004). Met provides essential signals for liver regeneration. *Proceedings of the National Academy of Sciences of the United States of America*, *101*(29), 10608–10613. https://doi.org/10.1073/PNAS.0403412101

Bourgine, J., Billaut-Laden, I., Happillon, M., Lo-Guidice, J. M., Maunoury, V., Imbenotte, M., & Broly, F. (2012). Gene expression profiling of systems involved in the metabolism and the disposition of xenobiotics: comparison between human intestinal biopsy samples and colon cell lines. *Drug Metabolism and Disposition: The Biological Fate of Chemicals*, *40*(4), 694–705. https://doi.org/10.1124/DMD.111.042465

Bradbury, A., & Plückthun, A. (2015). Reproducibility: Standardize antibodies used in research. *Nature*, *518*(7537), 27–29. https://doi.org/10.1038/518027A

Briscoe, J., & Thérond, P. P. (2013). The mechanisms of Hedgehog signalling and its roles in development and disease. *Nature Reviews. Molecular Cell Biology*, *14*(7), 418–431. https://doi.org/10.1038/NRM3598

Brown, K. D. (1995). The epidermal growth factor/transforming growth factor-α family and their receptors. *European Journal of Gastroenterology and Hepatology*, *7*(10), 914–922. https://doi.org/10.1097/00042737-199510000-00002

Busser, B., Sancey, L., Brambilla, E., Coll, J. L., & Hurbin, A. (2011). The multiple roles of amphiregulin in human cancer. *Biochimica et Biophysica Acta*, *1816*(2), 119–131. https://doi.org/10.1016/J.BBCAN.2011.05.003

Bustin, S. A., Benes, V., Garson, J. A., Hellemans, J., Huggett, J., Kubista, M., Mueller, R., Nolan, T., Pfaffl, M. W., Shipley, G. L., Vandesompele, J., & Wittwer, C. T. (2009). The MIQE guidelines: minimum information for publication of quantitative real-time PCR experiments. *Clinical chemistry*, *55*(4), 611–622. https://doi.org/10.1373/clinchem.2008.112797

Carmeliet P. (2005). Angiogenesis in life, disease and medicine. Nature, 438(7070), 932–936. https://doi.org/10.1038/nature04478

Carmeliet, P., & Jain, R. K. (2011). Molecular mechanisms and clinical applications of angiogenesis. *Nature 2011 473:7347*, *473*(7347), 298–307. https://doi.org/10.1038/nature10144

Carpenter, G., & Cohen, S. (1979). Epidermal growth factor. Annual review of biochemistry, 48, 193–216. https://doi.org/10.1146/annurev.bi.48.070179.001205

Cederbaum, A. I. (2012). Alcohol metabolism. *Clinics in Liver Disease*, *16*(4), 667–685. https://doi.org/10.1016/J.CLD.2012.08.002

Chalasani, N., Fontana, R. J., Bonkovsky, H. L., Watkins, P. B., Davern, T., Serrano, J., Yang, H., & Rochon, J. (2008). Causes, Clinical Features, and Outcomes From a Prospective Study of Drug-Induced Liver Injury in the United States. *Gastroenterology*, *135*(6). https://doi.org/10.1053/J.GASTRO.2008.09.011

Chalothorn, D., Moore, S. M., Zhang, H., Sunnarborg, S. W., Lee, D. C., & Faber, J. E. (2005). Heparin-binding epidermal growth factor-like growth factor, collateral vessel development, and angiogenesis in skeletal muscle ischemia. *Arteriosclerosis, Thrombosis, and Vascular Biology*, *25*(9), 1884–1890. https://doi.org/10.1161/01.ATV.0000175761.59602.16

Chapouly, C., Guimbal, S., Hollier, P. L., & Renault, M. A. (2019). Role of Hedgehog Signaling in Vasculature Development, Differentiation, and Maintenance. *International Journal of Molecular Sciences*, *20*(12), E3076–E3076. https://doi.org/10.3390/IJMS20123076

Cheng, W. L., Feng, P. H., Lee, K. Y., Chen, K. Y., Sun, W. L., Van Hiep, N., Luo, C. S., & Wu, S. M. (2021). The Role of EREG/EGFR Pathway in Tumor Progression. *International Journal of Molecular Sciences 2021, Vol. 22, Page 12828*, *22*(23), 12828. https://doi.org/10.3390/IJMS222312828

Chiang, J. Y. L., & Ferrell, J. M. (2018). Bile Acid Metabolism in Liver Pathobiology. *Gene Expression*, *18*(2), 71–87. https://doi.org/10.3727/105221618X15156018385515

Citri, A., & Yarden, Y. (2006). EGF–ERBB signalling: towards the systems level. *Nature Reviews Molecular Cell Biology 2006 7:7*, *7*(7), 505–516. https://doi.org/10.1038/nrm1962

Colombo, C., Maria Battezzati, P., Crosignani, A., & Costantini, D. (2002). *liver Disease in Cystic Fibrosis: A Prospective Study on Incidence, Risk Factors, and Outcome*. https://doi.org/10.1002/hep.1840360613

Cook, P. W., Piepkorn, M., Clegg, C. H., Plowman, G. D., DeMay, J. M., Brown, J. R., & Pittelkow, M. R. (1997). Transgenic expression of the human amphiregulin gene induces a psoriasis-like phenotype. *The Journal of Clinical Investigation*, *100*(9), 2286–2294. https://doi.org/10.1172/JCI119766

Cooper, M. A., Fehniger, T. A., & Caligiuri, M. A. (2001). The biology of human natural killer-cell subsets. *Trends in Immunology*, *22*(11), 633–640. https://doi.org/10.1016/S1471-4906(01)02060-9

Cooper, M. A., Fehniger, T. A., Turner, S. C., Chen, K. S., Ghaheri, B. A., Ghayur, T., Carson, W. E., & Caligiuri, M. A. (2001). Human natural killer cells: a unique innate immunoregulatory role for the CD56(bright) subset. *Blood*, *97*(10), 3146–3151. https://doi.org/10.1182/BLOOD.V97.10.3146

Crispe, I. N. (2014). Immune tolerance in liver disease. *Hepatology (Baltimore, Md.)*, *60*(6), 2109–2117. https://doi.org/10.1002/HEP.27254

Crispe, I. N., & Bigorgne, A. E. (2010). TLRs in Hepatic Cellular Crosstalk. *Gastroenterology Research and Practice*, *2010*. https://doi.org/10.1155/2010/618260

Dang, C. V. (2012). MYC on the path to cancer. *Cell*, *149*(1), 22–35. https://doi.org/10.1016/J.CELL.2012.03.003

Dao, D. T., Anez-Bustillos, L., Adam, R. M., Puder, M., & Bielenberg, D. R. (2018). Heparin-Binding Epidermal Growth Factor-Like Growth Factor as a Critical Mediator of Tissue Repair and Regeneration. *The American Journal of Pathology*, *188*(11), 2446–2456. https://doi.org/10.1016/J.AJPATH.2018.07.016

Davies, L. C., Jenkins, S. J., Allen, J. E., & Taylor, P. R. (2013). Tissue-resident macrophages. *Nature Immunology*, *14*(10), 986–995. https://doi.org/10.1038/NI.2705

Debray, D., Kelly, D., Houwen, R., Strandvik, B., & Colombo, C. (2011). Best practice guidance for the diagnosis and management of cystic fibrosis-associated liver disease. *Journal of Cystic Fibrosis*, *10*(2), 29–36. www.elsevier.com/locate/jcf

Derynck, R. (1990). Transforming growth factor-alpha. *Molecular Reproduction and Development*, *27*(1), 3–9. https://doi.org/10.1002/MRD.1080270104

Derynck, R., Akhurst, R. J., & Balmain, A. (2001). TGF-beta signaling in tumor suppression and cancer progression. *Nature Genetics*, *29*(2), 117–129. https://doi.org/10.1038/NG1001-117

Derynck, R., & Budi, E. H. (2019). Specificity, versatility, and control of TGF-β family signaling. *Science Signaling*, *12*(570). https://doi.org/10.1126/SCISIGNAL.AAV5183

Derynck, R., Roberts, A. B., Winkler, M. E., Chen, E. Y., & Goeddel, D. V. (1984). Human transforming growth factor-alpha: precursor structure and expression in E. coli. *Cell*, *38*(1), 287–297. https://doi.org/10.1016/0092-8674(84)90550-6

Derynck, R., & Zhang, Y. E. (2003). Smad-dependent and Smad-independent pathways in TGF-beta family signalling. *Nature*, *425*(6958), 577–584. https://doi.org/10.1038/NATURE02006

Dranoff, G. (2004). Cytokines in cancer pathogenesis and cancer therapy. *Nature Reviews Cancer*, *4*(1), 11–22. https://doi.org/10.1038/NRC1252

Drixler, T. A., Vogten, J. M., Gebbink, M. F. B. G., Carmeliet, P., Voest, E. E., & Borel Rinkes, I. H. M. (2003). Plasminogen mediates liver regeneration and angiogenesis after experimental partial hepatectomy. *The British Journal of Surgery*, *90*(11), 1384–1390. https://doi.org/10.1002/BJS.4275

Dunbar, A. J., & Goddard, C. (2000). Structure-function and biological role of betacellulin. *The International Journal of Biochemistry & Cell Biology*, *32*(8), 805–815. https://doi.org/10.1016/S1357-2725(00)00028-5

Duval, K., Grover, H., Han, L. H., Mou, Y., Pegoraro, A. F., Fredberg, J., & Chen, Z. (2017). Modeling Physiological Events in 2D vs. 3D Cell Culture. *Physiology (Bethesda, Md.)*, *32*(4), 266–277. https://doi.org/10.1152/PHYSIOL.00036.2016

Eisenberg, E., & Levanon, E. Y. (2013). Human housekeeping genes, revisited. *Trends in Genetics : TIG*, *29*(10), 569–574. https://doi.org/10.1016/J.TIG.2013.05.010

Eslam, M., Newsome, P. N., Sarin, S. K., Anstee, Q. M., Targher, G., Romero-Gomez, M., Zelber-Sagi, S., Wai-Sun Wong, V., Dufour, J. F., Schattenberg, J. M., Kawaguchi, T., Arrese, M., Valenti, L., Shiha, G., Tiribelli, C., Yki-Järvinen, H., Fan, J. G., Grønbæk, H., Yilmaz, Y., … George, J. (2020). A new definition for metabolic dysfunction-associated fatty liver disease: An international expert consensus statement. *Journal of Hepatology*, *73*(1), 202–209. https://doi.org/10.1016/J.JHEP.2020.03.039

Exton, J. H. (1987). Mechanisms of hormonal regulation of hepatic glucose metabolism. *Diabetes/Metabolism Reviews*, *3*(1), 163–183. https://doi.org/10.1002/DMR.5610030108

Fausto, N. (2004). Liver regeneration and repair: hepatocytes, progenitor cells, and stem cells. *Hepatology (Baltimore, Md.)*, *39*(6), 1477–1487. https://doi.org/10.1002/HEP.20214

Fausto, N., & Campbell, J. S. (2003). The role of hepatocytes and oval cells in liver regeneration and repopulation. *Mechanisms of Development*, *120*(1), 117–130. https://doi.org/10.1016/S0925-4773(02)00338-6

Fazel Modares, N., Polz, R., Haghighi, F., Lamertz, L., Behnke, K., Zhuang, Y., Kordes, C., Häussinger, D., Sorg, U. R., Pfeffer, K., Floss, D. M., Moll, J. M., Piekorz, R. P., Ahmadian, M. R., Lang, P. A., & Scheller, J. (2019). IL-6 Trans-signaling Controls Liver Regeneration After Partial Hepatectomy. *Hepatology (Baltimore, Md.)*, *70*(6), 2075–2091. https://doi.org/10.1002/HEP.30774

Felipo, V. (2013). Hepatic encephalopathy: effects of liver failure on brain function. *Nature Reviews Neuroscience 2013 14:12*, *14*(12), 851–858. https://doi.org/10.1038/nrn3587

Fennema, E., Rivron, N., Rouwkema, J., van Blitterswijk, C., & De Boer, J. (2013). Spheroid culture as a tool for creating 3D complex tissues. *Trends in Biotechnology*, *31*(2), 108–115. https://doi.org/10.1016/j.tibtech.2012.12.003

Fischbach, C., Chen, R., Matsumoto, T., Schmelzle, T., Brugge, J. S., Polverini, P. J., & Mooney, D. J. (2007). Engineering tumors with 3D scaffolds. *Nature Methods 2007 4:10*, *4*(10), 855–860. https://doi.org/10.1038/nmeth1085

Forbes, S. J., Gupta, S., & Dhawan, A. (2015). Cell therapy for liver disease: From liver transplantation to cell factory. *Journal of Hepatology*, *62*(1 Suppl), S157–S169. https://doi.org/10.1016/J.JHEP.2015.02.040

Frankenberg, T., Rao, A., Chen, F., Haywood, J., Shneider, B. L., & Dawson, P. A. (2006). Regulation of the mouse organic solute transporter alpha-beta, Ostalpha-Ostbeta, by bile acids. *American Journal of Physiology. Gastrointestinal and Liver Physiology*, *290*(5). https://doi.org/10.1152/AJPGI.00479.2005

Friedman, S. L. (2008a). Hepatic fibrosis -- overview. *Toxicology*, *254*(3), 120–129. https://doi.org/10.1016/J.TOX.2008.06.013

Friedman, S. L. (2008b). Hepatic stellate cells: protean, multifunctional, and enigmatic cells of the liver. *Physiological Reviews*, *88*(1), 125–172. https://doi.org/10.1152/PHYSREV.00013.2007

Friedman, S. L. (2010). Evolving challenges in hepatic fibrosis. *Nature Reviews Gastroenterology & Hepatology 2010 7:8*, *7*(8), 425–436. https://doi.org/10.1038/nrgastro.2010.97

Gao, B. (2016). Basic liver immunology. *Cellular and Molecular Immunology*, *13*(3), 265–266. https://doi.org/10.1038/CMI.2016.09

Gao, B., & Bataller, R. (2011). Alcoholic liver disease: Pathogenesis and new therapeutic targets. *Gastroenterology*, *141*(5), 1572–1585. https://doi.org/10.1053/J.GASTRO.2011.09.002

Gao, B., Radaeva, S., & Park, O. (2009). Liver natural killer and natural killer T cells: immunobiology and emerging roles in liver diseases. *Journal of Leukocyte Biology*, *86*(3), 513–528. https://doi.org/10.1189/JLB.0309135

Garcia-Tsao, G., Groszmann, R. J., Fisher, R. L., Conn, H. O., Atterbury, C. E., & Glickman, M. (1985). Portal pressure, presence of gastroesophageal varices and variceal bleeding. *Hepatology (Baltimore, Md.)*, *5*(3), 419–424. https://doi.org/10.1002/HEP.1840050313

Garcia-Tsao, G., & Lim, J. (2009). Management and treatment of patients with cirrhosis and portal hypertension: recommendations from the Department of Veterans Affairs Hepatitis C Resource Center Program and the National Hepatitis C Program. *The American Journal of Gastroenterology*, *104*(7), 1802–1829. https://doi.org/10.1038/AJG.2009.191

Gebhardt, R. (1992). Metabolic zonation of the liver: regulation and implications for liver function. *Pharmacology & Therapeutics*, *53*(3), 275–354. https://doi.org/10.1016/0163-7258(92)90055-5

Gentek, R., Molawi, K., & Sieweke, M. H. (2014). Tissue macrophage identity and self-renewal. *Immunological Reviews*, *262*(1), 56–73. https://doi.org/10.1111/IMR.12224

Ghobrial, R. M., Freise, C. E., Trotter, J. F., Tong, L., Ojo, A. O., Fair, J. H., Fisher, R. A., Emond, J. C., Koffron, A. J., Pruett, T. L., & Olthoff, K. M. (2008). Donor morbidity after living donation for liver transplantation. *Gastroenterology*, *135*(2), 468–476. https://doi.org/10.1053/J.GASTRO.2008.04.018

Ginès, P., Cárdenas, A., Arroyo, V., & Rodés, J. (2004). Management of cirrhosis and ascites. The New England journal of medicine, 350(16), 1646–1654. https://doi.org/10.1056/NEJMra035021

Godoy, P., Hewitt, N. J., Albrecht, U., Andersen, M. E., Ansari, N., Bhattacharya, S., Bode, J. G., Bolleyn, J., Borner, C., Böttger, J., Braeuning, A., Budinsky, R. A., Burkhardt, B., Cameron, N. R., Camussi, G., Cho, C. S., Choi, Y. J., Craig Rowlands, J., Dahmen, U., … Hengstler, J. G. (2013). Recent advances in 2D and 3D in vitro systems using primary hepatocytes, alternative hepatocyte sources and non-parenchymal liver cells and their use in investigating mechanisms of hepatotoxicity, cell signaling and ADME. *Archives of Toxicology*, *87*(8), 1315–1530. https://doi.org/10.1007/S00204-013-1078-5

Goldstein, J. L., DeBose-Boyd, R. A., & Brown, M. S. (2006). Protein sensors for membrane sterols. *Cell*, *124*(1), 35–46. https://doi.org/10.1016/J.CELL.2005.12.022

Gordillo, M., Evans, T., & Gouon-Evans, V. (2015). *Orchestrating liver development*. https://doi.org/10.1242/dev.114215

Griffith, L. G., & Swartz, M. A. (2006). Capturing complex 3D tissue physiology in vitro. *Nature Reviews. Molecular Cell Biology*, *7*(3), 211–224. https://doi.org/10.1038/NRM1858

Gu, Y., Mohammad, I. S., & Liu, Z. (2020). Overview of the STAT-3 signaling pathway in cancer and the development of specific inhibitors (Review). *Oncology Letters*, *19*(4), 2585–2594. https://doi.org/10.3892/OL.2020.11394/DOWNLOAD

Hadjittofi, C., Feretis, M., Martin, J., Harper, S., & Huguet, E. (2021). Liver regeneration biology: Implications for liver tumour therapies. *World Journal of Clinical Oncology*, *12*(12), 1101–1156. https://doi.org/10.5306/wjco.v12.i12.1101

Hanahan, D., & Weinberg, R. A. (2011). Hallmarks of cancer: the next generation. *Cell*, *144*(5), 646–674. https://doi.org/10.1016/J.CELL.2011.02.013

Harada, K. I., Shiota, G., & Kawasaki, H. (1999). Transforming growth factor-alpha and epidermal growth factor receptor in chronic liver disease and hepatocellular carcinoma. *Liver*, *19*(4), 318–325. https://doi.org/10.1111/J.1478-3231.1999.TB00056.X

Harris, R. C., Chung, E., & Coffey, R. J. (2003). EGF receptor ligands. *Experimental Cell Research*, *284*(1), 2–13. https://doi.org/10.1016/S0014-4827(02)00105-2

Haycock, J. W. (2011). 3D cell culture: a review of current approaches and techniques. *Methods in Molecular Biology (Clifton, N.J.)*, *695*, 1–15. https://doi.org/10.1007/978-1-60761-984-0_1

He, G., & Karin, M. (2010). NF-κB and STAT3 – key players in liver inflammation and cancer. *Cell Research 2011 21:1*, *21*(1), 159–168. https://doi.org/10.1038/cr.2010.183

Hernandez-Gea, V., & Friedman, S. L. (2011). Pathogenesis of liver fibrosis. *Annual Review of Pathology*, *6*, 425–456. https://doi.org/10.1146/ANNUREV-PATHOL-011110-130246

Heubi, J. E., Setchell, K. D. R., & Bove, K. E. (2007). Inborn errors of bile acid metabolism. *Seminars in Liver Disease*, *27*(3), 282–294. https://doi.org/10.1055/S-2007-985073

Heymann, F., & Tacke, F. (2016). Immunology in the liver — from homeostasis to disease. *Nature Reviews Gastroenterology & Hepatology 2016 13:2*, *13*(2), 88–110. https://doi.org/10.1038/nrgastro.2015.200

Higashiyama, S., Iwabuki, H., Morimoto, C., Hieda, M., Inoue, H., & Matsushita, N. (2008). Membrane-anchored growth factors, the epidermal growth factor family: Beyond receptor ligands. *Cancer Science*, *99*(2), 214–220. https://doi.org/10.1111/j.1349-7006.2007.00676.x

Hirsch, F. R., Varella-Garcia, M., Bunn, P. A., Di Maria, M. V., Veve, R., Bremnes, R. M., Barón, A. E., Zeng, C., & Franklin, W. A. (2003). Epidermal growth factor receptor in non-small-cell lung carcinomas: correlation between gene copy number and protein expression and impact on prognosis. *Journal of Clinical Oncology : Official Journal of the American Society of Clinical Oncology*, *21*(20), 3798–3807. https://doi.org/10.1200/JCO.2003.11.069

Hirschhaeuser, F., Menne, H., Dittfeld, C., West, J., Mueller-Klieser, W., & Kunz-Schughart, L. A. (2010). Multicellular tumor spheroids: An underestimated tool is catching up again. *Journal of Biotechnology*, *148*(1), 3–15. https://doi.org/10.1016/j.jbiotec.2010.01.012

Hoffmann, K., Nagel, A. J., Tanabe, K., Fuchs, J., Dehlke, K., Ghamarnejad, O., Lemekhova, A., & Mehrabi, A. (2020). Markers of liver regeneration—the role of growth factors and cytokines: a systematic review. *BMC Surgery*, *20*(1). https://doi.org/10.1186/S12893-019-0664-8

Hofmann, A. F. (1999). Bile Acids: The Good, the Bad, and the Ugly. *News in Physiological Sciences : An International Journal of Physiology Produced Jointly by the International Union of Physiological Sciences and the American Physiological Society*, *14*(1), 24–29. https://doi.org/10.1152/PHYSIOLOGYONLINE.1999.14.1.24

Hohenester, S., Maillette de Buy Wenniger, L., Paulusma, C. C., van Vliet, S. J., Jefferson, D. M., Oude Elferink, R. P., & Beuers, U. (2012). A biliary HCO3- umbrella constitutes a protective mechanism against bile acid-induced injury in human cholangiocytes. *Hepatology (Baltimore, Md.)*, *55*(1), 173–183. https://doi.org/10.1002/HEP.24691

Hritz, I., Mandrekar, P., Velayudham, A., Catalano, D., Dolganiuc, A., Kodys, K., Kurt-Jones, E., & Szabo, G. (2008). The critical role of toll-like receptor (TLR) 4 in alcoholic liver disease is independent of the common TLR adapter MyD88. *Hepatology (Baltimore, Md.)*, *48*(4), 1224–1231. https://doi.org/10.1002/HEP.22470

Huang, W., Han, N., Du, L., Wang, M., Chen, L., & Tang, H. (2021). A narrative review of liver regeneration-from models to molecular basis. *Ann Transl Med*, *9*(22), 1705. https://doi.org/10.21037/atm-21-5234

Huh, C. G., Factor, V. M., Sánchez, A., Uchida, K., Conner, E. A., & Thorgeirsson, S. S. (2004). Hepatocyte growth factor/c-met signaling pathway is required for efficient liver regeneration and repair. *Proceedings of the National Academy of Sciences of the United States of America*, *101*(13), 4477–4482. https://doi.org/10.1073/PNAS.0306068101

Hutmacher, D. W. (2010). Biomaterials offer cancer research the third dimension. *Nature Materials*, *9*(2), 90–93. https://doi.org/10.1038/NMAT2619

Hynes, N. E., & MacDonald, G. (2009). ErbB receptors and signaling pathways in cancer. *Current Opinion in Cell Biology*, *21*(2), 177–184. https://doi.org/10.1016/J.CEB.2008.12.010

Jameson, G. (2021). Investigating the phenotype and functional roles of human liver-resident natural killer (NK) cells (Doctoral dissertation). Trinity College Dublin, School of Medicine

Jenne, C. N., & Kubes, P. (2013). Immune surveillance by the liver. *Nature Immunology*, *14*(10), 996–1006. https://doi.org/10.1038/NI.2691

Jorissen, R. N., Walker, F., Pouliot, N., Garrett, T. P. J., Ward, C. W., & Burgess, A. W. (2003). Epidermal growth factor receptor: Mechanisms of activation and signalling. *Experimental Cell Research*, *284*(1), 31–53. https://doi.org/10.1016/S0014-4827(02)00098-8

Jungermann, K., & Kietzmann, T. (1996). Zonation of parenchymal and nonparenchymal metabolism in liver. *Annual Review of Nutrition*, *16*, 179–203. https://doi.org/10.1146/ANNUREV.NU.16.070196.001143

Kapałczyńska, M., Kolenda, T., Przybyła, W., Zajączkowska, M., Teresiak, A., Filas, V., Ibbs, M., Bliźniak, R., Łuczewski, Ł., & Lamperska, K. (2018). 2D and 3D cell cultures - a comparison of different types of cancer cell cultures. *Archives of Medical Science : AMS*, *14*(4), 910–919. https://doi.org/10.5114/AOMS.2016.63743

Kawamoto, M., Yamaji, T., Saito, K., Shirasago, Y., Satomura, K., Endo, T., Fukasawa, M., Hanada, K., & Osada, N. (2020). Identification of Characteristic Genomic Markers in Human Hepatoma HuH-7 and Huh7.5.1-8 Cell Lines. *Frontiers in Genetics*, *11*. https://doi.org/10.3389/FGENE.2020.546106/FULL)

Khan, M. G. M., Ghosh, A., Variya, B., Santharam, M. A., Kandhi, R., Ramanathan, S., & Ilangumaran, S. (2019). Hepatocyte growth control by SOCS1 and SOCS3. *Cytokine*, *121*. https://doi.org/10.1016/J.CYTO.2019.154733

Kisseleva, T., & Brenner, D. (2021). Molecular and cellular mechanisms of liver fibrosis and its regression. *Nature Reviews. Gastroenterology & Hepatology*, *18*(3), 151–166. https://doi.org/10.1038/S41575-020-00372-7

Knolle, P. A., & Thimme, R. (2014). Hepatic immune regulation and its involvement in viral hepatitis infection. *Gastroenterology*, *146*(5), 1193–1207. https://doi.org/10.1053/J.GASTRO.2013.12.036

Koledova, Z. (2017). 3D Cell Culture: An Introduction. *Methods in Molecular Biology (Clifton, N.J.)*, *1612*. https://doi.org/10.1007/978-1-4939-7021-6_1

Komposch, K., & Sibilia, M. (2015). EGFR Signaling in Liver Diseases. *International Journal of Molecular Sciences*, *17*(1). https://doi.org/10.3390/IJMS17010030

Konishi, T., Schuster, R. M., & Lentsch, A. B. (2018). Proliferation of hepatic stellate cells, mediated by YAP and TAZ, contributes to liver repair and regeneration after liver ischemia-reperfusion injury. *American Journal of Physiology - Gastrointestinal and Liver Physiology*, *314*(4), G471–G482. https://doi.org/10.1152/AJPGI.00153.2017/ASSET/IMAGES/LARGE/ZH30031874160008.JPEG

Krenkel, O., & Tacke, F. (2017). Liver macrophages in tissue homeostasis and disease. *Nature Reviews Immunology 2017 17:5*, *17*(5), 306–321. https://doi.org/10.1038/nri.2017.11

Kubes, P., & Jenne, C. (2018). Immune Responses in the Liver. *Annual Review of Immunology*, *36*, 247–277. https://doi.org/10.1146/ANNUREV-IMMUNOL-051116-052415

Kubes, P., Jenne, C., & Snyder, J. (2018). Immune Responses in the Liver. *Annual Review of Immunology*, 44. https://doi.org/10.1146/annurev-immunol

Kuten Pella, O., Hornyák, I., Horváthy, D., Fodor, E., Nehrer, S., & Lacza, Z. (2022). Albumin as a Biomaterial and Therapeutic Agent in Regenerative Medicine. International journal of molecular sciences, 23(18), 10557. https://doi.org/10.3390/ijms231810557

Lalor, P. F., Hields, P. S., Grant, A. J., & Adams, D. H. (2002). Recruitment of lymphocytes to the human liver. *Immunology and Cell Biology*, *80*(1), 52–64. https://doi.org/10.1046/J.1440-1711.2002.01062.X

Lee, G. Y., Kenny, P. A., Lee, E. H., & Bissell, M. J. (2007). Three-dimensional culture models of normal and malignant breast epithelial cells. *Nature Methods*, *4*(4), 359–365. https://doi.org/10.1038/NMETH1015

Leiskau, C., & Baumann, U. (2017). Structure, Function, and Repair of the Liver. *Diseases of the Liver and Biliary System in Children*, 1–17. https://doi.org/10.1002/9781119046936.CH1

Lemmon, M. A., & Schlessinger, J. (2010). Cell signaling by receptor tyrosine kinases. *Cell*, *141*(7), 1117–1134. https://doi.org/10.1016/J.CELL.2010.06.011

Li, X., Pérez, L., Pan, Z., & Fan, H. (2007). The transmembrane domain of TACE regulates protein ectodomain shedding. *Cell Research 2007 17:12*, *17*(12), 985–998. https://doi.org/10.1038/cr.2007.98

Liberal, R., Mieli-Vergani, G., & Vergani, D. (2013). Clinical significance of autoantibodies in autoimmune hepatitis. *Journal of Autoimmunity*, *46*, 17–24. https://doi.org/10.1016/J.JAUT.2013.08.001

Liu, H. X., Keane, R., Sheng, L., & Wan, Y. J. Y. (2015). Implications of microbiota and bile acid in liver injury and regeneration. *Journal of Hepatology*, *63*(6), 1502–1510. https://doi.org/10.1016/J.JHEP.2015.08.001

Liu, M., & Chen, P. (2017). Proliferation-inhibiting pathways in liver regeneration (Review). *Molecular Medicine Reports*, *16*(1), 23–35. https://doi.org/10.3892/MMR.2017.6613/HTML

Livak, K. J., & Schmittgen, T. D. (2001). Analysis of relative gene expression data using real-time quantitative PCR and the 2(-Delta Delta C(T)) Method. *Methods (San Diego, Calif.)*, *25*(4), 402–408. https://doi.org/10.1006/METH.2001.1262

López-Luque, J., & Fabregat, I. (2018). Revisiting the liver: from development to regeneration - what we ought to know! *The International Journal of Developmental Biology*, *62*(6-7–8), 441–451. https://doi.org/10.1387/IJDB.170264JL

Lorente, S., Hautefeuille, M., & Sanchez-Cedillo, A. (2020). The liver, a functionalized vascular structure. *Scientific Reports 2020 10:1*, *10*(1), 1–10. https://doi.org/10.1038/s41598-020-73208-8

Luetteke, N. C., Qiu, T. H., Fenton, S. E., Troyer, K. L., Riedel, R. F., Chang, A., & Lee, D. C. (1999a). Targeted inactivation of the EGF and amphiregulin genes reveals distinct roles for EGF receptor ligands in mouse mammary gland development. *Development (Cambridge, England)*, *126*(12), 2739–2750. https://doi.org/10.1242/DEV.126.12.2739

Luetteke, N. C., Qiu, T. H., Fenton, S. E., Troyer, K. L., Riedel, R. F., Chang, A., & Lee, D. C. (1999b). Targeted inactivation of the EGF and amphiregulin genes reveals distinct roles for EGF receptor ligands in mouse mammary gland development. *Development*, *126*(12), 2739–2750. https://doi.org/10.1242/DEV.126.12.2739

Machida, J., Yoshiura, K. I., Funkhauser, C. D., Natsume, N., Kawai, T., & Murray, J. C. (1999). Transforming growth factor-α (TGFA): Genomic structure, boundary sequences, and mutation analysis in nonsyndromic cleft lip/palate and cleft palate only. *Genomics*, *61*(3), 237–242. https://doi.org/10.1006/geno.1999.5962

Manns, M. P., Czaja, A. J., Gorham, J. D., Krawitt, E. L., Mieli-Vergani, G., Vergani, D., & Vierling, J. M. (2010). Diagnosis and management of autoimmune hepatitis. *Hepatology*, *51*(6), 2193–2213. https://doi.org/10.1002/HEP.23584

Marí, M., & Morales, A. (2017). Bone morphogenetic protein-9/activin-like kinase 1 axis a new target for hepatic regeneration and fibrosis treatment in liver injury. *Hepatobiliary Surgery and Nutrition*, *6*(6), 414–416. https://doi.org/10.21037/HBSN.2017.11.02

Massagué, J. (2012). TGFβ signalling in context. *Nature Reviews Molecular Cell Biology 2012 13:10*, *13*(10), 616–630. https://doi.org/10.1038/nrm3434

Mead, J. E., & Fausto, N. (1989). Transforming growth factor alpha may be a physiological regulator of liver regeneration by means of an autocrine mechanism. *Proceedings of the National Academy of Sciences of the United States of America*, *86*(5), 1558. https://doi.org/10.1073/PNAS.86.5.1558

Medzhitov, R., & Janeway, C. (2000). Innate immune recognition: mechanisms and pathways. *Immunological Reviews*, *173*, 89–97. https://doi.org/10.1034/J.1600-065X.2000.917309.X

Mehta, V. B., & Besner, G. E. (2007). HB-EGF promotes angiogenesis in endothelial cells via PI3-kinase and MAPK signaling pathways. *Growth Factors (Chur, Switzerland)*, *25*(4), 253–263. https://doi.org/10.1080/08977190701773070

Merlen, G., Ursic-Bedoya, J., Jourdainne, V., Kahale, N., Glenisson, M., Doignon, I., Rainteau, D., & Tordjmann, T. (2017). Bile acids and their receptors during liver regeneration: "Dangerous protectors." *Molecular Aspects of Medicine*, *56*, 25–33. https://doi.org/10.1016/J.MAM.2017.03.002

Metallo, C. M., & Vander Heiden, M. G. (2013). Understanding metabolic regulation and its influence on cell physiology. *Molecular Cell*, *49*(3), 388–398. https://doi.org/10.1016/J.MOLCEL.2013.01.018

Miaczynska, M., Christoforidis, S., Giner, A., Shevchenko, A., Uttenweiler-Joseph, S., Habermann, B., Wilm, M., Parton, R. G., & Zerial, M. (2004). APPL proteins link Rab5 to nuclear signal transduction via an endosomal compartment. *Cell*, *116*(3), 445–456. https://doi.org/10.1016/S0092-8674(04)00117-5

Michalopoulos, G. K. (2007). Liver regeneration. *Journal of Cellular Physiology*, *213*(2), 286–300. https://doi.org/10.1002/JCP.21172

Michalopoulos, G. K. (2010). Liver regeneration after partial hepatectomy: Critical analysis of mechanistic dilemmas. *American Journal of Pathology*, *176*(1), 2–13. https://doi.org/10.2353/AJPATH.2010.090675

Michalopoulos, G. K. (2013). Principles of liver regeneration and growth homeostasis. *Comprehensive Physiology*, *3*(1), 485–513. https://doi.org/10.1002/CPHY.C120014

Michalopoulos, G. K. (2017). Hepatostat: Liver regeneration and normal liver tissue maintenance. *Hepatology*, *65*(4), 1384–1392. https://doi.org/10.1002/HEP.28988

Michalopoulos, G. K., & Bhushan, B. (2020). Liver regeneration: biological and pathological mechanisms and implications. *Nature Reviews Gastroenterology & Hepatology 2020 18:1*, *18*(1), 40–55. https://doi.org/10.1038/s41575-020-0342-4

Michalopoulos, G. K., & DeFrances, M. C. (1997). Liver regeneration. *Science (New York, N.Y.)*, *276*(5309), 60–65. https://doi.org/10.1126/SCIENCE.276.5309.60

Min, J. S., DeAngelis, R. A., Reis, E. S., Gupta, S., Maurya, M. R., Evans, C., Das, A., Burant, C., Lambris, J. D., & Subramaniam, S. (2016). Systems analysis of the complement-induced priming phase of liver regeneration. *Journal of Immunology (Baltimore, Md. : 1950)*, *197*(6), 2500. https://doi.org/10.4049/JIMMUNOL.1600628

Mitra, A., Raychaudhuri, S. K., & Raychaudhuri, S. P. (2012). IL-22 induced cell proliferation is regulated by PI3K/Akt/mTOR signaling cascade. *Cytokine*, *60*(1), 38–42. https://doi.org/10.1016/J.CYTO.2012.06.316

Morales-González, Á., Bautista, M., Madrigal-Santillán, E., Posadas-Mondragón, A., Anguiano-Robledo, L., Madrigal-Bujaidar, E., Álvarez-González, I., Fregoso-Aguilar, T., Gayosso-Islas, E., Sánchez-Moreno, C., & Morales-González, J. A. (2017). Nrf2 modulates cell proliferation and antioxidants defenses during liver regeneration induced by partial hepatectomy. *International Journal of Clinical and Experimental Pathology*, *10*(7), 7801–7811. https://ipn.elsevierpure.com/en/publications/nrf2-modulates-cell-proliferation-and-antioxidants-defenses-durin

Natarajan, A., Wagner, B., & Sibilia, M. (2007). The EGF receptor is required for efficient liver regeneration. *Proceedings of the National Academy of Sciences of the United States of America*, *104*(43), 17081–17086. https://doi.org/10.1073/PNAS.0704126104

Nelson, C. M., & Bissell, M. J. (2006). Of extracellular matrix, scaffolds, and signaling: tissue architecture regulates development, homeostasis, and cancer. *Annual Review of Cell and Developmental Biology*, *22*, 287–309. https://doi.org/10.1146/ANNUREV.CELLBIO.22.010305.104315

Notas, G., Kisseleva, T., & Brenner, D. (2009). NK and NKT cells in liver injury and fibrosis. *Clinical Immunology*, *130*(1), 16–26. https://doi.org/10.1016/J.CLIM.2008.08.008

Odell, I. D., Steach, H., Gauld, S. B., Reinke-Breen, L., Karman, J., Carr, T. L., Wetter, J. B., Phillips, L., Hinchcliff, M., & Flavell, R. A. (2022). Epiregulin is a dendritic cell–derived EGFR ligand

that maintains skin and lung fibrosis. *Science Immunology*, *7*(78). https://doi.org/10.1126/SCIIMMUNOL.ABQ6691/SUPPL_FILE/SCIIMMUNOL.ABQ6691 _MDAR_REPRODUCIBILITY_CHECKLIST.PDF

Ohtani, O. (1988). Three-dimensional organization of the collagen fibrillar framework of the human and rat livers. *Archives of Histology and Cytology*, *51*(5), 473–488. https://doi.org/10.1679/AOHC.51.473

Pawson, T., & Nash, P. (2003). Assembly of cell regulatory systems through protein interaction domains. *Science (New York, N.Y.)*, *300*(5618), 445–452. https://doi.org/10.1126/SCIENCE.1083653

Péan, N., Doignon, I., Garcin, I., Besnard, A., Julien, B., Liu, B., Branchereau, S., Spraul, A., Guettier, C., Humbert, L., Schoonjans, K., Rainteau, D., & Tordjmann, T. (2013). The receptor TGR5 protects the liver from bile acid overload during liver regeneration in mice. *Hepatology (Baltimore, Md.)*, *58*(4), 1451–1460. https://doi.org/10.1002/HEP.26463

Peng, H., Wisse, E., & Tian, Z. (2015). Liver natural killer cells: subsets and roles in liver immunity. *Cellular & Molecular Immunology 2016 13:3*, *13*(3), 328–336. https://doi.org/10.1038/cmi.2015.96

Peng, X. E., Chen, F. L., Liu, W., et al. (2016). Lack of association between SREBF-1c gene polymorphisms and risk of non-alcoholic fatty liver disease in a Chinese Han population. Scientific Reports, 6, 32110. https://doi.org/10.1038/srep32110

Pietrangelo, A. (2010). Hereditary hemochromatosis: Pathogenesis, diagnosis, and treatment. *Gastroenterology*, *139*(2). https://doi.org/10.1053/J.GASTRO.2010.06.013

Plowman, G. D., Whitney, G. S., Neubauer, M. G., Green, J. M., McDonald, V. L., Todaro, G. J., & Shoyab, M. (1990). Molecular cloning and expression of an additional epidermal growth factor receptor-related gene. *Proceedings of the National Academy of Sciences of the United States of America*, *87*(13), 4905. https://doi.org/10.1073/PNAS.87.13.4905

Postic, C., & Girard, J. (2008). Contribution of de novo fatty acid synthesis to hepatic steatosis and insulin resistance: lessons from genetically engineered mice. *The Journal of Clinical Investigation*, *118*(3), 829–838. https://doi.org/10.1172/JCI34275

Preziosi, M., Okabe, H., Poddar, M., Singh, S., & Monga, S. P. (2018). Endothelial Wnts regulate β-catenin signaling in murine liver zonation and regeneration: A sequel to the Wnt-Wnt situation. *Hepatology Communications*, *2*(7), 845–860. https://doi.org/10.1002/HEP4.1196

Puerta, A. B. F., Prado, M. M., Frampton, A. E., & Jiao, L. R. (2016). Gene of the month: HGF. *Journal of Clinical Pathology*, *69*(7), 575–579. https://doi.org/10.1136/JCLINPATH-2015-203575

Ravi, M., Paramesh, V., Kaviya, S. R., Anuradha, E., & Paul Solomon, F. D. (2015). 3D cell culture systems: advantages and applications. *Journal of Cellular Physiology*, *230*(1), 16–26. https://doi.org/10.1002/JCP.24683

Rehm, J., Samokhvalov, A. V., & Shield, K. D. (2013). Global burden of alcoholic liver diseases. *Journal of Hepatology*, *59*(1), 160–168. https://doi.org/10.1016/J.JHEP.2013.03.007

Reuben, A., Koch, D. G., & Lee, W. M. (2010). Drug-induced acute liver failure: Results of a U.S. multicenter, prospective study. *Hepatology*, *52*(6), 2065–2076. https://doi.org/10.1002/HEP.23937

Rhee, S. G. (2001). Regulation of phosphoinositide-specific phospholipase C. *Annual Review of Biochemistry*, *70*, 281–312. https://doi.org/10.1146/ANNUREV.BIOCHEM.70.1.281

Richardson, S. R., & O'Malley, G. F. (2022). Glucose-6-Phosphate Dehydrogenase Deficiency. StatPearls. https://www.ncbi.nlm.nih.gov/books/NBK470315/

Roberts, E. A., & Schilsky, M. L. (2008). Diagnosis and treatment of Wilson disease: an update. *Hepatology (Baltimore, Md.)*, *47*(6), 2089–2111. https://doi.org/10.1002/HEP.22261

Roepstorff, K., Grandal, M. V., Henriksen, L., Knudsen, S. L. J., Lerdrup, M., Grøvdal, L., Willumsen, B. M., & Van Deurs, B. (2009). Differential effects of EGFR ligands on endocytic sorting of the receptor. *Traffic (Copenhagen, Denmark)*, *10*(8), 1115–1127. https://doi.org/10.1111/J.1600-0854.2009.00943.X

Romee, R., & Miller, J. S. (2015). ADAM17 and CD56lowCD16low NK cells. *Haematologica*, *100*(8), e331. https://doi.org/10.3324/HAEMATOL.2015.129213

Roskoski, R. (2014). The ErbB/HER family of protein-tyrosine kinases and cancer. *Pharmacological Research*, *79*, 34–74. https://doi.org/10.1016/J.PHRS.2013.11.002

Rossol, M., Heine, H., Meusch, U., Quandt, D., Klein, C., Sweet, M. J., & Hauschildt, S. (2011). LPS-induced cytokine production in human monocytes and macrophages. *Critical Reviews in Immunology*, *31*(5), 379–446. https://doi.org/10.1615/CRITREVIMMUNOL.V31.I5.20

Russell D. W. (2003). The enzymes, regulation, and genetics of bile acid synthesis. Annual review of biochemistry, 72, 137–174. https://doi.org/10.1146/annurev.biochem.72.121801.161712

Russell, J. O., & Monga, S. P. (2018). Wnt/β-Catenin Signaling in Liver Development, Homeostasis, and Pathobiology. *Annual Review of Pathology*, *13*, 351–378. https://doi.org/10.1146/ANNUREV-PATHOL-020117-044010

Russell, R. M. (2000). The vitamin A spectrum: from deficiency to toxicity. *The American Journal of Clinical Nutrition*, *71*(4), 878–884. https://doi.org/10.1093/AJCN/71.4.878

Schlessinger, J. (2000). Cell signaling by receptor tyrosine kinases. *Cell*, *103*(2), 211–225. https://doi.org/10.1016/S0092-8674(00)00114-8

Schlessinger, J., Plotnikov, A. N., Ibrahimi, O. A., Eliseenkova, A. V., Yeh, B. K., Yayon, A., Linhardt, R. J., & Mohammadi, M. (2000). Crystal structure of a ternary FGF-FGFR-heparin complex reveals a dual role for heparin in FGFR binding and dimerization. *Molecular Cell*, *6*(3), 743–750. https://doi.org/10.1016/S1097-2765(00)00073-3

Schmidt-Arras, D., & Rose-John, S. (2016). IL-6 pathway in the liver: From physiopathology to therapy. *Journal of Hepatology*, *64*(6), 1403–1415. https://doi.org/10.1016/J.JHEP.2016.02.004

Schreiber, A. B., Winkler, M. E., & Derynck, R. (1986). Transforming Growth Factor-α: a More Potent Angiogenic Mediator than Epidermal Growth Factor. *Science*, *232*(4755), 1250–1253. https://doi.org/10.1126/SCIENCE.2422759

Schuppan, D., & Kim, Y. O. (2013). Evolving therapies for liver fibrosis. *The Journal of Clinical Investigation*, *123*(5), 1887–1901. https://doi.org/10.1172/JCI66028

Schwabe, R. F., Tabas, I., & Pajvani, U. B. (2020). Mechanisms of Fibrosis Development in Nonalcoholic Steatohepatitis. *Gastroenterology*, *158*(7), 1913–1928. https://doi.org/10.1053/J.GASTRO.2019.11.311

Seki, E., & Schwabe, R. F. (2015). Hepatic inflammation and fibrosis: functional links and key pathways. *Hepatology (Baltimore, Md.)*, *61*(3), 1066–1079. https://doi.org/10.1002/HEP.27332

Semenza G. L. (2011). Oxygen sensing, homeostasis, and disease. The New England journal of medicine, 365(6), 537–547. https://doi.org/10.1056/NEJMra1011165

Seshacharyulu, P., Ponnusamy, M. P., Haridas, D., Jain, M., Ganti, A. K., & Batra, S. K. (2012). Targeting the EGFR signaling pathway in cancer therapy. *Expert Opinion on Therapeutic Targets*, *16*(1), 15–31. https://doi.org/10.1517/14728222.2011.648617

Shachaf, C. M., Kopelman, A. M., Arvanitis, C., Karlsson, Å., Beer, S., Mandl, S., Bachmann, M. H., Borowsky, A. D., Ruebner, B., Cardiff, R. D., Yang, Q., Bishop, J. M., Contag, C. H., & Felsher, D. W. (2004). MYC inactivation uncovers pluripotent differentiation and tumour dormancy in hepatocellular cancer. *Nature*, *431*(7012), 1112–1117. https://doi.org/10.1038/NATURE03043

Shibuya, M. (2006). Vascular endothelial growth factor (VEGF)-receptor2: Its biological functions, major signaling pathway, and specific ligand VEGF-E. *Endothelium: Journal of Endothelial Cell Research*, *13*(2), 63–69. https://doi.org/10.1080/10623320600697955

Shimasaki, N., Jain, A., & Campana, D. (2020). NK cells for cancer immunotherapy. *Nature Reviews. Drug Discovery*, *19*(3), 200–218. https://doi.org/10.1038/S41573-019-0052-1

Shoyab, M., Plowman, G. D., McDonald, V. L., Bradley, J. G., & Todaro, G. J. (1989). Structure and function of human amphiregulin: a member of the epidermal growth factor family. *Science*, *243*(4894), 1074–1076. https://doi.org/10.1126/SCIENCE.2466334

Sielska, M., Przanowski, P., Pasierbińska, M., Wojnicki, K., Poleszak, K., Wojtas, B., Grzeganek, D., Ellert-Miklaszewska, A., Ku, M. C., Kettenmann, H., & Kaminska, B. (2020). Tumour-derived CSF2/granulocyte macrophage colony stimulating factor controls myeloid cell accumulation and progression of gliomas. *British Journal of Cancer 2020 123:3*, *123*(3), 438–448. https://doi.org/10.1038/s41416-020-0862-2

Singal, A. K., & Shah, V. H. (2019). Current trials and novel therapeutic targets for alcoholic hepatitis. *Journal of Hepatology*, *70*(2), 305–313. https://doi.org/10.1016/J.JHEP.2018.10.026

Singal, A., Volk, M. L., Waljee, A., Salgia, R., Higgins, P., Rogers, M. A. M., & Marrero, J. A. (2009). Meta-analysis: surveillance with ultrasound for early-stage hepatocellular carcinoma

in patients with cirrhosis. *Alimentary Pharmacology & Therapeutics*, *30*(1), 37–47. https://doi.org/10.1111/J.1365-2036.2009.04014.X

Singh, A. B., & Harris, R. C. (2005). Autocrine, paracrine and juxtacrine signaling by EGFR ligands. *Cellular Signalling*, *17*(10), 1183–1193. https://doi.org/10.1016/J.CELLSIG.2005.03.026

Sorkin, A., & Von Zastrow, M. (2009). Endocytosis and signalling: intertwining molecular networks. *Nature Reviews Molecular Cell Biology 2009 10:9*, *10*(9), 609–622. https://doi.org/10.1038/nrm2748

Starzl, T. E., Marchioro, T. L., Porter, K. A., & Brettschneider, L. (1967). Homotransplantation of the liver. *Transplantation*, *5*(4), 790–803. https://doi.org/10.1097/00007890-196707001-00003

Sternberger, L. A. (1979). *Immunocytochemistry*. 354. https://archive.org/details/immunocytochemis0000ster_t9i2

Stickel, F., & Hampe, J. (2012). Genetic determinants of alcoholic liver disease. *Gut*, *61*(1), 150–159. https://doi.org/10.1136/GUTJNL-2011-301239

Stravitz, R. T., & Lee, W. M. (2019). Acute liver failure. *The Lancet*, *394*(10201), 869–881. https://doi.org/10.1016/S0140-6736(19)31894-X

Streetz, K. L., Luedde, T., Manns, M. P., & Trautwein, C. (2000). Interleukin 6 and liver regeneration. *Gut*, *47*(2), 309–312. https://doi.org/10.1136/GUT.47.2.309

Sun, C., Sun, H., Zhang, C., & Tian, Z. (2014). NK cell receptor imbalance and NK cell dysfunction in HBV infection and hepatocellular carcinoma. *Cellular & Molecular Immunology 2014 12:3*, *12*(3), 292–302. https://doi.org/10.1038/cmi.2014.91

Sun, R., & Gao, B. (2004). Negative regulation of liver regeneration by innate immunity (natural killer cells/interferon-γ). *Gastroenterology*, *127*(5), 1525–1539. https://doi.org/10.1053/j.gastro.2004.08.055

Susan Standring. (2020). Gray's Anatomy: 42nd edition | | ISBN: 9780702077050 | ANZ Elsevier Health Bookshop : Books. *Gray's Anatomy*, *Hardcover*, 955–985. https://www.goliardicats.it/it/libri/medicina/medicina-stranieri/gray-s-anatomy-anatomical-basis-clinical-practice-42nd.html

Takahashi, M., Ota, S., Shimada, T., Hamada, E., Kawabe, T., Okudaira, T., Matsumura, M., Kaneko, N., Terano, A., Nakamura, T., & Omata, M. (1995). Hepatocyte growth factor is the most potent endogenous stimulant of rabbit gastric epithelial cell proliferation and migration in primary culture. *Journal of Clinical Investigation*, *95*(5), 1994. https://doi.org/10.1172/JCI117884

Takebayashi-Suzuki, K., & Suzuki, A. (2020). Intracellular Communication among Morphogen Signaling Pathways during Vertebrate Body Plan Formation. *Genes*, *11*(3). https://doi.org/10.3390/GENES11030341

Tao, Y., Wang, M., Chen, E., & Tang, H. (2017). Liver Regeneration: Analysis of the Main Relevant Signaling Molecules. *Mediators of Inflammation*, *2017*. https://doi.org/10.1155/2017/4256352

Tapper, E. B., & Parikh, N. D. (2018). observational study. *BMJ*, *362*, 2817. https://doi.org/10.1136/bmj.k2817

Taub, R. (2004). Liver regeneration: from myth to mechanism. *Nature Reviews. Molecular Cell Biology*, *5*(10), 836–847. https://doi.org/10.1038/NRM1489

Terunuma, H., Deng, X., Dewan, Z., Fujimoto, S., & Yamamoto, N. (2008). Potential role of NK cells in the induction of immune responses: Implications for NK cell-based immunotherapy for cancers and viral infections. *International Reviews of Immunology*, *27*(3), 93–110. https://doi.org/10.1080/08830180801911743

Thomson, A. W., & Knolle, P. A. (2010). Antigen-presenting cell function in the tolerogenic liver environment. *Nature Reviews. Immunology*, *10*(11), 753–766. https://doi.org/10.1038/NRI2858

Tiniakos, D. G., Vos, M. B., & Brunt, E. M. (2010). Nonalcoholic Fatty Liver Disease: Pathology and Pathogenesis. *Https://Doi.Org/10.1146/Annurev-Pathol-121808-102132*, *5*, 145–171. https://doi.org/10.1146/ANNUREV-PATHOL-121808-102132

Trefts, E., Gannon, M., & Wasserman, D. H. (2017). The liver. *Current Biology : CB*, *27*(21), R1147–R1151. https://doi.org/10.1016/J.CUB.2017.09.019

Tsochatzis, E. A., Bosch, J., & Burroughs, A. K. (2014). Liver cirrhosis. *Lancet (London, England)*, *383*(9930), 1749–1761. https://doi.org/10.1016/S0140-6736(14)60121-5

Tsuchida, T., & Friedman, S. L. (2017). Mechanisms of hepatic stellate cell activation. *Nature Reviews Gastroenterology & Hepatology 2017 14:7*, *14*(7), 397–411. https://doi.org/10.1038/nrgastro.2017.38

Umata, T. (2004). Mechanism for Activation of Heparin-Binding EGF-Like Growth Factor Induced by Stimuli. *Journal of UOEH*, *26*(1), 85–97. https://doi.org/10.7888/juoeh.26.85

Valizadeh, A., Majidinia, M., Samadi-Kafil, H., Yousefi, M., & Yousefi, B. (2019). The roles of signaling pathways in liver repair and regeneration. *Journal of Cellular Physiology*, *234*(9), 14966–14974. https://doi.org/10.1002/JCP.28336

van de Laarschot, L. F. M., Jansen, P. L. M., Schaap, F. G., & Olde Damink, S. W. M. (2016). The role of bile salts in liver regeneration. *Hepatology International*, *10*(5), 733–740. https://doi.org/10.1007/S12072-016-9723-8

Vandesompele, J., De Preter, K., Pattyn, F., Poppe, B., Van Roy, N., De Paepe, A., & Speleman, F. (2002). Accurate normalization of real-time quantitative RT-PCR data by geometric averaging of multiple internal control genes. *Genome Biology*, *3*(7). https://doi.org/10.1186/GB-2002-3-7-RESEARCH0034

Vinci, M., Gowan, S., Boxall, F., Patterson, L., Zimmermann, M., Court, W., Lomas, C., Mendiola, M., Hardisson, D., & Eccles, S. A. (2012). Advances in establishment and analysis of three-dimensional tumor spheroid-based functional assays for target validation and drug evaluation. *BMC Biology*, *10*. https://doi.org/10.1186/1741-7007-10-29

Vivier, E., Raulet, D. H., Moretta, A., Caligiuri, M. A., Zitvogel, L., Lanier, L. L., Yokoyama, W. M., & Ugolini, S. (2011). Innate or adaptive immunity? The example of natural killer cells. *Science (New York, N.Y.)*, *331*(6013), 44–49. https://doi.org/10.1126/SCIENCE.1198687

Vivier, E., Tomasello, E., Baratin, M., Walzer, T., & Ugolini, S. (2008). Functions of natural killer cells. *Nature Immunology*, *9*(5), 503–510. https://doi.org/10.1038/NI1582

Wan, J., Benkdane, M., Teixeira-Clerc, F., Bonnafous, S., Louvet, A., Lafdil, F., Pecker, F., Tran, A., Gual, P., Mallat, A., Lotersztajn, S., & Pavoine, C. (2014). M2 Kupffer cells promote M1 Kupffer cell apoptosis: a protective mechanism against alcoholic and nonalcoholic fatty liver disease. *Hepatology (Baltimore, Md.)*, *59*(1), 130–142. https://doi.org/10.1002/HEP.26607

Weaver, V. M., Petersen, O. W., Wang, F., Larabell, C. A., Briand, P., Damsky, C., & Bissell, M. J. (1997). Reversion of the Malignant Phenotype of Human Breast Cells in Three-Dimensional Culture and In Vivo by Integrin Blocking Antibodies. *The Journal of Cell Biology*, *137*(1). http://rupress.org/jcb/article-pdf/137/1/231/1842891/16405.pdf

Weigelt, B., Lo, A. T., Park, C. C., Gray, J. W., & Bissell, M. J. (2010). HER2 signaling pathway activation and response of breast cancer cells to HER2-targeting agents is dependent strongly on the 3D microenvironment. *Breast Cancer Research and Treatment*, *122*(1), 35–43. https://doi.org/10.1007/S10549-009-0502-2

Wherry, E. J., & Kurachi, M. (2015). Molecular and cellular insights into T cell exhaustion. *Nature Reviews. Immunology*, *15*(8), 486–499. https://doi.org/10.1038/NRI3862

WHO. (2017). Epidemiological update: increasing mortality calls for action 03. *Global Hepatitis Report, 2017*, 7–20.

Wu, T., Ji, Y., Ashley Moseman, E., Xu, H. C., Manglani, M., Kirby, M., Anderson, S. M., Handon, R., Kenyon, E., Elkahloun, A., Wu, W., Lang, P. A., Gattinoni, L., McGavern, D. B., & Schwartzberg, P. L. (2016). The TCF1-Bcl6 axis counteracts type I interferon to repress exhaustion and maintain T cell stemness. *Science Immunology*, *1*(6). https://doi.org/10.1126/SCIIMMUNOL.AAI8593

Yamamoto, K., Blum, R., & Kaufman, D. S. (2020). ADAM17-Deficient Pluripotent Stem Cell-Derived Natural Killer Cells Possess Improved Antibody-Dependent Cellular Cytotoxicity and Antitumor Activity. *Blood*, *136*(Supplement 1), 2–2. https://doi.org/10.1182/BLOOD-2020-137766

Yang, L. L. (2020). Anatomy and physiology of the liver. *Anesthesia for Hepatico-Pancreatic-Biliary Surgery and Transplantation*, 15–40. https://doi.org/10.1007/978-3-030-51331-3_2/COVER

Yarden, Y., & Sliwkowski, M. X. (2001). Untangling the ErbB signalling network. *Nature Reviews. Molecular Cell Biology*, *2*(2), 127–137. https://doi.org/10.1038/35052073

Younossi, Z. M., Koenig, A. B., Abdelatif, D., Fazel, Y., Henry, L., & Wymer, M. (2016). Global epidemiology of nonalcoholic fatty liver disease—Meta-analytic assessment of prevalence, incidence, and outcomes. *Hepatology*, *64*(1), 73–84. https://doi.org/10.1002/HEP.28431/SUPPINFO

Zaiss, D. M. W., Gause, W. C., Osborne, L. C., & Artis, D. (2015). Emerging functions of amphiregulin in orchestrating immunity, inflammation, and tissue repair. *Immunity*, *42*(2), 216–226. https://doi.org/10.1016/J.IMMUNI.2015.01.020

Zaiss, D. M. W., van Loosdregt, J., Gorlani, A., Bekker, C. P. J., Gröne, A., Sibilia, M., van Bergen en Henegouwen, P. M. P., Roovers, R. C., Coffer, P. J., & Sijts, A. J. A. M. (2013). Amphiregulin enhances regulatory T cell-suppressive function via the epidermal growth factor receptor. *Immunity*, *38*(2), 275–284. https://doi.org/10.1016/J.IMMUNI.2012.09.023

Zanger, U. M., & Schwab, M. (2013). Cytochrome P450 enzymes in drug metabolism: regulation of gene expression, enzyme activities, and impact of genetic variation. *Pharmacology & Therapeutics*, *138*(1), 103–141. https://doi.org/10.1016/J.PHARMTHERA.2012.12.007

Zhang, H., Berezov, A., Wang, Q., Zhang, G., Drebin, J., Murali, R., & Greene, M. I. (2007). ErbB receptors: from oncogenes to targeted cancer therapies. *The Journal of Clinical Investigation*, *117*(8), 2051–2058. https://doi.org/10.1172/JCI32278

Zhang, H., Shi, J. H., Jiang, H., Wang, K., Lu, J. Y., Jiang, X., Ma, X., Chen, Y. X., Ren, A. J., Zheng, J., Xie, Z., Guo, S., Xu, X., & Zhang, W. J. (2018). ZBTB20 regulates EGFR expression and hepatocyte proliferation in mouse liver regeneration. Cell death & disease, 9(5), 462. https://doi.org/10.1038/s41419-018-0514-0

Zhou, J., Sun, X., Yang, L., Wang, L., Ran, G., Wang, J., Cao, Q., Wu, L., Bryant, A., Ling, C., & Pi, L. (2020). Hepatocyte nuclear factor 4α negatively regulates connective tissue growth factor during liver regeneration. *The FASEB Journal*, *34*(4), 4970–4983. https://doi.org/10.1096/FJ.201902382R

Zlotnik, A., & Yoshie, O. (2000). Chemokines: a new classification system and their role in immunity. *Immunity*, *12*(2), 121–127. https://doi.org/10.1016/S1074-7613(00)80165-X

Zou, Y., Lee, J., Nambiar, S. M., Hu, M., Rui, W., Bao, Q., Chan, J. Y., & Dai, G. (2014). Nrf2 is involved in maintaining hepatocyte identity during liver regeneration. *PloS One*, *9*(9). https://doi.org/10.1371/JOURNAL.PONE.0107423